1-26-2022

Deformed No-Core Shell Model and Symplectic Effective Field Theory

David Kekejian

DEFORMED NO-CORE SHELL MODEL AND SYMPLECTIC EFFECTIVE FIELD THEORY

A Dissertation

Submitted to the Graduate Faculty of the
Louisiana State University and
Agricultural and Mechanical College
in partial fulfillment of the
requirements for the degree of
Doctor of Philosophy

in

The Department of Physics and Astronomy

by
David Kekejian
B.S. Physics, Yerevan State University, 2014
May 2022

Acknowledgments

I want to sincerely thank everyone who supported me during the duration of my PhD. Without your support this thesis work would not have been possible.

First of all, I would like to thank my advisor Jerry Draayer for his leadership and oversight over this project. His enthusiasm towards this project and careful planning made this possible. Exceptional praise to Kristina Launey to whom I am indebted for all the help and support she has given me during these past years. The useful discussions I had with her was priceless for the advancement of my research project. With her professionalism, grace and patience, she has been the heart and soul of our research group and the key to the successful end of this thesis.

Special thanks to Lavrent Khachatryan who helped and sheltered me when I first arrived in USA. The collaboration we did together gave me valuable experience which I appreciate a lot. Also to Ravi Rau for the useful discussions that kept my passion towards physics alive. Further acknowledgement to my collaborators Viktor Mokeev at JLab and Craig Roberts at Nanjing University for their constant support and useful insight into my research project. Finally to all my professors at YSU in Armenia for influencing and equipping me with the necessary knowledge to become a successful scientist.

I also want to thank my friends, Arshag Danageozian, Grigor Sargsyan, Samuel Cupp, David Howe, Hazem Fleifel, Derek Walker, Robert Cottingham, Nick Walker, Kevin Becker, Hunter Meyer and Margaret Carey. My interactions with all of you added color and excitement to my life during these past years of graduate school. All the hang-outs, conversations, debates, trivia and board game nights that we had together gave me the strength needed to keep going and carry this project to the end.

Finally I would like to thank my parents, especially my mother to whom I owe endless gratitude. This section is not enough to describe all the love and emotional support she has provided me with. Furthermore, I sincerely thank all my relatives for their encouragement, kind words and for being there when I needed them.

Table of Contents

Abstract

Most nuclei are deformed! This simple fact has been established since Bohr and Mottelson, and successfully demonstrated from first principles by nuclear structure calculations carried out using the *ab-initio* Symmetry-Adapted No-Core Shell Model (SA-NCSM) using realistic interactions. This simple fact has been the main driver towards understanding the underlying physics; namely, that symplectic symmetry describes deformation and is a dominant symmetry in all nuclei independent of $\mathcal{A}$ (nucleon number) and of the realistic interaction used. These two simple observations laid the foundation of this thesis work to explore the applications of symplectic symmetry towards defining a deformed symplectic model algebra. We show how a deformed no-core shell model could be constructed that allows one to carry out nuclear structure calculations in smaller model spaces without the need of huge computational resources. Furthermore, we develop the overlaps (transformation coefficients) between deformed and non-deformed spherical, cylindrical and Cartesian harmonic oscillator basis states that could also be utilized for reducing computational complexities within the scope of nuclear physics studies. Finally, the emergence of symplectic symmetry within a simple field theoretical framework that paved the way for the development of the Symplectic Effective Field Theory (SpEFT) is presented.

SpEFT is in principle applicable to any nucleus across the nuclear chart and can reproduce energy spectra, B(E2) strengths and radii, using only a laptop computer without the need of supercomputing resources, since it takes full advantage of the underlying symmetry. It accurately depicts how rotations and vibrations in nuclei occur, and how they affect nuclear observables. Results from the application of this theory on ^{12}C, ^{20}Ne and ^{166}Er are presented, and are in remarkable agreement with experiment.

1 Introduction

The dominance of deformation in nuclear physics has long been recognized. The tale is a long one, beginning with the work of Niels Bohr in the 30s on the liquid drop model, followed by that of Pierre and Marie Curie in the 40s that led to the development of single-particle shell model, along with additional work in the 50s on the collective model of Aage Bohr (son of Niels) and Ben Mottelson [1] along with Sven Nilsson's addition of single-particle features to the ever-evolving picture of collective motion in nuclei (Copenhagen School), that extended to the work of Walter Greiner and Amand Faessler teams in Germany that embraced a more robust picture of the internal dynamics as required for studies of fission and fusion processes [2], etc.

Complementary to this work on collective models and various derivatives thereof, in the late 50s, JP (Phil) Elliott [3] in England, with his then-student Malcolm Harvey, advanced the first glimpse at a roadmap that has led to the unveiling of the microscopic origin of collectivity within a nuclear shell-model framework. In short, this pioneering effort recognized and built upon the importance of the SU(3) symmetry group, which is the single-shell symmetry group of the three-dimensional harmonic oscillator (3D-HO). An extended application of this theory (see below) allows one to organize the spatial parts of many-particle nuclear configurations into a collection of Pauli-allowed shapes, which is a logical first-step of a far more robust theory for grouping many-nucleons configurations into cluster-like shell-model configurations on the lowest rung of what is now known to be an algebraically defined pyramid of deformed eigensolutions coupled through enhanced B(E2) linkages.

Through efforts within, as well as between and among these expanding schools of thought (macroscopic collective models versus microscopic shell models), were further advanced through important follow-on efforts focused on gaining a better understanding of the importance of various pairing and quasi-particle excitation modes, other algebraic theories such as the interacting boson model and various extensions to it that exposed the presence of regular patterns (simplicities) within what otherwise could have been seen as a very com-

plex (perhaps even chaotic) spectroscopy through the 70s and 80s. And in parallel with these activities, significant progress was also being made on the development of various effective interactions; namely, the building of realistic interactions. They are called realistic because all the parameters of the interaction are fitted to nucleon-nucleon scattering data. While this initiative may have at first been seen as late-to-the-game, it was and still is a very natural follow-on to the work of Elliott and his coworkers, as a provider of interactions that are well-poised to challenge any and all phenomenologies by confronting each with realistic *ab initio* Hamiltonians not biased in the direction of any preferred phenomenology. These efforts led to the development of the so-called no-core shell model (NCSM) [4–6], which was advanced in the late 90s by Bruce Barrett, Peter Navratil, and James Vary as a comprehensive, parameter-free shell-model theory for atomic nuclei. This NCSM framework was further enabled by complementary advances in high-performance computing required to validate its thesis.

What we report on below builds forward from these developments towards a symmetry-adapted version (SA-NCSM) [7–13] of the NCSM, which like its predecessor, is a fully microscopic theory, but one that takes full advantage of the dynamical symmetry group of the complete, multi-shell isotropic harmonic oscillator; namely, it is underpinned by the Sp(3,$\mathbf{R}$) symmetry group, which when restricted to a single shell reduces to Elliott's SU(3) theory. This symplectic theory [14], perhaps best understood through the work of the late David Rowe and his student George Rosensteel in the early 70s and on into the 80s and beyond, allows one to create an alternative complete shell-model theory from the ground up that implicitly and explicitly exposes the ubiquitous nature of the dominance of deformation in atomic nuclei. Specifically, this approach is a version of the SA-NCSM, called the symplectic NCSM (NCSpM) [15, 16], a theory that embraces and exploits the dynamical symmetry [Sp(3,$\mathbf{R}$)] of the 3D harmonic oscillator, which has now been shown to reproduce – typically to a 70-80 percent level in its probability distribution – the structure of atomic nuclei within a single irreducible representation (irrep) of the symplecitc group. And further, by construc-

tion automatically yields observed B(E2) values without the need for introducing an ad hoc effective charge into the theory. Each such symplectic structure is but a small fraction of the full NCSM shell-model space, which means it can be used to integrate coherent-state-like structures into the theory that is capable of reproducing observed B(E2) strengths.

It is against this synoptic review of the 20th-Century nuclear physics landscape that we now turn our attention to the singular purpose of this thesis; that is, showing for the first time – at this dawn of the 21st Century – that the NCSpM has even deeper (*ab initio*) roots than previously appreciated, roots that are part-and-parcel to a truly *ab initio* framework for a simply defined effective field theory for atomic nuclei.

2 A Historical Overview of Symmetry Groups in Nuclear Physics

During the past century, different models were developed in order to describe distinct emergent phenomena in nuclear physics. Shortly after the discovery of the nucleus [17–20] and its constituent proton and neutron, researchers thought that nuclei must be chaotic and therefore it would not be feasible to describe them within a many-body quantum mechanical framework. However, the subsequent observation of strong binding energies at specific numbers of neutrons N and protons Z called magic numbers [21], and the spins of odd mass nuclei as well as single-particle separation energies [22], led to the independent development of the nuclear shell model (SM) by Goppert-Mayer and by Haxel, Jensen, Suess [23, 24].

2.1 Nuclear Shell Model

The Shell Model (SM) is a microscopic theory, patterned in part after the atomic case that treats the nucleus as a closed core interacting with single particles in valence shells. It is formulated on the assumption that the nuclear Hamiltonian can be expressed as a sum of independent single-particle Hamiltonians augmented with a residual interaction between the nucleons. This single-particle Hamiltonian can be expressed as $h = \frac{p^2}{2\mathcal{M}} + U$ where U is the average potential that a single nucleon experiences inside the nucleus and $\mathcal{M}$ is the effective mass of the nucleon. A suitable initial choice for such a potential is one that is easily solvable analytically, for example the spherical harmonic oscillator (HO) potential $U(r) = \mathcal{M}\Omega^2 r^2/2$ where Ω is the oscillator frequency.

In order to obtain the full sequence of magic numbers associated with shell closures, it is necessary to include a single-particle spin-orbit interaction $(l \cdot s)$ that splits different l (orbital angular momentum) states into $j + 1/2$ and $j - 1/2$ (total angular momentum) states. Furthermore, one must add an additional self-interaction l^2 term to this independent particle picture with a negative strength to lower the energies of levels with higher l values relative to those with lower l [25].

Whereas this, the most elementary Shell Model picture, can be used to capture single-particle effects in nuclei, it fails to describe effects due to the collective motion of the core

such as enhanced quadrupole moments and well-developed rotational bands in heavy nuclei. In order to address these issues within a Shell Model framework, the Nilsson Model was developed [25].

2.2 Nilsson Model

The Nilsson Model is a simple mean-field theory that replaces the spherical harmonic oscillator potential with an axially deformed one. Essentially, the Nilsson Model is a deformed version of the single-particle Shell Model where $\Omega_\parallel$ (parallel to the symmetry axis) $\neq \Omega_\perp$ (perpendicular to the symmetry axis). The $\Omega_\parallel$ and $\Omega_\perp$ are chosen in a way such that $\Omega_\parallel^2 \Omega_\perp = \Omega^3$ which follows from volume conservation of the nucleus that tracks back to the incompressibility of nuclear matter. This choice of different oscillator strengths parallel and perpendicular to symmetry axis of the system lifts the degeneracy of the m (projection of j onto preferred axis) levels associated with each j value in such a way that the resulting single-particle energy levels associated with different m values fan out in regular patterns.

However, this choice for the Hamiltonian mixes j values of different single-particle states so that the Nilsson Model does not preserve rotational invariance as j is no longer a good quantum number. In applications of the Nilsson model, the only remaining good quantum number is the projection of j, m_z, on the symmetry axis. If one wants to retain a rotationally invariant Hamiltonian, which tracks to the isotropy of space, and still enjoy a Shell-Model description of nuclear structure, one has to stop treating the core as closed and move to a No-Core Shell Model (NCSM) description of nuclear phenomena [4–6, 26].

2.3 No-Core Shell Model (NCSM)

In contrast with the single-particle Shell Model picture described above, the NCSM allows for the excitation of particles out of the core. It starts with a basis of Slater determinants that has a fixed total M and M_z (total projection onto the preferred z-axis) constructed from single-particle basis states [27, 28], for example, as introduced above for the Shell Model, those of the three-dimensional harmonic oscillator. This is called the M-scheme basis. One can imagine this geometrically as carving out horizontal slices of fixed N values in the

harmonic oscillator ladder of levels. Since the Hamiltonian has to be rotationally invariant, the basis is built up from single-particle states that have good j and m quantum numbers. The Hamiltonians utilized in NCSM calculations include realistic *ab initio* interactions. The name *ab initio* implies interactions that are fit to two- and sometimes three-body phase shift scattering data along with Deuteron and Triton/^{3}He binding energies and the half-life of the Triton.

A NCSM implementation built upon an M-scheme basis, quickly runs into the so-called scale explosion problem. Because the NCSM allows for all possible configurations, the size of the basis grows combinatorially with increasing nucleon number and the number of excitations above the core that are included in the analysis, which is why one must truncate the model space at some reasonable $N_{\max}$ value, where $N_{\max}$ is the maximum number of HO excitations (quanta) allowed above the minimum required in a particular application of the theory. Fig. (2.1) is a schematic interpretation of the $N_{\max}$ cutoff: the greater the $N_{\max}$ cutoff, the more deformed structures one can describe. A robust application of the NCSM in

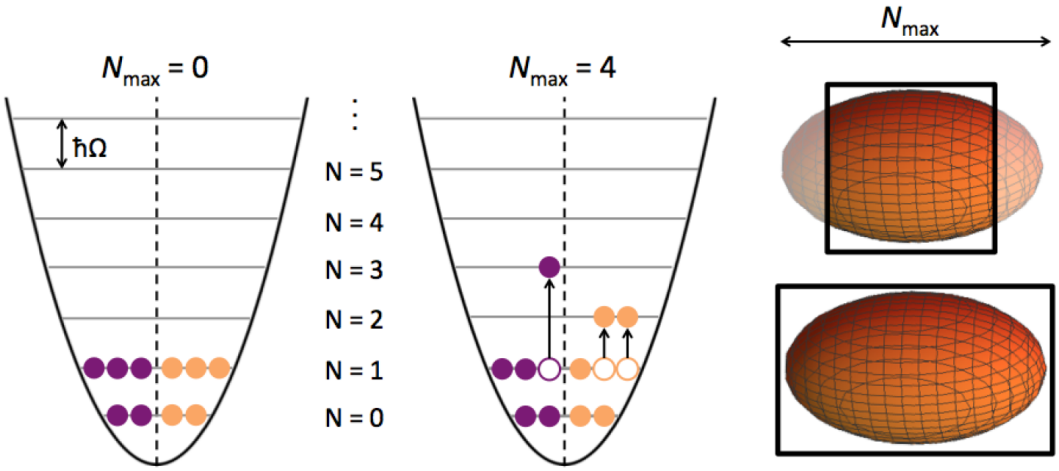

Figure 2.1. A schematic interpretation of $N_{\max}$ is shown in (a). In the $N_{\max}$=0 space, no excitations are allowed, whereas in the $N_{\max}$=4 space, all possible excitations up to and including $4\hbar\Omega$ are allowed, where Ω is the HO frequency. A pictorial rendering of $N_{\max}$ is shown in (b). A larger $N_{\max}$ allows one to probe more deformed structures, and thereby capture more physics.

an M-scheme basis on state-of-art supercomputers is currently limited to p shell nuclei [29]. Fig. (2.2) illustrates the scale-explosion issue for a Hamiltonian matrix as a function of $N_{\max}$ for several nuclei. To address current limitations of the NCSM and to be able to reproduce

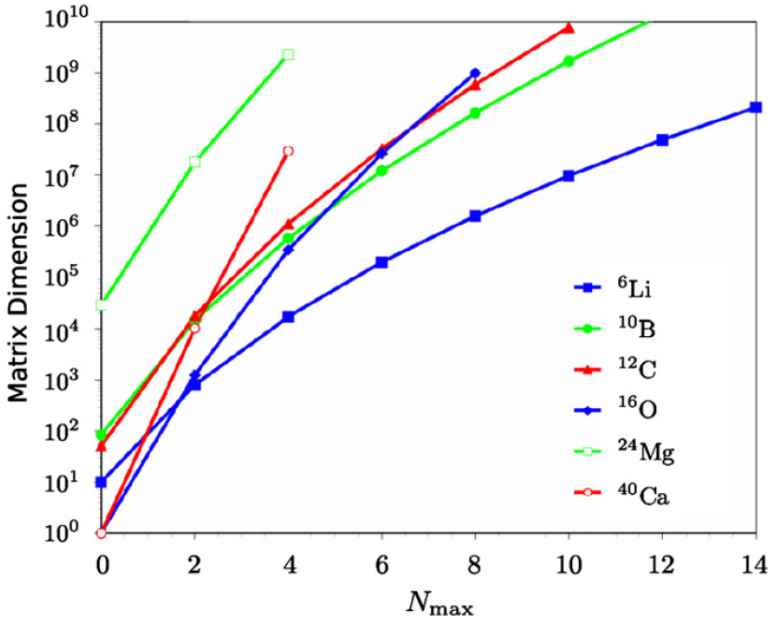

Figure 2.2. Dimension of the Hamiltonian matrix as a function of $N_{\max}$. Figure from [9].

observed collectivity in nuclei, especially strongly enhanced B(E2) transition rates between low-lying levels in nuclei, one really needs to appreciate the importance of symmetries in nuclei and the ability to reduce the complexity of the nuclear problem through their use, which has been demonstrated by our group in multiple ways [9–13].

2.4 Elliott SU(3) Model

Elliott's SU(3) Model [3] is a group theoretical construct with eight infinitesimal generators that span an SU(3) Lie algebra. These eight generators are the three antisymmetric angular momentum operators L_{ij}, which account for rotations, and five symmetric algebraic quadrupole operators Q^{a}_{ij}, that account for deformation. It is important to note that the algebraic quadrupole operators only act within an oscillator shell and they do not connect different major shells.

The SU(3) Model was the first group-theoretical model that tried to capture rotational

collectivity within a shell-model framework. One can find its roots in the Nilsson model which is a deformed version of the single-particle spherically-symmetric harmonic oscillator. Here, the deformation is achieved by adding a quadrupole-quadrupole interaction ($Q^a \cdot Q^a$) to the Hamiltonian, where Q^a is the single-shell algebraic part of the total quadrupole operator (Q). While Q reduces to Q^a within a single shell, it includes couplings to neighboring shells, couplings that are essential for building up collectivity that is required to reproduce observed strongly enhanced B(E2) strengths in nuclei.

As a result of using Q^a rather than Q, this implementation of the SU(3) symmetry underestimates B(E2) strengths, which in turn has to be compensated for by introducing effective nucleon charges. It is for similar reasons that this simplest implementation of the SU(3) scheme, which includes an L^2 term that yields the $L(L+1)$ spectrum of a rigid rotor, fails to describe the more dynamic nature of nuclear rotations which typically show some quite significant departures from a simple $L(L+1)$ rigid-rotor spectrum.

Nevertheless, SU(3) can be considered to be a quasi-dynamical symmetry of the nuclear Hamiltonian. It is not an exact symmetry because its generators do not commute with more robust Hamiltonians that attempt to incorporate other nuclear features. In particular, these include terms such as pairing and a spin-orbit interaction which couple different representations of SU(3) and therefore break the simplest SU(3) picture [30, 31], but this mixing/breaking of SU(3) does not seem to overpower the strong coherence that is found within SU(3) rotational bands. Indeed, it is this feature that gives rise to the quasi-dynamical symmetry concept [32, 33]. It is the simple SU(3) model of Elliott that proved to be crucial in gaining an understanding of why deformed equilibrium states favor maximal spacial symmetry within a shell model framework, and further, underpins the development of the Symplectic Sp(3,$\mathbf{R}$) Model, which in its simplest form is a multi-shell generalization of the Elliott SU(3) model that provides a much better platform for advance nuclear structure studies.

2.5 Symplectic Model

The Sp(3,$\mathbf{R}$) symmetry group [14, 34], like SU(3), is a quasi-dynamical symmetry of the Hamiltonian. However, it extends the simplest Elliott SU(3) picture by including the physical quadrupole operator Q_{ij} rather than the more restricted algebraic Q^a_{ij} one so that the action is not limited to a single-shell picture but incorporates couplings to the neighboring HO shells. In addition to the three angular momentum operators L_{ij} and six mass quadrupole operators Q_{ij}, the Sp(3,$\mathbf{R}$) also includes six symmetric vorticity operators S_{ij}, which can describe irrotational flow in nuclei, and six symmetric kinetic energy operators K_{ij}. Altogether these 21 generators form a Lie algebra of the symplectic group Sp(3,$\mathbf{R}$). It is the group of all possible real linear transformations of a nucleon's six position ($q_{i\mathrm{n}}$) and linear momentum ($p_{i\mathrm{n}}$) coordinates, such that the overarching Heisenberg algebra is preserved:

$$[q_{i\mathrm{n}}, p_{j\mathrm{n}}] = \iota\hbar\delta_{ij}, \tag{2.1}$$

where i, j=1,2,3 denote the three spatial directions z, x and y, n denotes the n-th nucleon and ι is the imaginary number. The generators of the Sp(3,$\mathbf{R}$) algebra are expressed in the following way

$$\begin{aligned} Q_{ij} &= \sum_{\mathrm{n}}^{\mathcal{A}} q_{i\mathrm{n}} q_{j\mathrm{n}}, \\ K_{ij} &= \sum_{\mathrm{n}}^{\mathcal{A}} p_{i\mathrm{n}} p_{j\mathrm{n}}, \\ L_{ij} &= \sum_{\mathrm{n}}^{\mathcal{A}} \left(q_{i\mathrm{n}} p_{j\mathrm{n}} - q_{j\mathrm{n}} p_{i\mathrm{n}} \right), \\ S_{ij} &= \sum_{\mathrm{n}}^{\mathcal{A}} \left(q_{i\mathrm{n}} p_{j\mathrm{n}} + p_{i\mathrm{n}} q_{j\mathrm{n}} \right), \end{aligned} \tag{2.2}$$

where $\mathcal{A}$ is the total number of nucleons. It is also possible to express this set of generators in terms of the raising and lowering HO ladder operators $b^+_{i\mathrm{n}}$ and $b^-_{i\mathrm{n}}$ where the former creates the n-th nucleon in the i-th direction and the latter annihilates one. These operators are

defined as follows:

$$q_{i\mathrm{n}} = (b^{+}_{i\mathrm{n}} + b^{-}_{i\mathrm{n}})/\sqrt{2},$$
$$p_{i\mathrm{n}} = \iota(b^{+}_{i\mathrm{n}} - b^{-}_{i\mathrm{n}})/\sqrt{2}, \tag{2.3}$$

where the oscillator length $\sqrt{\hbar/m\Omega}$ is taken as unity for simplicity. From a structure perspective, the 21 generators of Sp(3,R) span the space of all independent operators that are quadratic in the system's momentum and coordinate variables. These can be rearranged into 6 $2\hbar\omega$ raising operators with SU(3) tensor character (2,0) and the conjugate 6 $2\hbar\omega$ lowering operators with SU(3) tensor character (0,2), plus 9 other $0\hbar\omega$ horizontal operators that are generators of the compact (finite-dimensional) U(3) subalgebra of Sp(3,$\mathbf{R}$), that can be further reduced into the eight generators of SU(3), with SU(3) tensor character (1,1), and another single operator with SU(3) tensor character (0,0) that is an operator that counts the total number of oscillator quanta at any level within the symplectic irrep. Then, the symplectic generators could be expressed as

$$Q_{ij} = Q^{a}_{ij} + A_{ij} + B_{ij},$$
$$K_{ij} = Q^{a}_{ij} - A_{ij} - B_{ij},$$
$$L_{ij} = -\iota(C_{ij} - C_{ji}),$$
$$S_{ij} = 2\iota(A_{ij} - B_{ij}), \tag{2.4}$$

where the following operators

$$A_{ij} = \frac{1}{2}\sum_{\mathrm{n}}^{\mathcal{A}} b_{i\mathrm{n}}^{+} b_{j\mathrm{n}}^{+},$$
$$B_{ij} = \frac{1}{2}\sum_{\mathrm{n}}^{\mathcal{A}} b_{i\mathrm{n}}^{-} b_{j\mathrm{n}}^{-},$$
$$C_{ij} = \frac{1}{2}\sum_{\mathrm{n}}^{\mathcal{A}} (b_{i\mathrm{n}}^{+} b_{j\mathrm{n}}^{-} + b_{j\mathrm{n}}^{-} b_{i\mathrm{n}}^{+}), \tag{2.5}$$

are the symplectic operators. All the operators mentioned above are written in their Cartesian representation.

One can also cast them as spherical tensors $A^{(2,0)}_{L_0M_0}$ [35]. For A_{ij} we have

$$A_{xx} = \frac{1}{2\sqrt{2}}(A^{(2,0)}_{2+2} + \frac{2}{\sqrt{3}}A^{(2,0)}_{00} - \frac{2}{\sqrt{6}}A^{(2,0)}_{20} + A^{(2,0)}_{2-2}),$$
$$A_{yy} = -\frac{1}{2\sqrt{2}}(A^{(2,0)}_{2+2} - \frac{2}{\sqrt{3}}A^{(2,0)}_{00} + \frac{2}{\sqrt{6}}A^{(2,0)}_{20} + A^{(2,0)}_{2-2}),$$
$$A_{zz} = \frac{1}{\sqrt{6}}A^{(2,0)}_{00} + \frac{1}{\sqrt{3}}A^{(20)}_{20},$$
$$A_{xy} = -\frac{\iota}{2\sqrt{2}}(A^{(2,0)}_{2+2} - A^{(2,0)}_{2-2}),$$
$$A_{xz} = -\frac{1}{2\sqrt{2}}(A^{(2,0)}_{2+1} - A^{(2,0)}_{2-1}),$$
$$A_{yz} = \frac{\iota}{2\sqrt{2}}(A^{(2,0)}_{2+1} + A^{(2,0)}_{2-1}). \tag{2.6}$$

The above transformations are identical for B_{ij} since $B_{ij} = A^{+}_{ij}$ and therefore

$$B^{(0,2)}_{L_0M_0} = (-1)^{L_0-M_0}(A^{(2,0)}_{L_0-M_0})^{+}. \tag{2.7}$$

As for C_{ij} we have

$$
\begin{aligned}
C_{xx} &= \frac{1}{2\sqrt{2}}(C^{(1,1)}_{2+2} - \frac{2}{\sqrt{6}}C^{(1,1)}_{20} + C^{(1,1)}_{2-2}) + \frac{1}{3}C^{(0,0)}_{00}, \\
C_{yy} &= -\frac{1}{2\sqrt{2}}(C^{(1,1)}_{2+2} + \frac{2}{\sqrt{6}}C^{(1,1)}_{20} + C^{(1,1)}_{2-2}) + \frac{1}{3}C^{(0,0)}_{00}, \\
C_{zz} &= \frac{1}{3}C^{(0,0)}_{00} + \frac{1}{\sqrt{3}}C^{(1,1)}_{20}, \\
C_{xy} &= -\frac{\iota}{2\sqrt{2}}(C^{(1,1)}_{2+2} - C^{(1,1)}_{2-2} - \sqrt{2}C^{(1,1)}_{10}), \\
C_{yx} &= -\frac{\iota}{2\sqrt{2}}(C^{(1,1)}_{2+2} - C^{(1,1)}_{2-2} + \sqrt{2}C^{(1,1)}_{10}), \\
C_{xz} &= -\frac{1}{2\sqrt{2}}(C^{(1,1)}_{2+1} - C^{(1,1)}_{2-1} - C^{(1,1)}_{1+1} - C^{(1,1)}_{1-1}), \\
C_{zx} &= -\frac{1}{2\sqrt{2}}(C^{(1,1)}_{2+1} - C^{(1,1)}_{2-1} + C^{(1,1)}_{1+1} + C^{(1,1)}_{1-1}), \\
C_{yz} &= \frac{\iota}{2\sqrt{2}}(C^{(1,1)}_{2+1} + C^{(1,1)}_{2-1} - C^{(1,1)}_{1+1} + C^{(1,1)}_{1-1}), \\
C_{zy} &= \frac{\iota}{2\sqrt{2}}(C^{(1,1)}_{2+1} + C^{(1,1)}_{2-1} + C^{(1,1)}_{1+1} - C^{(1,1)}_{1-1}).
\end{aligned} \tag{2.8}
$$

Using the definitions above in Eqs. (2.6), (2.8), and (2.4), it is easy to identify the following SU(3) tensors

$$
\begin{aligned}
\sum_i C_{ii} &= C^{(0,0)}_{00} = \frac{\mathrm{HO}}{\hbar\Omega}, \\
C^{(1,1)}_{10} &= L_{10} = L, \\
Q_{00} &= \sum_i (A_{ii} + B_{ii} + C_{ii}) = \frac{\mathrm{HO}}{\hbar\Omega} + \sqrt{\frac{3}{2}}(A^{(2,0)}_{00} + B^{(0,2)}_{00}), \\
Q_{2M} &= \sqrt{3}(A^{(2,0)}_{2M} + B^{(0,2)}_{2M} + C^{(1,1)}_{2M}),
\end{aligned} \tag{2.9}
$$

where HO is the harmonic oscillator Hamiltonian (the number operator), $Q_{00} = r^2$ is the monopole operator and Q_{2M} is the quadrupole operator. One could also express them in terms of fermion creation and annihilation operators [36].

It should be clear from the above discussion that unlike the Elliott SU(3) Model which

is a 'compact' algebraic theory with basis states that are confined to a single HO shell, the Symplectic Model is a 'non-compact' algebraic theory, with basis states that are infinite in number because its defining algebra structure includes raising operators (A_{ij}) that add (create) a pair of HO quanta to the system as well as lowering (B_{ij}) operators that subtract (annihilate) a pair of HO quanta from the system, in addition to the subset of generators L_{ij} and Q^a_{ij} of the Elliott SU(3) algebra that only act within a single HO shell. This hierarchical structure is a key feature of the theory that can be used to parse the entire (infinite) HO shell-model space into a collection of symplectic subspaces (each of which is itself infinite in size).

2.6 No-Core Symplectic Shell Model (NCSpM)

As suggested above, the Symplectic Model is a multi-shell extension of the Elliott SU(3) Model. All states within a Sp(3,**R**) representation are labeled by a common set of three quantum numbers $N_\sigma(\lambda_\sigma, \mu_\sigma)$. These are associated with the subset of all states within a symplectic representation that are annihilated by a single application of any of the B_{ij} lowering operators; and secondly, the two SU(3) quantum numbers (λ, μ) that are uniquely defined by the so-called SU(3) lowest-weight (bandhead) configuration with respect to shifts of quanta between and among the three spatial (z, x and y) directions by the generators C_{ij} of SU(3) acting within the n-th shell of the HO. In short, the λ and μ labels of the Elliott SU(3) Model along with N serve as a common label for all states within a symplectic representation - all states can be generated by applying the shift operators of SU(3) for states within a shell and the A_{ij} raising operators enables one to reach states that make up the next higher rung of states within that symplectic representation, and so on. It is interesting to note that a $(\lambda = N_z - N_x, \mu = N_x - N_y) = (0,0)$ state denotes a spherical shape, while $(\lambda,0)$ has a prolate shape, and $(0,\mu)$ signals an oblate shape, see Fig. (2.3). N_i denotes the total number of oscillator quanta in the i-th direction. It is because of this underlying hierarchical structure that a $N_\sigma(\lambda_\sigma, \mu_\sigma)$ set is used to tag each and every Sp(3,**R**) state with the parent equilibrium deformation of its simplest state, the Sp(3,**R**)$\supset$SU(3)

bandhead configuration. (Here the index σ is added to label bandhead configurations). The mathematical construction of the basis states within one symplectic irrep is as follows: First identify the bandhead configuration $|\sigma\rangle$ of a given nucleus which is the lowest energy configuration of $\mathcal{A}$ nucleons allowed by the Pauli principle within the oscillator structure and then apply on it with A_{ij}, or $A^{(2,0)}$ its SU(3) tensor form, in such a way that we first create excitation quanta in z then x and then y directions in that order (this is done for convenience where z is the preferred direction over x, and x over y, a, without loss of generality) which results to generating six new states

$$(2,0,0)\otimes(n_z,n_x,n_y) = (n_z+2,n_x,n_y)\oplus(n_z+1,n_x+1,n_y)\oplus(n_z+1,n_x,n_y+1)$$
$$\oplus(n_z,n_x+2,n_y)\oplus(n_z,n_x+1,n_y+1)\oplus(n_z,n_x,n_y+2). \tag{2.10}$$

In terms of SU(3) coupled products the above equation becomes [37]

$$(2,0)\otimes(\lambda_\sigma,\mu_\sigma) = (\lambda_\sigma+2,\mu_\sigma)\oplus(\lambda_\sigma,\mu_\sigma+1)\oplus(\lambda_\sigma+1,\mu_\sigma-1)\oplus$$
$$(\lambda_\sigma-2,\mu_\sigma+2)\oplus(\lambda_\sigma-1,\mu_\sigma)\oplus(\lambda_\sigma,\mu_\sigma-2). \tag{2.11}$$

If we continue this process on the resulting states we will create all possible states within an irrep spanning to infinity. However for purposes of carrying out calculations we have to stop at some $N_{\max}$. The complete labeling of a sympletic basis state that is constructed from its $|\sigma\rangle$ bandhead irrep is $|\sigma n\rho\omega\kappa LM\rangle$ where $\sigma \equiv N_\sigma(\lambda_\sigma\mu_\sigma)$ labels the bandhead as discussed, $n \equiv N_n(\lambda_n\mu_n)$ labels the excited state that coupled to the bandhead yields the final configuration labeled by $\omega \equiv N_\omega(\lambda_\omega\mu_\omega)$ with ρ multiplicity, L angular momentum with κ multiplicity and its M projection. A schematic demonstration of this is as follows

$$|\sigma n\rho\omega\kappa LM\rangle = [[A^{(2,0)}\times A^{(2,0)}\times A^{(2,0)}\times\cdots\times A^{(2,0)}]^n|\sigma\rangle]^{\rho\omega}_{\kappa LM}. \tag{2.12}$$

The underlying symmetry groups associated with each set of quantum numbers are

$$Sp(3,\mathbf{R}) \supset U(3) \supset SO(3) \supset SO(2). \qquad (2.13)$$
$$\sigma \quad n\rho \quad \omega \quad \kappa \quad L \quad M$$

This symmetry group chain clearly illustrates the resulting states from applying the operators to every non-closed valence shell that is included in the U(3)⊃SU(3)⊃SO(3) reduction which illustrates the symmetry group chain of a single-shell of the 3D-HO and its dynamical extension to the symmetry group, Sp(3,**R**) of the 3D-HO as a whole [14]. And since U(3)⊃SU(3)⊃SO(3) is a compact subgroup structure with finite-dimensional irreps, while Sp(3,**R**) is a noncompact group with infinite-dimensional irreps, one can see how this 'oscillator as a whole' formulation takes one from a compact SM picture to a bonified NCSM theory. As we will see ahead, this feature can also be used to help address the explosive growth issue that has plagued our field for decades, while at the same time eliminating the need for introducing an effective charge into the theory.

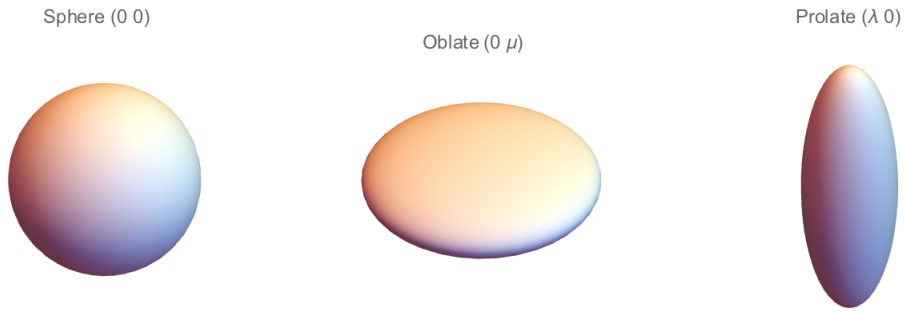

Figure 2.3. A geometrical depiction of three special bandhead configurations.

From this it should be clear that the full shell-model space for a particular application can be parsed into a collection of symplectic representations that in aggregate spans the entire space. This also means that within the NCSpM picture the shell model space can be build up in a very systematic way; namely, the symplectic basis parses the entire HO basis into vertical slices that are built upon the lowest allowed harmonic oscillator energy with a given (λ, μ) deformed state, the so-called bandhead configuration. In particular, all states

at the bandhead level can be generated by applications of the SU(3) raising operators, while jumps up a level can be reached by applying the symplectic raising operators, with each such application moving one up to the next higher plateau, etc., see Fig. (2.4).

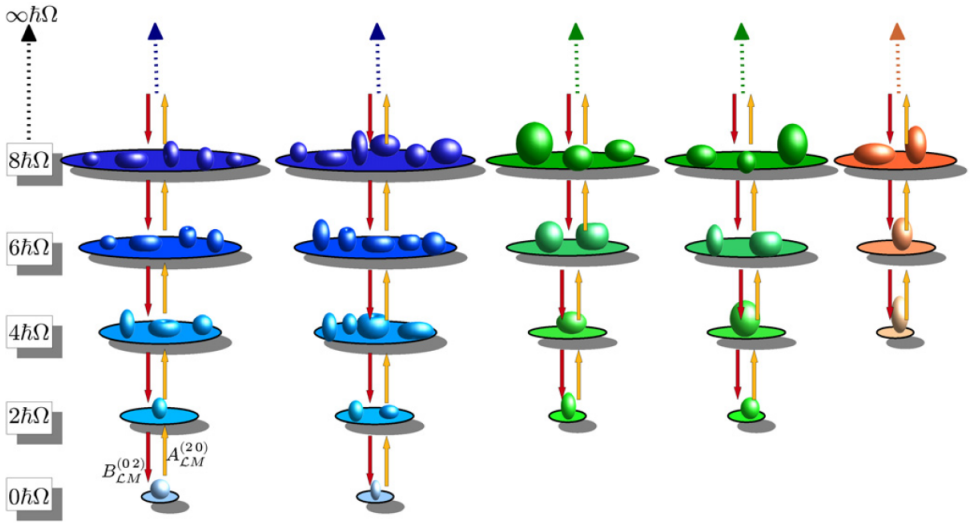

Figure 2.4. A schematic illustration of a symplectic basis (vertical slice) in terms of HO basis states (horizontal slices) for 0p-0h configuration (blue), 2p-2h (green) and 4p-4h (orange). Each ellipsoid corresponds to a given deformation of the nucleus described by (λ, μ). One ellipsoid can be derived from the other by the symplectic operators shown in their spherical tensor forms. Figure from [9].

However, it is important to realize that in a many-particle generalization of the single-particle picture there are very important additional considerations that must be addressed. Specifically, in a many-particle framework there is always the possibility of exciting correlated clusters of nucleons. In going from the single-particle shell model to its many-particle generalization this feature is addressed through the addition of so-called particle-hole excitations to the picture, and more specifically n-particle-n-hole (np-nh) excitations to the overall landscape, with n greater than or equal to 1. Consistent with this, but still within the framework of a single-particle picture, the symplectic raising/lowering operators introduced above are examples of 1p-1h excitations that add/subtract 2 quanta to/from the system (2 being the minimum required to insure parity conservation). Other multi-particle-multi-hole excitations are not a natural part of the symplectic picture; they must be introduced by hand.

(As this same complication applies to the many-particle generalization of the single-particle model, and guidance for dealing with it carries forward from how it is addressed in that case, inclusive of any and all associated antisymmetrization requirements that must be respected because one is dealing with fermions and not bosons.) The good news of this story is that this complication can be dealt within the symplectic picture as it is dealt with in advancing from the single-particle picture to the many-particle framework, through the inclusion of only independent np-nh bandhead configurations in addition to the ones generated from symplectic excitations to ensure one spans the entire space.

Now that we understand how the NCSpM space is built, we will proceed with a step-by-step guide on how to calculate the matrix elements of the symplectic operators; namely, $A^{(2,0)}_{L_0M_0}$ and $C^{(1,1)}_{L_0M_0}$ where $L_0 = 0, 2$ for A, and $L_0 = 0, 1, 2$ for C. We are going to use their SU(3) spherical tensor forms since the available analytic matrix elements are given for SU(3) tensors. As for $B^{(0,2)}_{L_0M_0}$ it is simply given in Eq. (2.7).

The matrix element of $\langle f| A^{(2,0)}_{L_0M_0} |i\rangle$ between an initial state i and a final state f is given by

$$\langle \sigma n_f \rho_f \omega_f \kappa_f L_f M_f| A^{(2,0)}_{L_0M_0} |\sigma n_i \rho_i \omega_i \kappa_i L_i M_i\rangle = C^{L_fM_f}_{L_iM_i,L_0M_0} \times$$
$$\left\langle (\lambda_{\omega_i}, \mu_{\omega_i})\kappa_i L_i, (2,0)L_0 \middle| (\lambda_{\omega_f}, \mu_{\omega_f})\kappa_f L_f \right\rangle \langle \sigma n_f \rho_f \omega_f| \,|A^{(2,0)}|\, |\sigma n_i \rho_i \omega_i\rangle \,, \tag{2.14}$$

where $\left\langle (\lambda_{\omega_i}, \mu_{\omega_i})\kappa_i L_i, (2,0)L_0 \middle| (\lambda_{\omega_f}, \mu_{\omega_f})\kappa_f L_f \right\rangle$ is the SU(3)$\supset$SO(3) Clebsch-Gordon coefficient [38, 39], $C^{L_fM_f}_{L_iM_i,L_0M_0}$ is the SO(3)$\supset$SO(2) Clebsch-Gordon coefficient, and

$$\langle \sigma n_f \rho_f \omega_f| \,|A^{(2,0)}|\, |\sigma n_i \rho_i \omega_i\rangle = (-1)^{\lambda_{\omega_f}+\mu_{\omega_f}-\lambda_{\omega_i}-\mu_{\omega_i}} \sqrt{F(\sigma n_f \omega_f) - F(\sigma n_i \omega_i)}\, \langle n_f| \,|A|\, |n_i\rangle \times$$
$$U\big((\lambda_\sigma, \mu_\sigma)(\lambda_{n_i}, \mu_{n_i})(\lambda_{\omega_f}, \mu_{\omega_f})(2,0); (\lambda_{\omega_i}, \mu_{\omega_i})\rho_i(\lambda_{n_f}, \mu_{n_f})\rho_f\big), \tag{2.15}$$

is the matrix element of $A^{(2,0)}$ reduced with respect to SU(3) [37, 40]. U is the SU(3) Racah coefficient [38, 39] and $\langle n_f| \,|A|\, |n_i\rangle$ (the second pair of bars reflects the reduction in respect

to SU(3) and shouldn't be confused with absolute value) is

$$\langle n_f|\,|A|\,|n_i\rangle = \sqrt{\frac{(n_z+4)(n_z-n_x+2)(n_z-n_y+3)}{2(n_z-n_x+3)(n_z-n_y+4)}}\delta_{n_{z_i}+2,n_z}\delta_{n_{x_i},n_{x_f}}\delta_{n_{y_i},n_{y_f}}+$$
$$\sqrt{\frac{(n_x+3)(n_z-n_x)(n_z-n_y+2)}{2(n_z-n_x-1)(n_x-n_y+3)}}\delta_{n_{z_i},n_z}\delta_{n_{x_i}+2,n_{x_f}}\delta_{n_{y_i},n_{y_f}}+$$
$$\sqrt{\frac{(n_y+2)(n_x-n_y)(n_z-n_y+1)}{2(n_z-n_y)(n_x-n_y-1)}}\delta_{n_{z_i},n_z}\delta_{n_{x_i},n_{x_f}}\delta_{n_{y_i}+2,n_{y_f}}. \tag{2.16}$$

As for the $F(\sigma n_f\omega_f)$ function in Eq. (2.15) it is given by

$$F(\sigma n\omega) = \frac{1}{4}\Big(2(\omega_z^2+\omega_x^2+\omega_y^2)-(n_z^2+n_x^2+n_y^2)+4\omega_z-4\omega_y-6n_z-4n_x-2n_y\Big). \tag{2.17}$$

Similar to $\langle f|\,A^{(2,0)}_{L_0M_0}\,|i\rangle$ the matrix elements of $\langle f|\,C^{(1,1)}_{L_0M_0}\,|i\rangle$ are given by

$$\langle \sigma n_f\rho_f\omega_f\kappa_f L_fM_f|\,C^{(1,1)}_{L_0M_0}\,|\sigma n_i\rho_i\omega_i\kappa_i L_iM_i\rangle = C^{L_fM_f}_{L_iM_i,L_0M_0}\times$$
$$\Big\langle(\lambda_{\omega_i},\mu_{\omega_i})\kappa_iL_i,(1,1)L_0\Big|(\lambda_{\omega_f},\mu_{\omega_f})\kappa_fL_f\Big\rangle\,\langle\sigma n_f\rho_f\omega_f|\,|C^{(1,1)}|\,|\sigma n_i\rho_i\omega_i\rangle\,, \tag{2.18}$$

where similarly to the raising operator A, $\langle\sigma n_f\rho_f\omega_f|\,|C^{(1,1)}|\,|\sigma n_i\rho_i\omega_i\rangle$ [41] is given by

$$\langle\sigma n_f\rho_f\omega_f|\,|C^{(1,1)}|\,|\sigma n_i\rho_i\omega_i\rangle = \begin{cases}(-1)^\psi\frac{2}{\sqrt{3}}(\lambda_\omega^2+\mu_\omega^2+\lambda_\omega\mu_\omega+3\lambda_\omega+3\mu_\omega)\delta_{n_fn_i}\delta_{\omega_f\omega_i}, & \text{if } \rho{=}1\\ 0. & \text{if } \rho\neq 1\end{cases} \tag{2.19}$$

The phase in the above equation is $(-1)^\psi = 1$ if $\mu = 0$ and $(-1)^\psi = -1$ if $\mu \neq 0$.

Continuing with the earlier discussion, we see that the introduction of the symplectic concept enables one to identify which deformed configurations within a horizontal slice are more important than others, and this in turn enables one to exclude those that are expected to contribute less to the overall physics and in so doing gain huge savings in computational memory and time. As an important example, we note the ability of the NCSpM to reproduce the low lying spectrum of ^{12}C. It has been identified that the ground state can be described by

the $(0,4)$ symplectic irrep. The second excited state was identified to be a 2p-2h configuration that belongs to $(6,2)$ irrep. As for the Hoyle state in ^{12}C, which is the first excited 0^+ state that is believed to be a 4p-4h configuration, can be described by the $(12,0)$ irrep, with an energy of about 7.65 MeV relative to the ground state, that falls below the 2p-2h configuration due to the interaction preffering a more prolate shape, demonstrated by Dreyfuss et al. [15]. Specifically, by using a schematic interaction made out of symplectic generators given by

$$H_\gamma = \hbar\Omega \sum_i C_{ii} + \frac{\hbar\Omega}{8\gamma N_a}(e^{-\gamma(Q\cdot Q - <Q\cdot Q>_{N_n})} - 1), \tag{2.20}$$

where $\gamma = 1.7 \times 10^{-4}$ and $N_a = \sqrt{N_{\omega_f} N_{\omega_i}}$ is the geometrical average of the number of bosons between the initial and final states. As for $Q \cdot Q$, it is the scalar product of the quadrupole operator defined in Eq. (2.9) and $< Q \cdot Q >_{N_n}$ is the average (monopole) contribution of $Q \cdot Q$ within the subspace of N_n HO excitations called the centroid term [42], that is, the trace of $Q \cdot Q$ divided by the space dimension for a fixed N_n. This monopole part of the $Q \cdot Q$ interaction is considerably large and majorly affects the energy of the HO shells. Hence, its subtraction helps preserve the HO-based mean field, while retaining the $Q \cdot Q$-driven behavior of the wave functions. Furthermore, [15] implemented a spin-orbit mixing term that mixes symplectic irreps at the bandhead level between $(0,4)$ and $(1,2)$. Using this interaction, the authors were successful in obtaining a Hoyle-like state, which agreed with the experimental value, Fig. (2.5), within a model space of $N_{\max}$=20 using the NCSpM. This would have been impossible within the NCSM without utilizing any symmetries.

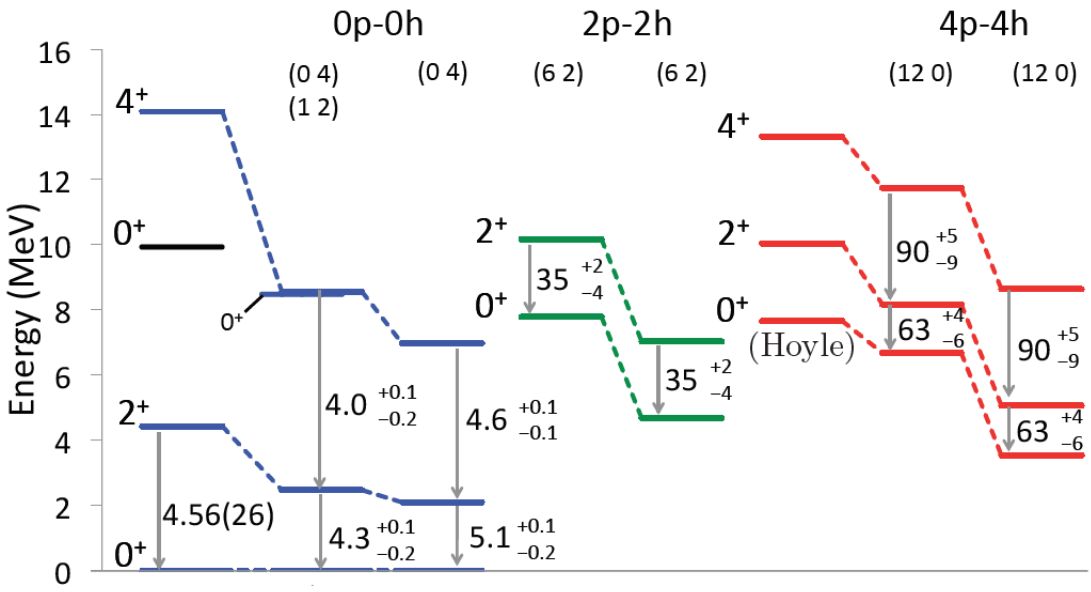

Figure 2.5. Low-lying spectrum and B(E2) values in W.u. of ^{12}C within NCSpM with spin-orbit mixing (second set) and without (third set) vs the experimental values. Figure from [43].

3 Deformed No-Core Symplectic Shell Model (DNCSpM)

In this chapter we summarize the work published in [44, 45]. We present how one can utilize the underlying deformation of nuclei to our own advantage by constructing deformed basis states, which in turn can be used to describe the same physics that in a non-deformed basis requires huge model spaces, in much smaller ones, and in so doing significantly reduce the overall computational complexity. The overarching scientific objective is to use this strategy to probe more deeply into the (*ab initio*) structure of light and heavy nuclei, short cutting a need to await the availability of more robust computational resources for advanced nuclear structure investigations.

This problem could be tackled in two ways, both of which are identical and are described in detail in this chapter. The first approach is to deform the symplectic algebra through canonical transformations and build a mirror deformed symplectic algebra, hence the name (DNCSpM). This allows us to express a given symplectic operator in terms of their deformed counterparts which then can be diagonalized in a deformed basis. The second approach is carried out by constructing the deformation into the single particle harmonic oscillator basis states and later calculating overlaps between deformed and non-deformed states by providing analytic results for transformation coefficients between spherical, cylindrical and Cartesian basis states of the 3D-HO. So while our interest in these expressions is driven by our need for them in nuclear physics studies, they can be invoked whenever and wherever the 3D-HO comes into play. Such applications include studies of coupled oscillators [46], the interaction of coherent and squeezed states with different frequencies [47], the construction of a deformed effective field theory [48], as well as for gaining a better understanding of how damped oscillators interact [49].

Parts of this chapter was previously published as D. Kekejian, J. P. Draayer, and K. D. Launey. Symmetries and canonical transformations in nuclei. AIP Conference Proceedings, 2150(1):040002, 2019.

3.1 Unitary Canonical Transformations of the Sp(3,R) Algebra

Classically, canonical transformations are transformations that preserve the Poisson brackets between the coordinates and momenta

$$\{q_i, p_j\} = \{\widetilde{q_i}, \widetilde{p_j}\} = \delta_{ij}. \tag{3.1}$$

This definition can be generalized for the quantum mechanical case as a transformation that preserves the commutation relation between the coordinate and momentum operators

$$[q_i, p_j] = [\widetilde{q_i}, \widetilde{p_j}] = \iota\hbar\delta_{ij}. \tag{3.2}$$

Further, in classical mechanics, a canonical transformation is a unitary transformation. However, this is not necessarily the case for the quantum case [50]. In quantum mechanics, a canonical transformation can be unitary or non-unitary [51, 52]. For constructing the deformed basis, we will limit ourselves to unitary transformations.

Now we define the following unitary canonical transformations

$$\begin{aligned} \widetilde{q_i} &= \frac{1}{\sqrt{\epsilon_i}} q_i, \\ \widetilde{p_i} &= \sqrt{\epsilon_i} p_i, \end{aligned} \tag{3.3}$$

where "$\sim$" denotes the quantities in the canonical space and ϵ_i is the transformation parameter which is a real positive quantity $\neq 0$. The physical implication of ϵ depends on the system that we study. If we choose $\epsilon_i = \Omega/\Omega_i$ then ϵ_i could be interpreted as a deformation parameter that transforms the non-deformed canonical set (q_i, p_i) into the deformed canonical set $(\widetilde{q_i}, \widetilde{p_i})$. While the isotropy of space is commonly invoked, which implies equal oscillator lengths in the three (x, y and z) directions, for many applications this is not an optimal choice since deformation often dominates the dynamics for example, in nuclear physics deformation dominates in nearly all cases, therefore it is best to incorporate deformation into the

picture from the onset. It is done under a constant volume constraint, which means $\Omega_x\Omega_y\Omega_z = \Omega^3$. This constraint has applications in deformed HO models that study equipotential surfaces [53] and is a direct implication of the incompressibility of nuclear matter [25].

The canonical transformations above not only preserve the Heisenberg algebra, but they also preserve the symplectic algebra [54]. This means that the commutation relations between all of the symplectic generators in the deformed space is the same as in the non-deformed space and the deformed symplectic algebra closes. Since the symplectic generators could be expressed in terms of raising and lowering operators, one needs to define the deformed equivalent of those operators in such a way that the symplectic and its underlying Heisenberg algebra are preserved. To do this we define the deformed operators as

$$\begin{aligned}\widetilde{b^+_{i\mathrm{n}}} &= \frac{1}{2}\Big(\frac{1}{\sqrt{\epsilon_i}}\big(b^+_{i\mathrm{n}} + b^-_{i\mathrm{n}}\big) + \sqrt{\epsilon_i}\big(b^+_{i\mathrm{n}} - b^-_{i\mathrm{n}}\big)\Big),\\ \widetilde{b^-_{i\mathrm{n}}} &= \frac{1}{2}\Big(\frac{1}{\sqrt{\epsilon_i}}\big(b^+_{i\mathrm{n}} + b^-_{i\mathrm{n}}\big) - \sqrt{\epsilon_i}\big(b^+_{i\mathrm{n}} - b^-_{i\mathrm{n}}\big)\Big).\end{aligned} \tag{3.4}$$

It is easy to see that the canonical transformations in Eq. (3.4) are equivalent to Eq. (3.3) therefore

$$[b^-_{i\mathrm{n}}, b^+_{j\mathrm{n}}] = [\widetilde{b^-_{i\mathrm{n}}}, \widetilde{b^+_{j\mathrm{n}}}] = \delta_{ij}, \tag{3.5}$$

which are equivalent to Eq. (3.2). The canonical transformations defined in Eq. (3.4) are symmetric with respect to the inverse transformations. The inverse transformations could be achieved if one does the following $O \to \widetilde{O}$, $\frac{1}{\sqrt{\epsilon_i}} \to \sqrt{\epsilon_i}$ and $\sqrt{\epsilon_i} \to \frac{1}{\sqrt{\epsilon_i}}$. To demonstrate this let us apply this procedure of inverse transformation on Eq. (3.4). Move $\sim$ by $(\widetilde{q_i} \to q_i, \widetilde{p_i} \to p_i)$, then flip the coefficients $\frac{1}{\sqrt{\epsilon_i}} \to \sqrt{\epsilon_i}$, $\sqrt{\epsilon_i} \to \frac{1}{\sqrt{\epsilon_i}}$ and we will get

$$\begin{aligned}q_i &= \sqrt{\epsilon_i}\widetilde{q_i},\\ p_i &= \frac{1}{\sqrt{\epsilon_i}}\widetilde{p_i},\end{aligned} \tag{3.6}$$

which are the inverse transformations. The fact that the canonical transformations are

symmetric in respect to an inverse transformation suggests that the canonical sets (q_i, p_i) and $(\widetilde{q_i}, \widetilde{p_i})$ are mathematically equivalent. The fact that we chose to call the former set non-deformed and the latter deformed is purely formal and is done for clarity. This is also evident from the observation that the canonical transformations defined above are unitary. However, the physical significance of those transformations come from the fact that one could represent the canonical set (q_i, p_i), defined in an infinite phase space through mapping it onto a canonical set $(\widetilde{q_i}, \widetilde{p_i})$ that is defined in a finite phase space which could be achieved by a careful selection of the deformation parameters ϵ_{i}.

In order to demonstrate this let us first define the deformed equivalent of the symplectic operators given in Eq. (2.5) as

$$\begin{aligned}
\widetilde{A_{ij}} &= \frac{1}{2}\sum_{\mathrm{n}}^{\mathcal{A}} \widetilde{b_{i\mathrm{n}}^{+}}\widetilde{b_{j\mathrm{n}}^{+}}, \\
\widetilde{B_{ij}} &= \frac{1}{2}\sum_{\mathrm{n}}^{\mathcal{A}} \widetilde{b_{i\mathrm{n}}^{-}}\widetilde{b_{j\mathrm{n}}^{-}}, \\
\widetilde{C_{ij}} &= \frac{1}{2}\sum_{\mathrm{n}}^{\mathcal{A}} (\widetilde{b_{i\mathrm{n}}^{+}}\widetilde{b_{j\mathrm{n}}^{-}} + \widetilde{b_{j\mathrm{n}}^{-}}\widetilde{b_{i\mathrm{n}}^{+}}).
\end{aligned} \tag{3.7}$$

By plugging Eq. (3.4) into Eq. (3.7), using the fact that $B_{ij} = A_{ij}^{+}$, $C_{ij} = C_{ji}^{+}$ and that the same holds for their deformed equivalents, one would get a relationship between the

deformed and non-deformed symplectic operators

$$
\begin{aligned}
\widetilde{A_{ij}} &= \frac{1}{4}\Bigg(\frac{1}{\sqrt{\epsilon_i\epsilon_j}}(A_{ij}+B_{ij}+C_{ij}+C_{ji})+\sqrt{\frac{\epsilon_j}{\epsilon_i}}(A_{ij}-B_{ij}-C_{ij}+C_{ji}) \\
&\quad +\sqrt{\frac{\epsilon_i}{\epsilon_j}}(A_{ij}-B_{ij}+C_{ij}-C_{ji})+\sqrt{\epsilon_i\epsilon_j}(A_{ij}+B_{ij}-C_{ij}-C_{ji})\Bigg), \\
\widetilde{B_{ij}} &= \frac{1}{4}\Bigg(\frac{1}{\sqrt{\epsilon_i\epsilon_j}}(A_{ij}+B_{ij}+C_{ij}+C_{ji})+\sqrt{\frac{\epsilon_j}{\epsilon_i}}(-A_{ij}+B_{ij}+C_{ij}-C_{ji}) \\
&\quad +\sqrt{\frac{\epsilon_i}{\epsilon_j}}(-A_{ij}+B_{ij}-C_{ij}+C_{ji})+\sqrt{\epsilon_i\epsilon_j}(A_{ij}+B_{ij}-C_{ij}-C_{ji})\Bigg), \\
\widetilde{C_{ij}} &= \frac{1}{4}\Bigg(\frac{1}{\sqrt{\epsilon_i\epsilon_j}}(A_{ij}+B_{ij}+C_{ij}+C_{ji})+\sqrt{\frac{\epsilon_j}{\epsilon_i}}(-A_{ij}+B_{ij}+C_{ij}-C_{ji}) \\
&\quad +\sqrt{\frac{\epsilon_i}{\epsilon_j}}(A_{ij}-B_{ij}+C_{ij}-C_{ji})+\sqrt{\epsilon_i\epsilon_j}(-A_{ij}-B_{ij}+C_{ij}+C_{ji})\Bigg), \\
\widetilde{C_{ji}} &= \frac{1}{4}\Bigg(\frac{1}{\sqrt{\epsilon_i\epsilon_j}}(A_{ij}+B_{ij}+C_{ij}+C_{ji})+\sqrt{\frac{\epsilon_j}{\epsilon_i}}(A_{ij}-B_{ij}-C_{ij}+C_{ji}) \\
&\quad +\sqrt{\frac{\epsilon_i}{\epsilon_j}}(-A_{ij}+B_{ij}-C_{ij}+C_{ji})+\sqrt{\epsilon_i\epsilon_j}(-A_{ij}-B_{ij}+C_{ij}+C_{ji})\Bigg).
\end{aligned}
\tag{3.8}
$$

Eq. (3.8) shows that any operator that belongs to the deformed set of operators $\left(\widetilde{A_{ij}},\widetilde{B_{ij}},\widetilde{C_{ij}}\right)$ are a superposition of all the other operators that belong to the non-deformed set $\left(A_{ij},B_{ij},C_{ij}\right)$ and because of the symmetrical property of the inverse transformation, the opposite is also true. By utilizing this fact, it is possible to express a given Hamiltonian through the set of $\left(\widetilde{A_{ij}},\widetilde{B_{ij}},\widetilde{C_{ij}}\right)$ using the transformation rules given in Eq. (3.8). This allows us to calculate the eigenvalues of a given Hamiltonian in a smaller model space by using an appropriate deformation parameter. Let us demonstrate this by taking H_γ defined in Eq. (2.20) and diagonalize it in a deformed basis state; namely, calculate $\langle\widetilde{f}|\,H_\gamma\,|\widetilde{i}\rangle$. This is done by expressing $Q\cdot Q$ in terms of deformed symplectic operators. To find it we need to do the following in steps:

1) First express the quadrupole SU(3) tensor operators in terms of their Cartesian operators.

2) Deform the Cartesian quadrupole operators defined in Eq. (2.2) according to the inverse transformations defined in Eq. (3.6).

3) Express the deformed Cartesian operators in terms of their deformed SU(3) operators using the equations in step one.

Step one is as follows

$$Q_{2\pm M} = \begin{cases} \sqrt{\frac{3}{2}}(Q_{xx} - Q_{yy} \pm 2\iota Q_{xy}), & \text{if M=2} \\ \mp\sqrt{6}(Q_{xz} \pm \iota Q_{yz}), & \text{if M=1} \\ (2Q_{zz} - Q_{yy} - Q_{xx}). & \text{if M=0} \end{cases} \tag{3.9}$$

Step two is

$$Q_{ij} = \sqrt{\epsilon_i \epsilon_j}\widetilde{Q_{ij}}. \tag{3.10}$$

As for the final step we will have

$$Q_{2\pm M} = \begin{cases} \frac{1}{4}(\epsilon_x + \epsilon_y \pm 2\sqrt{\epsilon_x\epsilon_y})\widetilde{Q_{2+2}} + \frac{1}{4}(\epsilon_x + \epsilon_y \mp 2\sqrt{\epsilon_x\epsilon_y})\widetilde{Q_{2-2}} + \frac{1}{2\sqrt{6}}(\epsilon_y - \epsilon_x)\widetilde{Q_{20}}, & \text{if M=2} \\ \frac{1}{2}(\sqrt{\epsilon_y\epsilon_z} \pm \sqrt{\epsilon_x\epsilon_z})\widetilde{Q_{2+1}} + \frac{1}{2}(\sqrt{\epsilon_y\epsilon_z} \mp \sqrt{\epsilon_x\epsilon_z})\widetilde{Q_{2-1}}, & \text{if M=1} \\ \epsilon_z\widetilde{Q_{20}}. & \text{if M=0} \end{cases} \tag{3.11}$$

3.2 Many-Body Harmonic Oscillator Hamiltonian in Terms of Deformed Symplectic Operators

Let us consider the many body harmonic oscillator Hamiltonian and express it in terms of the deformed symplectic operators in $\hbar\Omega$ units

$$H = \sum_i C_{ii} = \frac{1}{4}\left(\epsilon_i(\widetilde{A_{ii}} + \widetilde{B_{ii}} + 2\widetilde{C_{ii}}) + \frac{1}{\epsilon_i}(-\widetilde{A_{ii}} - \widetilde{B_{ii}} + 2\widetilde{C_{ii}})\right). \tag{3.12}$$

For simplicity, if we pick ϵ_x=ϵ_y and apply the volume conservation constraint $\epsilon_x\epsilon_y\epsilon_z = 1$ during the canonical transformation, then Eq. (3.12) reduces to

$$H = \frac{1}{4}\left((\epsilon_z - \frac{1}{\epsilon_z})(\widetilde{A_{zz}} + \widetilde{B_{zz}}) + +2(\sqrt{\epsilon_z} + \frac{1}{\sqrt{\epsilon_z}})(\widetilde{C_{xx}} + \widetilde{C_{yy}}) + 2(\epsilon_z + \frac{1}{\epsilon_z})\widetilde{C_{zz}}\right). \quad (3.13)$$

Diagonalizing the Hamiltonian in Eq. (3.13) within a model space of $N_{\max}$=2 and $N_{\max}$=4 we get the following results shown in Fig. (3.1) and Fig. (3.2).

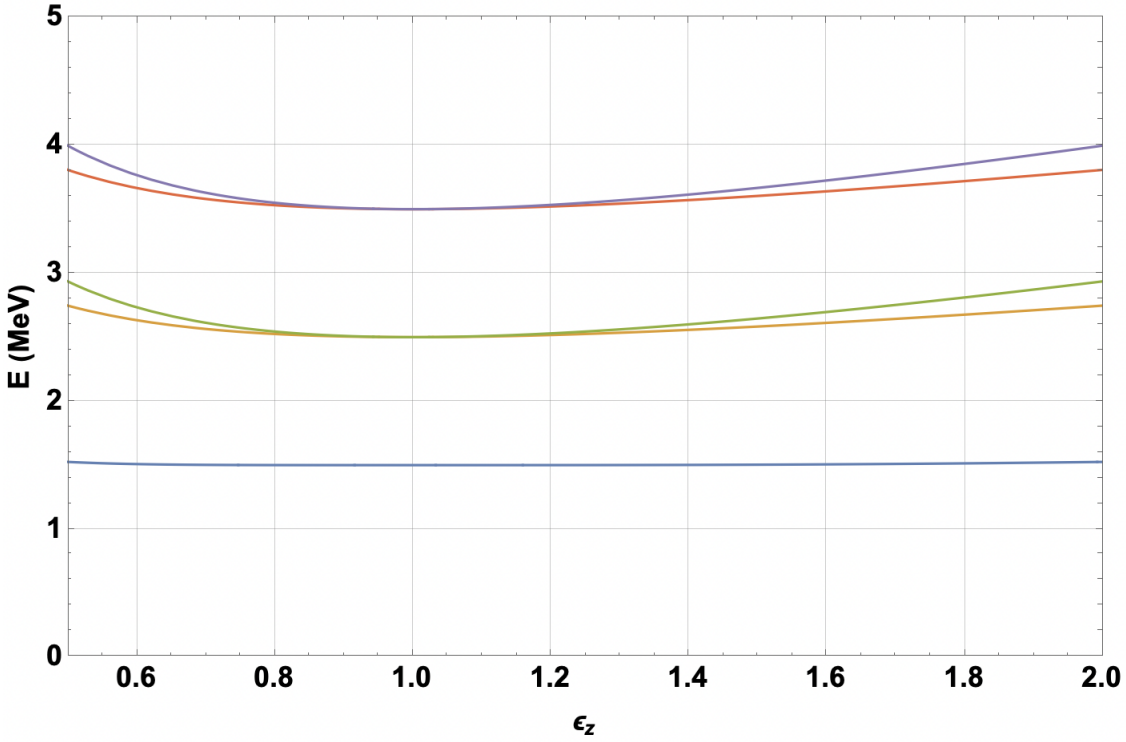

Figure 3.1. The eigenvalues (in $\hbar\Omega$ units) of a 3D Spherical Oscillator as a function of ϵ_z in the deformed model space of $N_{\max}$=2. Figure from [44].

We expected to see all the eigenvalues independent of ϵ_z, however Fig. (3.1) shows a slight dependence of the eigenvalues on ϵ_z. This is because we are attempting to map from an infinite Hilbert space onto a finite Hilbert space, which one can only do approximately by going to higher and higher $N_{\max}$ values; that is, the transformation from the non-deformed to deformed set of operators is not truly a unitary one. To get a unitary transformation, that will be independent of ϵ_z, one has to map it onto infinite deformed basis states which is not possible, but as the figures show, with increasing $N_{\max}$ the results seem to converge

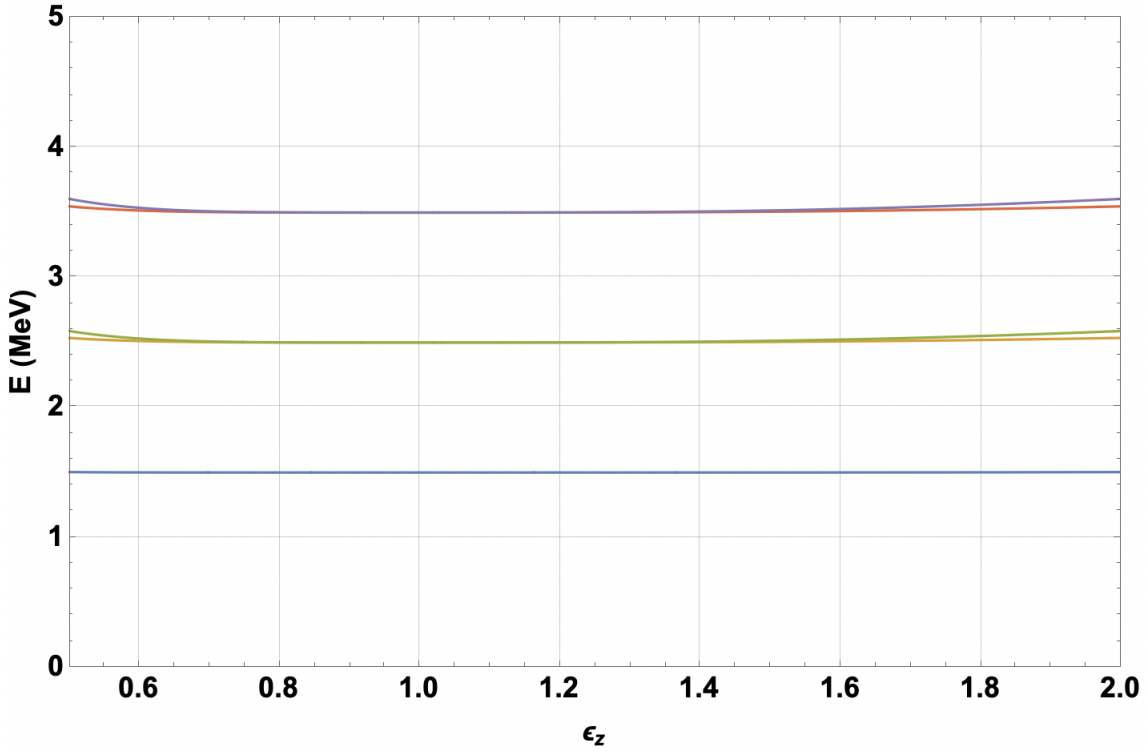

Figure 3.2. The eigenvalues (in $\hbar\Omega$ units) of a 3D Spherical Oscillator as a function of ϵ_z in the deformed model space of $N_{\max}$=4. Figure from [44].

very nicely to the low-lying eigenvalues by the time $N_{\max}$=4, as seen in Fig. (3.2) .

Note that when we applied the canonical transformations to the harmonic oscillator Hamiltonian in Eq. (3.13) the operator C_{ii} includes the zero point energy or the so-called vacuum energy. It is usually common practice in quantum mechanics and quantum field theories to renormalize the energy by discarding the vacuum contribution to the energy since it has no physical meaning. However, the vacuum term should be included when applying canonical transformations because it is part of the symplectic algebra Sp(3,$\mathbf{R}$). In order to unitarily map the symplectic operators to their deformed counterparts one also needs to map the vacuum to its deformed counterpart. After the mapping one could renormalize the energy by retrospectively eliminating the deformed vacuum. The vacuum term in C_{ii} is $\frac{3}{2}\mathcal{A}$ which, after applying the canonical transformation becomes $6\mathcal{A}(\sqrt{\epsilon_z}+\frac{1}{\sqrt{\epsilon_z}})+3\mathcal{A}(\epsilon_z+\frac{1}{\epsilon_z})$.

3.3 Overlaps of Non-Deformed Spherical Versus Cylindrical Harmonic Oscillator Basis States

To calculate the $\langle nn_z m|nlm\rangle$, we begin by expanding a given $|nlm\rangle$ state in terms of all possible cylindrical states $|nn_z m\rangle$,

$$|nlm\rangle = \sum_{n_z=0}^{n} \langle nn_z m|nlm\rangle \, |nn_z m\rangle \, , \tag{3.14}$$

where $n \geq 0$ is the major oscillator shell quantum number, l is the angular momentum quantum number that can take any even number $0, 2, ..., n$ if n is even or any odd number $1, 3, ..., n$ if n is odd, and m is the projection of l on to the z-axis which can take on any value from $-l$ to l. The spherical symmetry dictates that the m on the left must be equal to the m on the right, and therefore the sum is only over n_z which runs from 0 to n. To actually determine the $\langle nn_z m|nlm\rangle$ we write these states in terms of their respective coordinate representations,

$$\Psi_{n_r lm}(r,\theta,\phi) = \Omega^{(l+1)/2}\Omega^{1/4}\sqrt{\frac{2n_r!}{\Gamma(n_r+l+3/2)}}\sqrt{\frac{(2l+1)(l-m)!}{4\pi(l+m)!}}\times$$
$$r^l e^{-\Omega r^2/2} L_{n_r}^{l+1/2}(\Omega r^2) P_l^m(cos(\theta)) e^{\iota m\phi}. \tag{3.15}$$

$$\Psi_{n_\rho n_z m}(\rho,z,\phi) = \Omega^{(|m|+1)/2}\Omega^{1/4}\sqrt{\frac{n_\rho!}{2^{n_z}n_z!\Gamma(n_\rho+|m|+1)}}\times$$
$$\rho^{|m|} e^{-\Omega\rho^2/2} e^{-\Omega z^2/2} L_{n_\rho}^{|m|}(\Omega\rho^2) H_{n_z}(\sqrt{\Omega}z) e^{\iota m\phi}/\pi^{3/4}, \tag{3.16}$$

where $n_r = (n-l)/2$ and $n_\rho = (n-n_z-|m|)/2$ are the radial quantum numbers of their respective geometries. In what follows we will use radial quantum numbers in our derivations because they simplify the resulting expressions. Also for simplicity we put $\hbar = \mathcal{M} = 1$. If

This section was previously publised as D. Kekejian, J. P. Draayer, T. Dytrych, and K. D. Launey. Overlaps of deformed and non-deformed harmonic oscillator basis states. Physics Letters A, 384(7):126162, 2020.

one desires to recover the SI units, one can simply replace $\Omega \rightarrow \mathcal{M}\Omega/\hbar$. Because of axial symmetry, we can also, without loss of generality, drop the absolute value of m and consider only $m \geq 0$. The overlaps of the spherical and cylindrical basis states are therefore given by

$$\langle nn_z m|nlm\rangle = \int_0^{+\infty}\int_0^{\pi}\int_0^{2\pi} r^2 sin(\theta)\times$$
$$\Psi^*_{n_\rho n_z m}(rsin(\theta), rcos(\theta), \phi)\Psi_{n_r lm}(r,\theta,\phi)drd\theta d\phi. \tag{3.17}$$

The integral over ϕ in Eq. (3.17) is simply 2π. For the other integrals over θ and r, we expand the special functions – two associated Laguerre functions plus a Hermite polynomial and a Legendre polynomial – in their respective polynomial forms where we substitute $\rho = rsin(\theta)$, $z = rcos(\theta)$ and integrate the resulting expressions; that is,

$$L^m_{n_\rho}(\Omega r^2 sin^2(\theta)) = \sum_{k_\rho=0}^{n_\rho}(-1)^{k_\rho}\frac{(n_\rho+m)!}{(n_\rho-k_\rho)!(k_\rho+m)!k_\rho!}(\sqrt{\Omega}rsin(\theta))^{2k_\rho}, \tag{3.18}$$

$$L^{l+1/2}_{n_r}(\Omega r^2) = \sum_{k_r=0}^{n_r}(-1)^{k_r}\frac{(n_r+l+1/2)!}{(n_r-k_r)!(k_r+l+1/2)!k_r!}(\sqrt{\Omega}r)^{2k_r}, \tag{3.19}$$

$$H_{n_z}(\sqrt{\Omega}rcos(\theta)) = \sum_{k_z=0}^{[n_z/2]}(-1)^{k_z}\frac{n_z!}{(n_z-2k_z)!k_z!}(2\sqrt{\Omega}rcos(\theta))^{n_z-2k_z}, \tag{3.20}$$

$$P^m_l(cos(\theta)) = (-1)^m sin^m(\theta)\sum_{k_l=0}^{[\frac{l-m}{2}]}(-1)^{k_l}\frac{(2l-2k_l)!}{2^l(l-k_l)!(l-2k_l-m)!k_l!}(cos(\theta))^{l-2k_l-m}. \tag{3.21}$$

The $[n_z/2]$ and $[l-m/2]$ in the upper limits of the sums above denote the integer part of those quantities. If we collect the θ dependent terms first and exploit the equivalence

$$\int_0^{\pi} sin(\theta)sin^{2m+2k_\rho}(\theta)cos^{n_z-2k_z+l-2k_l-m}(\theta)d\theta =$$
$$-\int_0^{\pi}(1-cos^2(\theta))^{m+k_\rho}cos^{n_z-2k_z+l-2k_l-m}(\theta)dcos(\theta), \tag{3.22}$$

and substitute $u = cos(\theta)$, the θ integration simply reduces to

$$\int_{-1}^{+1}(1-u^2)^{m+k_\rho}u^{n_z-2k_z+l-2k_l-m}du =$$
$$\big(1+(-1)^{n_z-2k_z+l-2k_l-m}\big)(m+k_\rho)!\frac{\Gamma(\frac{n_z-2k_z+l-2k_l-m+1}{2})}{2\Gamma(\frac{m+2k_\rho+n_z+l-2k_z-2k_l+3}{2})}, \tag{3.23}$$

where $(1+(-1)^{n_z-2k_z+l-2k_l-m}) = 2$ because it follows from the definition of n_ρ and l that $n_z + l - m$ should always be even. It is also the only acceptable value for the integral above to be nonzero. As for the radial integrals we get

$$\int_0^{+\infty} r^{m+l+2+2k_\rho+2k_r+n_z-2k_z}e^{-\Omega r^2}dr =$$
$$\Omega^{-(m+l+3+2k_\rho+2k_r+n_z-2k_z)/2}\Gamma(\frac{m+l+2+2k_\rho+2k_r+n_z-2k_z+1}{2})/2. \tag{3.24}$$

Inserting these three factors into Eq. (3.17) yields the following analytical expression for the overlaps, which is a four-fold alternating sum,

$$\langle nn_zm|nlm\rangle = \frac{2\pi}{\pi^{3/4}}\sqrt{\frac{2n_r!}{\Gamma(n_r+l+3/2)}}\sqrt{\frac{(2l+1)(l-m)!}{4\pi(l+m)!}}\sqrt{\frac{n_\rho!}{2^{n_z}n_z!\Gamma(n_\rho+m+1)}}$$
$$\sum_{k_\rho=0}^{n_\rho}\sum_{k_r=0}^{n_r}\sum_{k_z=0}^{[n_z/2]}\sum_{k_l=0}^{[\frac{l-m}{2}]}(-1)^{m+k_\rho+k_r+k_z+k_l}2^{n_z-2k_z}\frac{(n_\rho+m)!}{(n_\rho-k_\rho)!k_\rho!}$$
$$\frac{(n_r+l+1/2)!}{(n_r-k_r)!(k_r+l+1/2)!k_r!}\frac{n_z!}{(n_z-2k_z)!k_z!}\frac{(2l-2k_l)!}{2^l(l-k_l)!(l-2k_l-m)!k_l!}$$
$$\frac{\Gamma(\frac{n_z-2k_z+l-2k_l-m+1}{2})}{2\Gamma(\frac{m+2k_\rho+n_z+l-2k_z-2k_l+3}{2})}\Gamma(\frac{m+l+3+2k_\rho+2k_r+n_z-2k_z}{2}). \tag{3.25}$$

Note that the overlap in Eq. (3.25) is independent of Ω, which is a result that follows simply from the completeness of the basis states as long as the transformation is carried out in the same space, deformed or non-deformed. Eq. (3.25) was tested and benchmarked against the results of [55] given in Eqs. (33-36). In this reference, the author presents interbasis

expansions between cylindrical and spherical coordinates up to $n = 3$. In formula in Eq. (3.25) can be considered to be an extension to the work of [55] since it provides the values of these types of interbasis expansions for any set of quantum numbers and is not limited to the size of the model space. In table 1, we present a comparison for some of the overlaps in [55] to our results using the formula in Eq. (3.25). Note that the overlaps in [55] are given in the $\langle n_\rho n_z m|nlm\rangle$ notation where $n_\rho = (n - n_z - |m|)/2$ as mentioned above.

Table 3.1. Overlaps of Non-Deformed Spherical Versus Cylindrical Harmonic Oscillator Basis States for states $n \leq 3$. Table from [45].

$\langle n_\rho n_z m\|nlm\rangle$	$\langle nn_z m\|nlm\rangle$	Results in [55] Eq. (33-36)	Results using our Eq. (3.25)
$\langle 000\|000\rangle$	$\langle 000\|000\rangle$	1	1
$\langle 001\|111\rangle$	$\langle 101\|111\rangle$	-1	-1
$\langle 020\|220\rangle$	$\langle 220\|220\rangle$	$\sqrt{2/3}$	0.816497
$\langle 020\|200\rangle$	$\langle 220\|200\rangle$	$-\sqrt{1/3}$	-0.577350
$\langle 110\|330\rangle$	$\langle 310\|330\rangle$	$\sqrt{3/5}$	0.774597
$\langle 110\|310\rangle$	$\langle 310\|310\rangle$	$\sqrt{2/5}$	0.632456
$\langle 021\|331\rangle$	$\langle 321\|331\rangle$	$-\sqrt{4/5}$	-0.894427
$\langle 021\|311\rangle$	$\langle 321\|311\rangle$	$\sqrt{1/5}$	0.447214

3.4 Overlaps of Deformed and Non-Deformed Harmonic Oscillator Basis States

Next we turn our attention to an expansion of non-deformed cylindrical states ($|nn_z m\rangle$) of Eq. (3.14) in terms of their deformed ($|\widetilde{n}\widetilde{n}_z m\rangle$) counterparts,

$$|nn_z m\rangle = \sum_{\widetilde{n}=0}^{\infty} \sum_{\widetilde{n}_z=0}^{\widetilde{n}} \langle \widetilde{n}\widetilde{n}_z m|nn_z m\rangle \, |\widetilde{n}\widetilde{n}_z m\rangle \, . \tag{3.26}$$

In this case the inner sum runs over $\widetilde{n}_z$ from 0 to $\widetilde{n}$, while the outer sum runs over $\widetilde{n}$ from 0 to infinity which in practice is taken to be some $\widetilde{N}_{\max}$ cutoff. The transformation coefficients, $\langle \widetilde{n}\widetilde{n}_z m|nn_z m\rangle$ in Eq. (3.26), are the key elements in this expansion. Once the $\langle \widetilde{n}\widetilde{n}_z m|nn_z m\rangle$ are known, the corresponding transformation between the non-deformed spherical states and their deformed counterparts follows directly through a double application of Eq. (3.25);

specifically,

$$\langle \widetilde{\widetilde{n}l}m|nlm\rangle = \sum_{\widetilde{n}_z}^{\widetilde{n}} \sum_{n_z}^{n} \langle \widetilde{\widetilde{n}l}m|\widetilde{\widetilde{n}}\widetilde{n}_z m\rangle \langle \widetilde{\widetilde{n}}\widetilde{n}_z m|nn_z m\rangle \langle nn_z m|nlm\rangle \,, \tag{3.27}$$

where the first $\langle \widetilde{\widetilde{n}l}m|\widetilde{\widetilde{n}}\widetilde{n}_z m\rangle$ and third $\langle nn_z m|nlm\rangle$ terms in this double sum follow from applications of Eq. (3.25). The missing ingredient in this whole picture is the transformation coefficient, $\langle \widetilde{\widetilde{n}}\widetilde{n}_z m|nn_z m\rangle$, between deformed cylindrical states and their non-deformed counterparts, to which we now turn our attention. A coordinate representation for the non-deformed ket, $|nn_z m\rangle$, was introduced in Eq. (3.16). The corresponding coordinate representation for the deformed bra, $\langle \widetilde{\widetilde{n}}\widetilde{n}_z m|$, captures the effect of the deformation; that is, $\Omega_x = \Omega_y$ (cylindrical symmetry) not equal to Ω_z and where $\Omega_x\Omega_y\Omega_z = \Omega^3$ to ensure overall volume conservation.

$$\Psi_{\widetilde{n}_\rho \widetilde{n}_z m}(\rho, z, \phi) = \Omega_x^{(m+1)/2}\Omega_z^{1/4} \sqrt{\frac{\widetilde{n}_\rho!}{2^{\widetilde{n}_z}\widetilde{n}_z!\Gamma(\widetilde{n}_\rho + m + 1)}}$$
$$\rho^m e^{-\Omega_x\rho^2/2} e^{-\Omega_z z^2/2} L^m_{\widetilde{n}_\rho}(\Omega_x\rho^2) H_{\widetilde{n}_z}(\sqrt{\Omega_z}z) e^{\imath m\phi}/\pi^{3/4}. \tag{3.28}$$

It follows from this that

$$\langle \widetilde{\widetilde{n}}\widetilde{n}_z m|nn_z m\rangle = \int_0^{+\infty}\int_{-\infty}^{+\infty}\int_0^{2\pi} \Psi^*_{\widetilde{n}_\rho \widetilde{n}_z m}(\rho, z, \phi)\Psi_{n_\rho n_z m}(\rho, z, \phi)$$
$$\rho d\rho dz d\phi. \tag{3.29}$$

The ϕ part again gives 2π. However, unlike the previous case considered in section 3.3 above, these integrals are separable. First, for the radial integral we have

$$\int_0^{+\infty} \rho^{2m} L^m_{\widetilde{n}_\rho}(\Omega_x\rho^2) L^m_{n_\rho}(\Omega\rho^2) e^{-(\Omega+\Omega_x)\rho^2/2}\rho d\rho$$
$$= \int_0^{+\infty} u^m L^m_{\widetilde{n}_\rho}(\Omega_x u) L^m_{n_\rho}(\Omega u) e^{-(\Omega+\Omega_x)u/2} du/2, \tag{3.30}$$

where we made the $\rho^2 = u$ and $2\rho d\rho = du$ substitution. Now, we write the associated Laguerre polynomials in their explicit forms as we did in Eq. (3.18) and Eq. (3.19) to get

$$\sum_{k_\rho=0}^{n_\rho}\sum_{\widetilde{k}_\rho=0}^{\widetilde{n}_\rho}(-1)^{k_\rho+\widetilde{k}_\rho}\frac{(n_\rho+m)!}{(n_\rho-k_\rho)!(k_\rho+m)!k_\rho!}\frac{(\widetilde{n}_\rho+m)!}{(\widetilde{n}_\rho-\widetilde{k}_\rho)!(\widetilde{k}_\rho+m)!\widetilde{k}_\rho!}\Omega^{k_\rho}\Omega_x^{\widetilde{k}_\rho}$$
$$\int_0^{+\infty}u^{k_\rho+\widetilde{k}_\rho+m}e^{-(\Omega+\Omega_x)u/2}du/2, \tag{3.31}$$

where the integral gives us

$$\int_0^{+\infty}u^{k_\rho+\widetilde{k}_\rho+m}e^{-(\Omega+\Omega_x)u}du/2 = 2^{k_\rho+\widetilde{k}_\rho+m}(k_\rho+\widetilde{k}_\rho+m)!$$
$$(\Omega+\Omega_x)^{-(k_\rho+\widetilde{k}_\rho+m+1)}. \tag{3.32}$$

And finally, for Eq. (3.30) we obtain the following expression

$$I_\rho = \sum_{k_\rho=0}^{n_\rho}\sum_{\widetilde{k}_\rho=0}^{\widetilde{n}_\rho}(-1)^{k_\rho+\widetilde{k}_\rho}2^{k_\rho+\widetilde{k}_\rho+m}\frac{(n_\rho+m)!}{(n_\rho-k_\rho)!(k_\rho+m)!k_\rho!}\frac{(\widetilde{n}_\rho+m)!}{(\widetilde{n}_\rho-\widetilde{k}_\rho)!(\widetilde{k}_\rho+m)!\widetilde{k}_\rho!}$$
$$(k_\rho+\widetilde{k}_\rho+m)!\frac{\Omega^{k_\rho}\Omega_x^{\widetilde{k}_\rho}}{(\Omega+\Omega_x)^{k_\rho+\widetilde{k}_\rho+m+1}}. \tag{3.33}$$

Now consider the integral over z,

$$\int_{-\infty}^{+\infty}e^{-(\Omega+\Omega_z)z^2/2}H_{n_z}(\sqrt{\Omega}z)H_{\widetilde{n}_z}(\sqrt{\Omega_z}z)dz$$
$$= \sqrt{\frac{2}{\Omega+\Omega_z}}\int_{-\infty}^{+\infty}e^{-u^2}H_{n_z}(\sqrt{\frac{2\Omega}{\Omega+\omega_z}}u)H_{\widetilde{n}_z}(\sqrt{\frac{2\Omega_z}{\Omega+\Omega_z}}u)du, \tag{3.34}$$

where we made the substitution $z = \sqrt{\frac{2}{\Omega+\Omega_z}}u$. We can simplify this result further by utilizing a multiplication theorem [56] for Hermite polynomials,

$$H_n(\gamma z) = \sum_{k=0}^{[n/2]}\gamma^{n-2k}(\gamma^2-1)^k\frac{n!}{(n-2k)!k!}H_{n-2k}(z). \tag{3.35}$$

Inserting Eq. (3.35) into Eq. (3.34), we get the following intermediate result

$$\sqrt{\frac{2}{\Omega+\Omega_z}}\sum_{k=0}^{[n_z/2]}\sum_{\widetilde{k}=0}^{[\widetilde{n}_z/2]}(-1)^{\widetilde{k}}(\sqrt{\frac{2\Omega}{\Omega+\Omega_z}})^{n_z-2k}(\sqrt{\frac{2\Omega_z}{\Omega+\Omega_z}})^{\widetilde{n}_z-2\widetilde{k}}(\frac{\Omega-\Omega_z}{\Omega+\Omega_z})^{k+\widetilde{k}}$$
$$\frac{\widetilde{n}_z!}{(\widetilde{n}_z-2\widetilde{k})!\widetilde{k}!}\frac{n_z!}{(n_z-2k)!k!}\int_{-\infty}^{+\infty}e^{-u^2}H_{\widetilde{n}_z-2\widetilde{k}}(u)H_{n_z-2k}(u)du, \tag{3.36}$$

where $\int_{-\infty}^{+\infty}e^{-u^2}H_{\widetilde{n}-2\widetilde{k}}(u)H_{n_z-2k}(u)du = \sqrt{\pi}2^{n_z-2k}(n_z-2k)!\delta_{n_z-2k,\widetilde{n}_z-2\widetilde{k}}$. And finally, we obtain the following for Eq. (3.34)

$$\sqrt{\frac{2\pi}{\Omega+\Omega_z}}\sum_{k=0}^{[n_z/2]}\sum_{\widetilde{k}=0}^{[\widetilde{n}_z/2]}(-1)^{\widetilde{k}}2^{n_z-2k}(\sqrt{\frac{2\Omega}{\Omega+\Omega_z}})^{n_z-2k}(\sqrt{\frac{2\Omega_z}{\Omega+\Omega_z}})^{\widetilde{n}_z-2\widetilde{k}}$$
$$\left(\frac{\Omega-\Omega_z}{\Omega+\Omega_z}\right)^{k+\widetilde{k}}\frac{\widetilde{n}_z!n_z!}{(n_z-2k)!k!\widetilde{k}!}\delta_{n_z-2k,\widetilde{n}_z-2\widetilde{k}}. \tag{3.37}$$

The only term that survives in Eq. (3.37) is when $\widetilde{k}=(\widetilde{n}_z-n_z+2k)/2$ which reduces it to

$$I_z=\sqrt{\frac{2\pi}{\Omega+\Omega_z}}\sum_{k=0}^{[n_z/2]}(-1)^{(\widetilde{n}_z-n_z+2k)/2}4^{n_z-2k}\left(\frac{\sqrt{\Omega\Omega_z}}{\Omega+\Omega_z}\right)^{n_z-2k}$$
$$\left(\frac{\Omega-\Omega_z}{\Omega+\Omega_z}\right)^{(\widetilde{n}_z-n_z+4k)/2}\frac{\widetilde{n}_z!n_z!}{(n_z-2k)!((\widetilde{n}_z-n_z+2k)/2)!k!}. \tag{3.38}$$

It follows from all of the above that the desired overlap is given by

$$\langle\widetilde{n}\widetilde{n}_z m|nn_z m\rangle=\frac{2\pi}{\pi^{3/2}}(\Omega\Omega_x)^{(m+1)/2}(\Omega\Omega_z)^{1/4}$$
$$\times\sqrt{\frac{\widetilde{n}_\rho!}{2^{\widetilde{n}_z}\widetilde{n}_z!\Gamma(\widetilde{n}_\rho+m+1)}}\sqrt{\frac{n_\rho!}{2^{n_z}n_z!\Gamma(n_\rho+m+1)}}\times I_\rho\times I_z. \tag{3.39}$$

Knowing $\langle\widetilde{n}\widetilde{n}_z m|nn_z m\rangle$ allows us to obtain an analytic expression for the $\langle\widetilde{n}\widetilde{l}m|nlm\rangle$ through Eq. (3.27). In particular, note that these expressions only depend on Ω and Ω_z, since $\Omega_x=\Omega_y$ follows from cylindrical symmetry and $\Omega_x\Omega_y\Omega_z=\Omega^3$ from volume conservation.

As for the overlaps of deformed and non-deformed Cartesian basis states, it is easy to

see from Eq. (3.38) that the overlaps between deformed and non-deformed Cartesian basis states would be given by

$$\langle \widetilde{n}_x \widetilde{n}_y \widetilde{n}_z | n_x n_y n_z \rangle = \frac{\Omega^{3/4} (\Omega_x \Omega_y \Omega_z)^{1/4} I_x \times I_y \times I_z}{\pi^{3/2} \sqrt{2^{\widetilde{n}_x + \widetilde{n}_y + \widetilde{n}_z + n_x + n_y + n_z} \widetilde{n}_x! \widetilde{n}_y! \widetilde{n}_z! n_x! n_y! n_z!}}. \tag{3.40}$$

In Eq. (3.40), I_x and I_y are given by Eq. (3.38) where the index z is replaced by x and y respectively. Unlike $\langle \widetilde{n}\widetilde{n}_z m | n n_z m \rangle$ and $\langle \widetilde{n}\widetilde{l} m | n l m \rangle$, these overlaps hold even for the $\Omega_x \neq \Omega_y$ case but don't have m as a good quantum number.

To understand the behavior of the probability distribution of these overlaps we present results for $\langle \widetilde{n}\widetilde{n}_z m | n n_z m \rangle$ below.

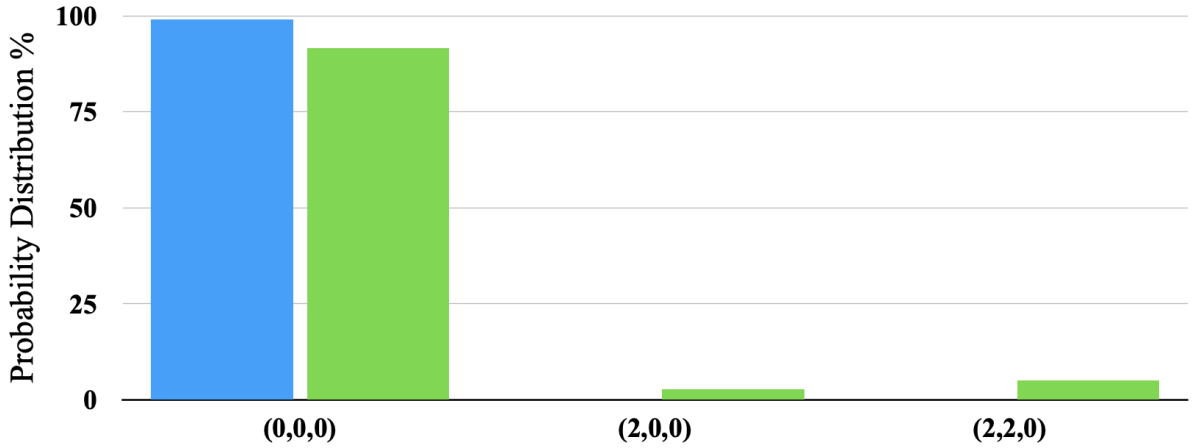

Figure 3.3. The probability distribution of the overlap between the deformed $|\widetilde{n}\widetilde{n}_z m\rangle = |000\rangle$ state and all other non-deformed states in a model space of N_{max}=10 for Ω=1 and Ω_z=0.8 (blue) and Ω_z=0.5 (green). Every state that is not plotted contributes less than 1% to the probability distribution.

As we can see from Fig. (3.3) and Fig. (3.4) the probability distribution for both $|\widetilde{n}\widetilde{n}_z m\rangle = |000\rangle$ and $|\widetilde{n}\widetilde{n}_z m\rangle = |110\rangle$ lie mostly in their non-deformed counterparts $|n n_z m\rangle = |000\rangle$ and $|n n_z m\rangle = |110\rangle$ respectively. As the deformation is turned on ($\Omega \neq \Omega_z$) the overlaps start distributing to other shapes. This distribution is proportional to how far Ω_z is from Ω and as evident for $\Omega_z = 0.5$ the distribution over other states versus its original non-deformed counterpart is bigger compared to $\Omega_z = 0.8$. This is more evident for higher lying states, see Fig. (3.5) and Fig. (3.6).

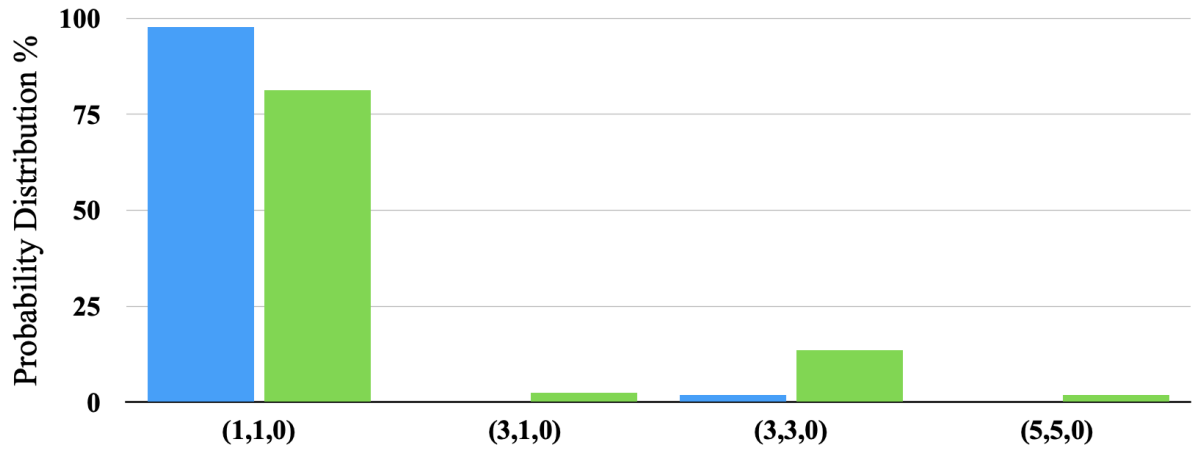

Figure 3.4. The probability distribution of the overlap between the deformed $|\widetilde{n}\widetilde{n}_z m\rangle = |110\rangle$ state and all other non-deformed states in a model space of N_{max}=10 for Ω=1 and Ω_z=0.8 (blue) and Ω_z=0.5 (green). Every state that is not plotted contributes less than 1% to the probability distribution.

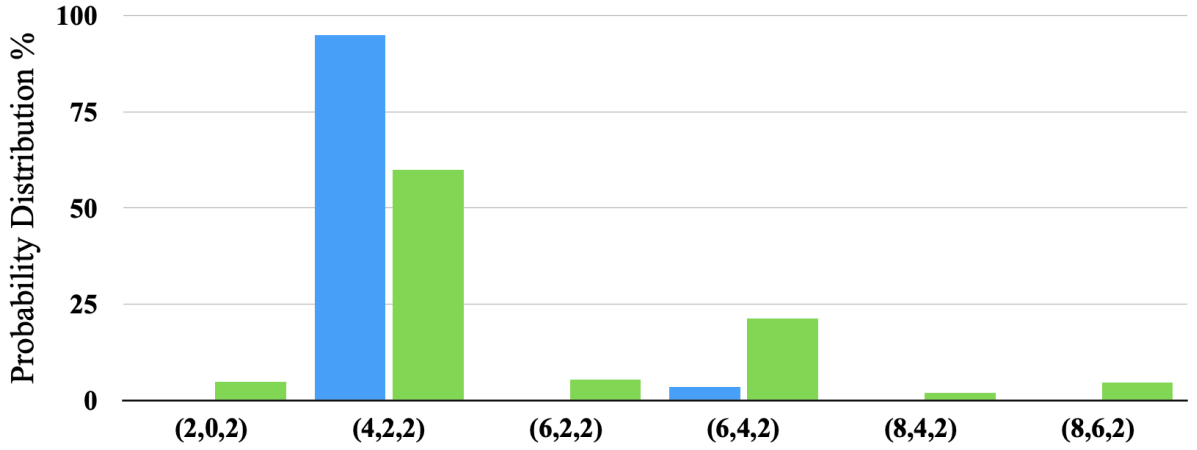

Figure 3.5. The probability distribution of the overlap between the deformed $|\widetilde{n}\widetilde{n}_z m\rangle = |422\rangle$ state and all other non-deformed states in a model space of N_{max}=10 for Ω=1 and Ω_z=0.8 (blue) and Ω_z=0.5 (green). Every state that is not plotted contributes less than 1% to the probability distribution.

The probability distribution for $|\widetilde{n}\widetilde{n}_z m\rangle = |642\rangle$ is very interesting. It is still proportional to how far Ω_z is from Ω but unlike lower lying deformed states $\widetilde{n} < 6$, $|\widetilde{n}\widetilde{n}_z m\rangle = |642\rangle$ has a bigger overlap with $|nn_z m\rangle = |862\rangle$ compared to $|nn_z m\rangle = |642\rangle$ for Ω_z=0.5 (green). This effect becomes even stronger as we move up the harmonic oscillator ladder (for bigger n and n_z values) see see Fig. (3.7) and Fig. (3.8).

Finally we see for $|\widetilde{n}\widetilde{n}_z m\rangle = |842\rangle$ has most of its overlap with other states other than

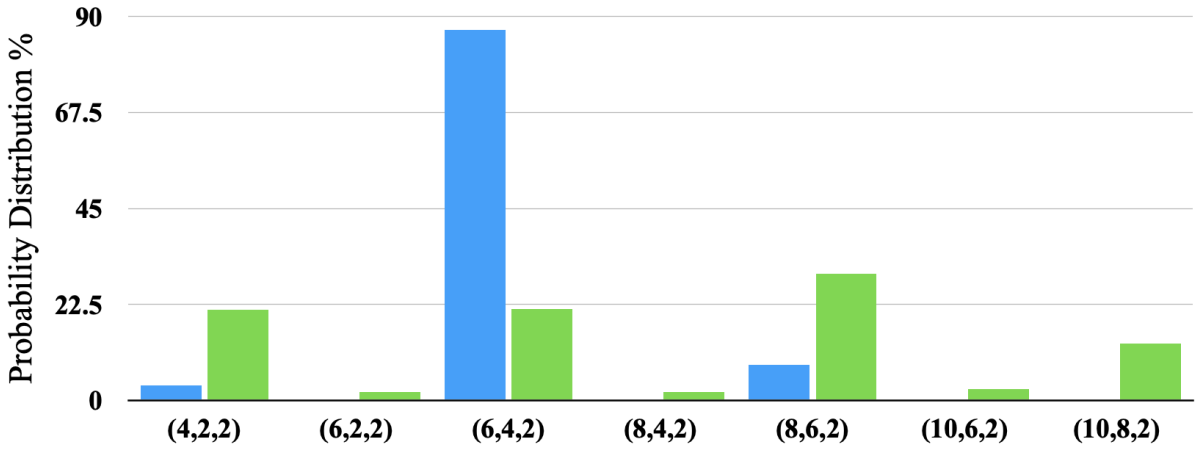

Figure 3.6. The probability distribution of the overlap between the deformed $|\widetilde{n}\widetilde{n}_z m\rangle = |642\rangle$ state and all other non-deformed states in a model space of N_{max}=10 for Ω=1 and Ω_z=0.8 (blue) and Ω_z=0.5 (green). Every state that is not plotted contributes less than 1% to the probability distribution.

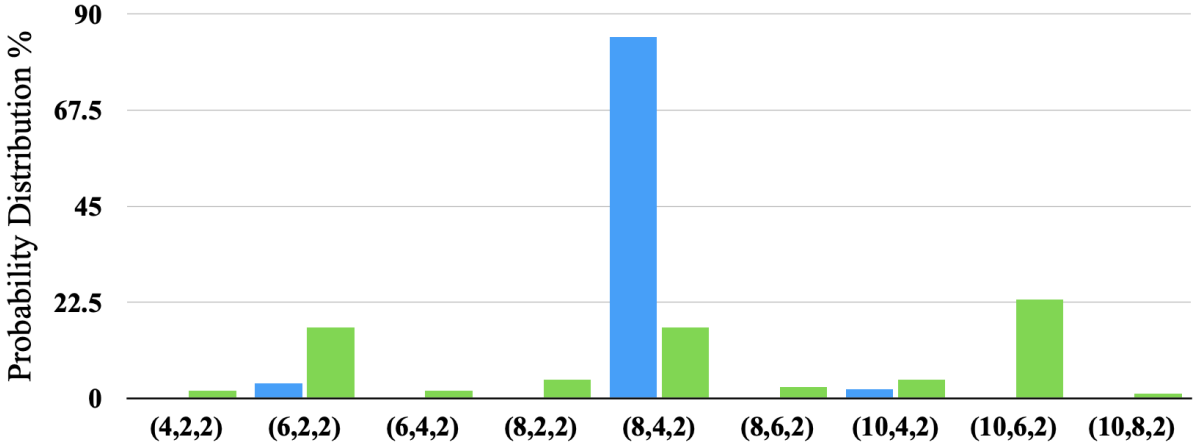

Figure 3.7. The probability distribution of the overlap between the deformed $|\widetilde{n}\widetilde{n}_z m\rangle = |842\rangle$ state and all other non-deformed states in a model space of N_{max}=10 for Ω=1 and Ω_z=0.8 (blue) and Ω_z=0.5 (green). Every state that is not plotted contributes less than 1% to the probability distribution.

its own non-deformed counterpart for Ω_z=0.5 (green). As for $|\widetilde{n}\widetilde{n}_z m\rangle = |862\rangle$, all of its overlap with its own non-deformed counterpart has disappeared and been distributed to other states. However for Ω_z=0.8 (blue) both of them retain majority of their overlap with their corresponding non-deformed counterparts.

To summarize, in all cases the leading overlap for Ω_z=0.8 (blue) is the overlap between two states (deformed and not) that share the same set of quantum number with nearly 99%.

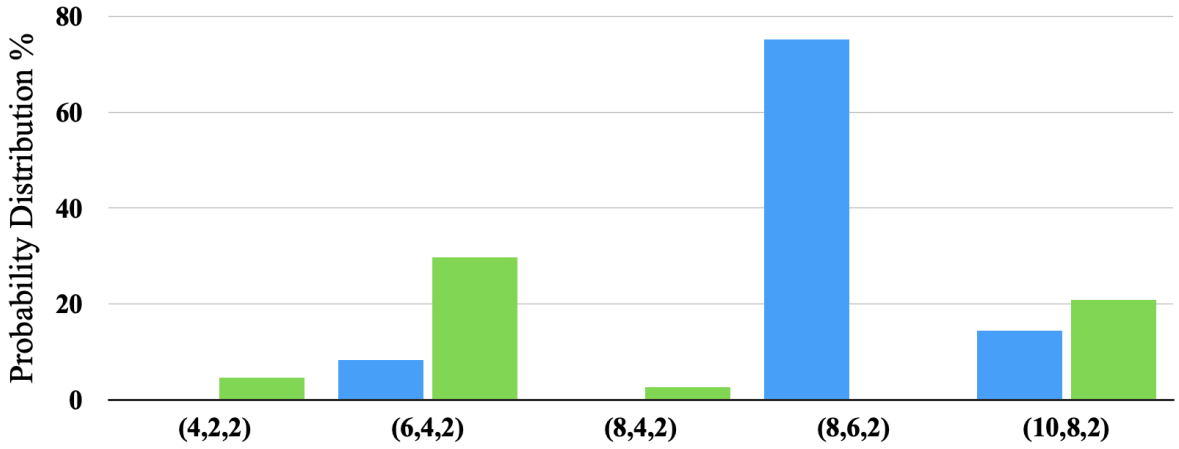

Figure 3.8. The probability distribution of the overlap between the deformed $|\widetilde{n}\widetilde{n}_z m\rangle = |862\rangle$ state and all other non-deformed states in a model space of N_{max}=10 for Ω=1 and Ω_z=0.8 (blue) and Ω_z=0.5 (green). Every state that is not plotted contributes less than 1% to the probability distribution.

The leading overlap for Ω_z=0.5 (green) is also the overlap between two states (deformed and not) that share the same set of quantum number for $n < 6$ but slightly less than the Ω_z=0.8 (blue) case. As for $n \geq 6$ The leading overlap for Ω_z=0.5 (green) becomes the next configuration(s) for which $\widetilde{n} - n$=2 and $\widetilde{n_z} - n_z$=2 is true. In these results we presented cases for randomly picked deformed states and only for $\Omega > \Omega_z$ (prolate). The described behavior is the same for all other deformed configurations and for $\Omega < \Omega_z$ (oblate).

4 Introduction to Quantum Field Theory

In this chapter we introduce basic field theory concepts. The Lagrangian and Hamiltonian formalism of a real scalar field will be introduced and quantized [57, 58]. Finally we show the origins of symplectic symmetry within a field theory framework that sets our motivation to build a symplectic effective field theory. We also discuss the renormalizability of field theories and summarize the known interactions.

4.1 The Four-Vector Notation

The position four vector x^μ has three spatial components ($\mu = 1, 2, 3$) and one time component ($\mu = 0$). It is denoted as $(ct, \mathbf{r})$ and is called a covariant four-vector. Its contravariant component which is a dual vector in the 4-dimensional space is x_μ and is denoted by $(ct, -\mathbf{r})$. As we can see by raising or lowering the covariant index of the four vector, the spatial component changes sign while the time component does not. For the rest of this thesis we are going to limit ourselves to this notation which is the notation followed by the Russian school of physics specifically in the Landau books [59]. Similarly, the momentum four vector p^μ is denoted as $(E/c, \mathbf{p})$ and a four vector derivative ∂^μ is $(\frac{1}{c}\frac{\partial}{\partial t}, \frac{\partial}{\partial \mathbf{r}})$.

A scalar product in the four dimensional space is always defined as the product of two four vectors, one covariant and one contravariant and this product is a Lorentz invariant meaning that it does not change under a Lorentz transformation. Let us see some examples

$$\begin{aligned} x^\mu x_\mu &= c^2 t^2 - \mathbf{r}^2, \\ p^\mu p_\mu &= (E/c)^2 - \mathbf{p}^2 = m^2 c^2. \end{aligned} \tag{4.1}$$

As evident from Eq. (4.1), $x^\mu x_\mu$ gives the interval which is the distance between two events in the 4-dimensional space-time and $p^\mu p_\mu$ gives the famous Einstein relation that connects the total energy and the momentum of a particle to its rest mass.

For the rest of this thesis we are going to use the natural units where $\hbar = c = 1$ for convenience. We pick these units because mathematically there is no difference between

time and space and between energy and momentum and we need to treat them on the same footing during the construction of a field theory. This significantly reduces the complexity of carrying the $\hbar$ and c everywhere during the derivation and quantization of the field theory. We will only recover those units when we want to interpret the physics of the final results. This notation reduces x^μ to $(t, \mathbf{r})$ and momentum reduces to the four wave vector $k^\mu(k^0, \mathbf{k})$. Within this notation everything will either have dimensions of mass $[m] = 1$ or dimensions of length $[x] = -1$. Multiplying dimensions results into adding them (dividing dimenions results into subtracting them). Some examples are $[V] = [x^3] = [x] + [x] + [x] = -3$, $[E] = [p] = 1$, $[t] = -1$, $[v] = [\frac{x}{t}] = [x] - [t] = -1 - (-1) = 0$.

4.2 Lagrangian and Hamiltonian Densities of a Real Scalar Field and Second Quantization

Let us consider the following four dimensional function $\varphi(\mathbf{r}, t)$ which we will call a field function. It is continuous and is defined on $(-\infty, \infty)$. This field function in general would describe the equations of motion of a particle once one constructs the Lagrangian density using them. A real scalar field in Quantum Field Theory (QFT) describes a boson with zero spin and zero electric charge, for example a π^0 meson. $\varphi(\mathbf{r}, t)$ though may be similar to the wave function used to describe a particle in Quantum Mechanics (QM), it is in fact not a wave function. In QFT a particle is defined everywhere in a 4-dimensional space-time through $\varphi(\mathbf{r}, t)$ and only excitations of this field in the vacuum will give rise to a particle description that one can use to construct a quantum mechanical description of the physics by assigning coordinates and momenta to that particular excitation (first quantization) given by Eqs. (2.3). Since QFT-s in general are four dimensional theories, we construct Lagrangian and Hamiltonian densities out of $\varphi(\mathbf{r}, t)$. This is needed because in four dimensions the action $\mathcal{S} = \int L dt$ is not Lorentz invariant but the $\mathcal{S} = \int \mathcal{L} d^4x$ is Lorentz invariant. Along this thesis, italic is used to denote the $\mathcal{L}, \mathcal{H}$ densities and L, H for regular quantities.

What follows is a systematic description of the second quantization, alternatively known as canonical quantization of a classical field theory. Therefore let us first consider the fol-

lowing Lagrangian density of a classical real scalar field

$$\mathcal{L} = \frac{1}{2}(\partial_\mu \varphi)(\partial^\mu \varphi) - \frac{m^2}{2}\varphi^2. \tag{4.2}$$

The action by definition is dimensionless $[S] = 0$ and since we know $[d^4x] = -4$ this implies that the Lagrangian density has $[\mathcal{L}] = 4$. From here it is easy to deduce that $[\varphi] = 1$ and $[\partial_\mu \varphi] = 2$. Plugging Eq. (4.2) into the 4-vector Euler-Lagrange equations which are derived from the principle of least action in four dimensions

$$\partial_\mu \frac{\partial \mathcal{L}}{\partial \varphi_{,\mu}} = \frac{\partial \mathcal{L}}{\partial \varphi}, \tag{4.3}$$

and expanding this equation $\frac{\partial}{\partial t}\frac{\partial \mathcal{L}}{\partial \dot{\varphi}} + \frac{\partial}{\partial \mathbf{r}}\frac{\partial \mathcal{L}}{\partial \varphi'} = \frac{\partial \mathcal{L}}{\partial \varphi}$ we would get

$$(\frac{\partial^2}{\partial t^2} - \frac{\partial^2}{\partial \mathbf{r}^2} + m^2)\varphi = 0. \tag{4.4}$$

This is the Klein-Gordon equation. Its classical analog is the wave equation that has a mass source which gives rise to the Yukawa potential. The Hamiltonian density is expressed in terms of the Lagrangian density

$$\mathcal{H} = \pi\dot{\varphi} - \mathcal{L} = \frac{1}{2}(\dot{\varphi}^2 + \nabla\varphi \cdot \nabla\varphi + m^2\varphi^2), \tag{4.5}$$

where $\dot{\varphi} \equiv \frac{\partial \varphi}{\partial t}$ and $\varphi' \equiv \frac{\partial \varphi}{\partial \mathbf{r}}$. As for $\pi = \frac{\partial \mathcal{L}}{\partial \dot{\varphi}}$ is the momentum of the field and should not be confused with P which is its classical counterpart. The fields that satisfy the equations of motion of this Lagrangian density are given by the plane wave solution and their corresponding Fourier transformation into momentum space is given by

$$\varphi(\mathbf{r}, t) = \frac{1}{(2\pi)^{3/2}} \int_{-\infty}^{+\infty} \psi(\mathbf{k}, E) e^{-\iota k^\mu x_\mu} dE d\mathbf{k}. \tag{4.6}$$

The above integration is over four variables, the three momenta ($\mathbf{k}$) (a vector in three space)

and the energy ($E = k^0$). Since Eq. (4.6) is a solution to Eq. (4.4), plugging it into it reduces it to

$$-((k^0)^2 - \mathbf{k}^2 - m^2)\psi(\mathbf{k}, k^0) = 0. \tag{4.7}$$

Since we are not interested in the trivial solution, $((k^0)^2 - \mathbf{k}^2 - m^2)$ must be zero. However, k^0 and/or $\mathbf{k}$ do not necessarily satisfy Einstein's equation for that fixed mass m but since the integral in the transformations are over all possible values one needs to specifically pick the k^0 and $\mathbf{k}$ values such that $((k^0)^2 - \mathbf{k}^2 - m^2) = 0$. This implies

$$\psi(\mathbf{k}, k^0) = \delta((k^0)^2 - \mathbf{k}^2 - m^2)\varphi(\mathbf{k}, k^0). \tag{4.8}$$

By substituting Eq. (4.8) into Eq. (4.6) and splitting the integral over k^0 into two parts we get

$$\begin{aligned}\varphi(\mathbf{r}, t) = &\frac{1}{(2\pi)^{3/2}} \int_0^{+\infty} \delta((k^0)^2 - \mathbf{k}^2 - m^2)\varphi(\mathbf{k}, k^0) e^{-\iota k^\mu x_\mu} dk^0 d\mathbf{k} \\ &+ \frac{1}{(2\pi)^{3/2}} \int_{-\infty}^{0} \delta((k^0)^2 - \mathbf{k}^2 - m^2)\varphi(\mathbf{k}, k^0) e^{-\iota k^\mu x_\mu} dk^0 d\mathbf{k}.\end{aligned} \tag{4.9}$$

Now let us make the following transformation in the second integral in Eq. (4.9) $k^\mu \to -k^\mu$. This reduces Eq. (4.9) into

$$\begin{aligned}\varphi(\mathbf{r}, t) = &\frac{1}{(2\pi)^{3/2}} \int_0^{+\infty} \delta((k^0)^2 - \mathbf{k}^2 - m^2)\varphi(\mathbf{k}, k^0) e^{-\iota k^\mu x_\mu} dk^0 d\mathbf{k} \\ &+ \frac{1}{(2\pi)^{3/2}} \int_0^{+\infty} \delta((k^0)^2 - \mathbf{k}^2 - m^2)\varphi(-\mathbf{k}, -k^0) e^{\iota k^\mu x_\mu} dk^0 d\mathbf{k}.\end{aligned} \tag{4.10}$$

Note that there is no minus sign from flipping the limits of the integral because the spatial integrals also flip limits. By using the following property of the delta function

$$\delta((k^0)^2 - \mathbf{k}^2 - m^2) = \frac{1}{|2k^0|}\Big(\delta(k^0 - \sqrt{\mathbf{k}^2 + m^2}) + \delta(k^0 + \sqrt{\mathbf{k}^2 + m^2})\Big), \tag{4.11}$$

and substituting Eq. (4.11) into Eq. (4.10) we would get

$$\varphi(\mathbf{r},t) = \frac{1}{(2\pi)^{3/2}}\int_0^{+\infty} \varphi(\mathbf{k},k^0)\frac{1}{|2k^0|}\delta(k^0-\sqrt{\mathbf{k}^2+m^2})e^{-\iota k^\mu x_\mu}dk^0d\mathbf{k}$$
$$+\frac{1}{(2\pi)^{3/2}}\int_0^{+\infty} \varphi(-\mathbf{k},-k^0)\frac{1}{|2k^0|}\delta(k^0-\sqrt{\mathbf{k}^2+m^2})e^{\iota k^\mu x_\mu}dk^0d\mathbf{k}, \tag{4.12}$$

where the integrals containing $\delta(k^0+\sqrt{\mathbf{k}^2+m^2})$ will be zero because k^0 only takes positive values in the limits. By integrating over k^0 in the above equation the delta functions drop out and it reduces to a transformation of spatial (momentum) coordinates only.

$$\varphi(\mathbf{r},t) = \frac{1}{(2\pi)^{3/2}}\int_{-\infty}^{+\infty} \frac{\varphi^+(\mathbf{k},k^0)}{\sqrt{|2k^0|}}e^{\iota k^\mu x_\mu}d\mathbf{k} + \frac{1}{(2\pi)^{3/2}}\int_{-\infty}^{+\infty} \frac{\varphi^-(\mathbf{k},k^0)}{\sqrt{|2k^0|}}e^{-\iota k^\mu x_\mu}d\mathbf{k}, \tag{4.13}$$

where $\varphi^-(\mathbf{k},k^0) = \frac{\varphi(\mathbf{k},k^0)}{\sqrt{|2k^0|}}$ and $\varphi^+(\mathbf{k},k^0) = \frac{\varphi(-\mathbf{k},-k^0)}{\sqrt{|2k^0|}}$ and $k^0 = \sqrt{\mathbf{k}^2+m^2}$ is not a variable in the integral anymore and is determined exactly. Until now everything we did is still a classical field theory in four dimensions. The quantization part comes in when we impose the commutation relations on the fields themselves

$$[\varphi(\mathbf{r}_1,t),\dot{\varphi}(\mathbf{r}_2,t)] = \iota\delta(\mathbf{r}_1-\mathbf{r}_2)$$
$$[\varphi(\mathbf{r}_1,t),\varphi(\mathbf{r}_2,t)] = [\dot{\varphi}(\mathbf{r}_1,t),\dot{\varphi}(\mathbf{r}_2,t)] = 0 \tag{4.14}$$

This is called second quantization of a classical field at equal times since $t_1 = t_2$. To summarize, it involves writing down a Lagrangian density appropriate for the physics we would like to describe. Following this is solving the equations of motion (Euler-Lagrange equations) and finding the fields that satisfy them and finally quantizing these fields as shown above. The second quantization turns the classical field $\varphi(\mathbf{r},t)$ into a quantum field $\hat{\varphi}(\mathbf{r},t)$ (operator). For simplicity we will omit the $\hat{\varphi}$ for the rest of this thesis since all our derivations refer to quantum fields.

Now let us see the consequence of this quantization on the coefficients $\varphi^-(\mathbf{k},k^0)$ and

$\varphi^+(\mathbf{k},k^0)$. First let us write the fields

$$\varphi(\mathbf{r}_1,t)=\frac{1}{(2\pi)^{3/2}}\Big(\int_{-\infty}^{+\infty}\frac{\varphi^+(\mathbf{k},k^0)}{\sqrt{|2k^0|}}e^{\iota k^0 t-\iota\mathbf{k}_1\cdot\mathbf{r}_1}d\mathbf{k}_1+\int_{-\infty}^{+\infty}\frac{\varphi^-(\mathbf{k},k^0)}{\sqrt{|2k^0|}}e^{-\iota k^0 t+\iota\mathbf{k}_1\cdot\mathbf{r}_1}d\mathbf{k}_1\Big),$$
$$\dot\varphi(\mathbf{r}_2,t)=\frac{1}{(2\pi)^{3/2}}\Big(\int_{-\infty}^{+\infty}\iota k^0\frac{\varphi^+(\mathbf{k},k^0)}{\sqrt{|2k^0|}}e^{\iota k^0 t-\iota\mathbf{k}_2\cdot\mathbf{r}_2}d\mathbf{k}_2-\int_{-\infty}^{+\infty}\iota k^0\frac{\varphi^-(\mathbf{k},k^0)}{\sqrt{|2k^0|}}e^{-\iota k^0 t+\iota\mathbf{k}_2\cdot\mathbf{r}_2}d\mathbf{k}_2\Big). \tag{4.15}$$

Now let us form $\varphi(\mathbf{r}_1,t)\dot\varphi(\mathbf{r}_2,t)$ for which we will get the following pairs with similar superscript signs and opposite superscript signs and use $\varphi^\pm(\mathbf{k},k^0)=\varphi^\pm_{\mathbf{k}}$ for short

$$\begin{aligned}\varphi(\mathbf{r}_1,t)\dot\varphi(\mathbf{r}_2,t)=&\frac{1}{(2\pi)^3}\int_{-\infty}^{+\infty}\varphi^+_{\mathbf{k}_1}\varphi^+_{\mathbf{k}_2}\frac{\iota k^0}{2k^0}e^{2\iota k^0 t-\iota\mathbf{k}_1\cdot\mathbf{r}_1-\iota\mathbf{k}_2\cdot\mathbf{r}_2}d\mathbf{k}_1d\mathbf{k}_2\\&-\frac{1}{(2\pi)^3}\int_{-\infty}^{+\infty}\varphi^-_{\mathbf{k}_1}\varphi^-_{\mathbf{k}_2}\frac{\iota k^0}{2k^0}e^{-2\iota k^0 t+\iota\mathbf{k}_1\cdot\mathbf{r}_1+\iota\mathbf{k}_2\cdot\mathbf{r}_2}d\mathbf{k}_1d\mathbf{k}_2\\&-\frac{1}{(2\pi)^3}\int_{-\infty}^{+\infty}\varphi^+_{\mathbf{k}_1}\varphi^-_{\mathbf{k}_2}\frac{\iota k^0}{2k^0}e^{-\iota\mathbf{k}_1\cdot\mathbf{r}_1+\iota\mathbf{k}_2\cdot\mathbf{r}_2}d\mathbf{k}_1d\mathbf{k}_2\\&+\frac{1}{(2\pi)^3}\int_{-\infty}^{+\infty}\varphi^-_{\mathbf{k}_1}\varphi^+_{\mathbf{k}_2}\frac{\iota k^0}{2k^0}e^{\iota\mathbf{k}_1\cdot\mathbf{r}_1-\iota\mathbf{k}_2\cdot\mathbf{r}_2}d\mathbf{k}_1d\mathbf{k}_2.\end{aligned} \tag{4.16}$$

So for the commutator we will have terms like $\varphi^+_{\mathbf{k}_1}\varphi^+_{\mathbf{k}_2}$ and $\varphi^-_{\mathbf{k}_1}\varphi^-_{\mathbf{k}_2}$ cancel, and only $\varphi^+_{\mathbf{k}_1}\varphi^-_{\mathbf{k}_2}$ and $\varphi^-_{\mathbf{k}_1}\varphi^+_{\mathbf{k}_2}$ will remain which gives us

$$\begin{aligned}[\varphi(\mathbf{r}_1,t),\dot\varphi(\mathbf{r}_2,t)]=&\frac{\iota}{2(2\pi)^3}\int_{-\infty}^{+\infty}(\varphi^-_{\mathbf{k}_2}\varphi^+_{\mathbf{k}_1}-\varphi^+_{\mathbf{k}_1}\varphi^-_{\mathbf{k}_2})e^{-\iota\mathbf{k}_1\cdot\mathbf{r}_1+\iota\mathbf{k}_2\cdot\mathbf{r}_2}d\mathbf{k}_1d\mathbf{k}_2+\\&\frac{\iota}{2(2\pi)^3}\int_{-\infty}^{+\infty}(\varphi^-_{\mathbf{k}_1}\varphi^+_{\mathbf{k}_2}-\varphi^+_{\mathbf{k}_2}\varphi^-_{\mathbf{k}_1})e^{\iota\mathbf{k}_1\cdot\mathbf{r}_1-\iota\mathbf{k}_2\cdot\mathbf{r}_2}d\mathbf{k}_1d\mathbf{k}_2=\iota\delta(\mathbf{r}_1-\mathbf{r}_2).\end{aligned} \tag{4.17}$$

In order for the above equation to be satisfied we have to have

$$[\varphi^-(\mathbf{k}_1),\varphi^+(\mathbf{k}_2)]=[b^-_{\mathbf{k}_1},b^+_{\mathbf{k}_2}]=\delta(\mathbf{k}_1-\mathbf{k}_2). \tag{4.18}$$

Eq.(4.18) tells us the physical interpretation of $\varphi^-(\mathbf{k},k^0)$ and $\varphi^+(\mathbf{k},k^0)$; namely, that they are the well known boson creation $b^+_{\mathbf{k}}$ and annihilation $b^-_{\mathbf{k}}$ operators . They create (annihilate)

a boson with momentum $\mathbf{k}$ and energy k^0 which has a continuous spectrum.

4.3 Harmonic Oscillator Hamiltonian in Quantum Field Theory

The way we identified our field in terms of its momentum representation in Eq. (4.13) makes it hard to make sense of the predictions because if we take the scalar product of any two states we would get $\langle \mathbf{k}_1 | \mathbf{k}_2 \rangle = \delta(\mathbf{k}_1 - \mathbf{k}_2)$. This implies that our states are not normalizable to one and therefore not square-integrable which is natural because until now we were dealing with plane waves defined everywhere in space-time. The proper way to solve this problem is to take the plane-wave states and build up localized wave packets, which are normalizable and for which the scattering process really is restricted to some finite region of space-time. This is achieved by discretizing the momentum vector $\mathbf{k}$ and forcing periodic boundary conditions on the exponential plane wave functions in Eq. (4.13) so the components of $\mathbf{k}$ need to satisfy the $k_i L = 2\pi \mathrm{n_i}$ boundary condition where n is an integer and L is the length of the discrete box element where the wave packet is localized. Note that if $V \longrightarrow \infty$ we will recover the continuous limit and should still get finite physical answers. This discretization reduces $\int d\mathbf{k} \to (\frac{2\pi}{L})^3 \sum_{\mathbf{k}}$ and $\varphi^{\pm}(\mathbf{k}, k^0) \to (\frac{L}{2\pi})^{3/2} b^{\pm}_{\mathbf{k}}$. With this in mind Eq. (4.13) reduces into

$$\varphi(\mathbf{r}, t) = \frac{1}{\sqrt{V}} \sum_{\mathbf{k}} b^{-}_{\mathbf{k}} \frac{1}{\sqrt{|2k^0|}} e^{-\iota k^{\mu} x_{\mu}} + b^{+}_{\mathbf{k}} \frac{1}{\sqrt{|2k^0|}} e^{\iota k^{\mu} x_{\mu}}. \tag{4.19}$$

This discretization tells us that the boson creation $b^{+}_{\mathbf{k}}$ and annihilation $b^{-}_{\mathbf{k}}$ operators now create (annihilate) a boson with momentum $\mathbf{k}$ and energy k^0 which has a discrete spectrum. Finally, let us calculate the Hamiltonian of this field which is $H = \lim_{L \to \infty} \int_{-L}^{+L} \mathcal{H} dV$. Where we are taking the limit so we can recover the continuum case. By plugging Eq. (4.19) into

Eq. (4.5) we would get the following for the Hamiltonian

$$H = \lim_{L\to\infty} \frac{1}{2V} \int_{-L}^{+L} \Bigg\{ \sum_{\mathbf{k},\mathbf{q}} m^2 \left(\frac{b^-_{\mathbf{k}}}{\sqrt{|2k^0|}} e^{-\iota k^\mu x_\mu} + \frac{b^+_{\mathbf{k}}}{\sqrt{|2k^0|}} e^{\iota k^\mu x_\mu} \right) \times \left(\frac{b^-_{\mathbf{q}}}{\sqrt{|2q^0|}} e^{-\iota q^\mu x_\mu} + \frac{b^+_{\mathbf{q}}}{\sqrt{|2q^0|}} e^{\iota q^\mu x_\mu} \right) + \left(\iota^2 k^0 q^0 + \iota^2 \mathbf{k}\cdot\mathbf{q} \right) \left(- \frac{b^-_{\mathbf{k}}}{\sqrt{|2k^0|}} e^{-\iota k^\mu x_\mu} + \frac{b^+_{\mathbf{k}}}{\sqrt{|2k^0|}} e^{\iota k^\mu x_\mu} \right) \times \left(- \frac{b^-_{\mathbf{q}}}{\sqrt{|2q^0|}} e^{-\iota q^\mu x_\mu} + \frac{b^+_{\mathbf{q}}}{\sqrt{|2q^0|}} e^{\iota q^\mu x_\mu} \right) \Bigg\} dV,$$

where we chose $\mathbf{q}$, a momentum vector to differentiate it from $\mathbf{k}$ when summing over. If $\mathbf{k} \neq -\mathbf{q}, \mathbf{q}$, then $H = 0$ because all the terms $b^+_{\mathbf{k}} b^+_{\mathbf{q}} e^{\iota(k^\mu + q^\mu)x_\mu}$, $b^-_{\mathbf{k}} b^-_{\mathbf{q}} e^{-\iota(k^\mu + q^\mu)x_\mu}$, $b^+_{\mathbf{k}} b^-_{\mathbf{q}} e^{\iota(k^\mu - q^\mu)x_\mu}$, $b^-_{\mathbf{k}} b^+_{\mathbf{q}} e^{-\iota(k^\mu - q^\mu)x_\mu}$ will vanish when we integrate over the volume because they are periodic from $-L$ to L. However, if we pick $\mathbf{k} = -\mathbf{q}$ which necessarily implies that $k^0 = q^0$ since they both describe the same m, then the terms like $b^+_{\mathbf{k}} b^-_{\mathbf{q}} e^{\iota(k^\mu - q^\mu)x_\mu}$, $b^-_{\mathbf{k}} b^+_{\mathbf{q}} e^{-\iota(k^\mu - q^\mu)x_\mu}$ will still be zero because of periodicity. As for the terms $b^+_{\mathbf{k}} b^+_{\mathbf{q}} e^{\iota(k^\mu + q^\mu)x_\mu}$ and $b^-_{\mathbf{k}} b^-_{\mathbf{q}} e^{-\iota(k^\mu + q^\mu)x_\mu}$, they also vanish because $(m^2 + \iota^2 k^0 k^0 + \iota^2 \mathbf{k}\cdot(-\mathbf{k})) = 0$. Therefore we are left with the option $\mathbf{k} = \mathbf{q}$. Once this is picked, terms like $b^+_{\mathbf{k}} b^+_{\mathbf{q}} e^{\iota(k^\mu + q^\mu)x_\mu}$, $b^-_{\mathbf{k}} b^-_{\mathbf{q}} e^{-\iota(k^\mu + q^\mu)x_\mu}$ will vanish because of periodicity but unlike before the terms $b^+_{\mathbf{k}} b^-_{\mathbf{q}} e^{\iota(k^\mu - q^\mu)x_\mu}$ and $b^-_{\mathbf{k}} b^+_{\mathbf{q}} e^{-\iota(k^\mu - q^\mu)x_\mu}$ will survive because $(m^2 - \iota^2 k^0 k^0 - \iota^2 \mathbf{k}\cdot(\mathbf{k})) = 2E^2_{\mathbf{k}}$. Since $e^{\iota(k^\mu - q^\mu)x_\mu}$ and $e^{-\iota(k^\mu - q^\mu)x_\mu}$ reduce to unity for $\mathbf{k} = \mathbf{q}$, the integral over the volume will give V that cancels the volume in the denominator therefore we can make the volume arbitrarily large without any physical consequences and recover the continuous case. The final form of the Hamiltonian will look like

$$H = \frac{1}{2} \sum_{\mathbf{k}} E_{\mathbf{k}} (b^+_{\mathbf{k}} b^-_{\mathbf{k}} + b^-_{\mathbf{k}} b^+_{\mathbf{k}}) = \sum_{\mathbf{k}} E_{\mathbf{k}} (b^+_{\mathbf{k}} b^-_{\mathbf{k}} + \frac{1}{2}), \tag{4.20}$$

which is the Hamiltonian of the harmonic oscillator. Eq. (4.20) shows all possible harmonic oscillator excitations that could exist in vacuum and the total energy of the field is the sum over all such possible excitations. Note that the energy of the vacuum itself is infinite

too. However, the energy of the vacuum, called zero point energy, has no physical meaning. In physics only energy differences have meaning since only differences are experimentally measurable therefore we could renormalize this Hamiltonian and omit the vacuum energy term. The main difference between QFT and QM could be easily summarized from Eq. (4.20). In QFT the harmonic oscillator Hamiltonian could be thought of as summing over infinite QM harmonic oscillator Hamiltonians, each with one specific value of $E_{\mathbf{k}}$.

4.4 Origins of NCSpM in a Quantum Effective Field Theory

The success with which the NCSpM was able to explain nuclear observables of light nuclei with a simple $Q \cdot Q$-driven schematic interaction suggests an underlying origin of the interaction in a field theory framework. This could first be seen from the fact that Eq. (4.2) gives the harmonic oscillator Hamiltonian which is part of the H_γ interaction given in Eq. (2.20) if we were to pick one value of $E_{\mathbf{k}} = \hbar\Omega_{\mathbf{k}}$. Furthermore φ^4 from Eq. (4.19) is proportional to pairs of $(b^{\pm}_{\mathbf{k}} b^{\pm}_{\mathbf{k}})$ and $(b^{\pm}_{\mathbf{k}} b^{\mp}_{\mathbf{k}})$, and therefore it includes $Q \cdot Q$.

A simple Lagrangian density that could capture the H_γ interaction given in Eq. (2.20) is as follows

$$\mathcal{L} = \frac{1}{2}(\partial_\mu \varphi)(\partial^\mu \varphi) - \frac{m^2}{2}\varphi^2(e^{-\gamma_e \varphi^2/m^2} - 1). \tag{4.21}$$

Here m is a mass-like term and γ_e is a dimensionless number and is believed to be tied to γ in Eq. (2.20). It denotes the strength of higher-order self- interacting fields which can be seen from expanding the exponential which gives

$$\mathcal{L} = \frac{1}{2}(\partial_\mu \varphi)(\partial^\mu \varphi) - \sum_{n=1}^{\infty} \frac{(-1)^n \gamma_e^n}{2m^{2n-2}} \varphi^{2n+2}. \tag{4.22}$$

Plugging this into Euler-Lagrange equations in Eq. (4.3) we get

$$\partial_\mu \partial^\mu \varphi = -m^2 \varphi(e^{-\gamma_e \varphi^2/m^2} - 1) + \gamma_e \varphi^3 e^{-\gamma_e \varphi^2/m^2}. \tag{4.23}$$

It is obvious that the plain-wave solution in Eq. (4.19) doesn't satisfy the above equation

and it is impossible to solve it exactly. However it can be solved perturbatively for γ_e at every order.

The steps are as follows:

1) Substitute the plain wave solution into Eq. (4.23). Expand the exponential term and pick terms only proportional to $\gamma_e^0 = 1$ which reduces the equation to $\partial_\mu \partial^\mu \varphi = 0$, which gives the plain wave solution with $E^2 = \mathbf{k}^2$ (massless boson excitations). This also explains why we subtracted one from the exponential in Eq. (4.21).

2) Substitute $\varphi = \varphi^{(0)} + \varphi^{(1)}$ into Eq. (4.23) where $\varphi^{(0)}$ is the plain wave solution from step 1 and solve it for $\varphi^{(1)}$ by keeping all terms up to the powers of γ_e^1. This gives the perturbative Next to Leading Order (NLO) correction to the plain wave solution. So the solution up to NLO will be $\varphi = \varphi^{(0)} + \varphi^{(1)}$.

3) Repeat step 2 but this time keep all powers up to γ_e^2. This will give N^{2}LO correction; namely, $\varphi^{(2)}$ and total solution up to N^{2}LO will be $\varphi = \varphi^{(0)} + \varphi^{(1)} + \varphi^{(2)}$.

4) Repeat this process up to the desired N^{n}LO correction.

As for the Hamiltonian density we get

$$\mathcal{H} = \frac{1}{2}\Big(\dot{\varphi}^2 + \nabla\varphi \cdot \nabla\varphi + m^2\varphi^2(e^{-\gamma_e\varphi^2/m^2} - 1)\Big). \tag{4.24}$$

For the purposes of this thesis we will refrain from solving the above mentioned Lagrangian density perturbatively since it involves calculating highly complicated diagrams and requires a deep technical knowledge of QFT that is beyond the scope of this thesis. However, it sets the motivation and foundation for constructing a Symplectic Effective Field Theory as discussed in Sec. 5.

4.5 Overview of Dimensional Analysis and Renormalizability

The Lagrangian density we introduced in Eq. (4.21) is *non-renormalizable* and hence would be an EFT. Field theories that include terms whose coefficients have dimension $d \geq 0$ are *renormalizable* and theories with $d < 0$ are *non-renormalizable*. Sometimes $d = 0$ theories

are also referred to as *super-renormalizable* because theories with coupling coefficients of dimension zero (dimensionless numbers) are easier to renormalize. Let us now discuss the main differences between them:

1) **Divergences**: They both include divergences (infinities). The divergences in *renormalizable* theories, called QFT-s, could be taken care of with a finite amount of terms added into the Lagrangian. However, *non-renormalizable* theories, called EFT-s, need an infinite amount of terms added to the Lagrangian to cancel those infinities. A rule of thumb is, to say for example for a coupling coefficient $[\lambda_n] = -n$ will include infinities of order n larger than the order before $n-1$. This is why we need to keep adding infinite terms to our theory to keep canceling the infinities from the order before. This is circumvented by introducing a *UV cutoff* (Ultra Violet).

2) **UV cutoffs**: Since we need to add an infinite amount of terms to an EFT to cancel the divergences at every order, we need to impose a *UV cutoff* on our theory. To demonstrate this let us take the coupling coefficient in Eq. (4.22). It has dimensions of $[\frac{\gamma_e^n}{2m^{2n-2}}] = -2(n-1)$ which for n=2 has dimensions of $1/E^2$. Now it is obvious why a *UV cutoff* is necessary. The next order $n = 3$ will be proportional to $1/E^4$, etc. Therefore higher order terms need to be added with a cutoff imposed on the value of E otherwise our theory won't make any physical predictions. This implies that terms in an EFT have to be added perturbatively whereas QFT-s don't have this problem of a *UV cutoff* therefore they could in theory be treated non-perturbatively.

3) **Predictablility**: How to pick a cutoff for an EFT? What values of energies are appropriate? The answer is: depends on the physics we are trying to study. For example, for atomic physics an appropriate value of $E \sim$ eV (electron Volts), for low energy nuclear physics $E \sim$ MeV. The cutoff sets an energy scale that determines the predictive power of an EFT. At the right energies, for example in case of nuclear physics, the relevant low energy phenomena is at $E \sim$ MeV versus its high energy counterpart that sets the cutoff around $E \sim$ GeV, they are highly predictable and easy to use [60]. At the wrong energies (near

or above the cutoff) they completely fail. Unlike EFT-s, QFT-s don't have this problem. They are supposed to be predictable at any energy scale which is why they are sometimes referred to as the $UV completion$ of an EFT. The $UV completion$ refers to their ability of being predictable at energies beyond the $UV cutoff$ set by the EFT hence "UV"-completing the EFT. QFT-s can be non-perturbative, however studying them perturbatively is much easier and their perturbative asymptotic limits yield EFT-s. However QFT-s are harder to use in general and have their own problems.

Let us summarize the four fundamental *renormalizable* and *non-renormalizable* interaction theories that exist today [57, 58]:

1) **The Electromagnetic Interaction**: This interaction is successfully described by the Schrodinger's equation of a charged particle, for example an electron interacting with an electromagnetic field. Quantum mechanics is *non-renormalizable*, perturbative and highly predictable for $E < m_e = 0.511$ MeV. Its $UV completion$ is Dirac's equation, who's perturbative limit gives the Schrodinger's equation. The full QFT description of it is done by Quantum Electrodynamics (QED) which is *renormalizable*. Its perturbative limit gives the Coulomb law and the fine structure constant. However, it has a Landau pole at $E \sim 10^{100}$ GeV and is perturbative up to this value. At this energy QED fails. This divergence of QED cannot be renormalized and is currently an open problem in physics.

2) **The Weak Interaction**: This interaction is successfully described by the Fermi theory which is *non-renormalizable*, perturbative and highly predictable for $E < G_F^{-1/2} \sim 300$ GeV, where G_F is the Fermi constant. Its $UV completion$ is the electroweak theory with W and Z bosons. It is *renormalizable* but only perturbative up to $E < 1$ TeV. One possible UV completion of the electroweak theory is to add a Higgs boson to it.

3) **The Strong Interaction**: This interaction is described by the chiral effective field theory which is *non-renormalizable* and is the low energy theory of pions. It is perturbative and highly predictive up to $E \ll 1200$ MeV. Its $UV completion$ is Quantum Chromodynamics (QCD) which is *renormalizable* and highly predictive at high energies. However unlike other

UV completion theories, QCD has no asymptotic states, meaning we can not talk about pions and pion scattering at high energies. The only thing we can do is match the two theories indirectly by external current correlations from electron or photon off pion scattering experiments. This implies that its perturbative limit at low energies are missing and an open problem in physics. This is why lattice QCD is used because it is a non-perturbative formulation of QCD and can carry out calculations on the lattice, and try to match those paramaters from low energy scattering data to high energy scattering data. Continuum QCD is another approach that is currently being utilized to study the origin of the nucleon mass.

4) **The Gravitational Interaction**: Is the least known interaction. Einstein quantum gravity or quantum loop gravity, is *non-renormalizable* and the low energy theory of gravity. It is perturbative and highly predictive up to $E < 10^{19}$GeV. Only problem is in order to measure any observable quantum effects of gravity we need to increase the sensitivity of our measurements. This is why Classical Einstein gravity is still been used. Assuming one day we measure any quantum effects, then we need to find a *UV completion* of the Einstein quantum gravity. One possible candidate is string theory.

5 Symplectic Effective Field Theory (SpEFT)

In this chapter we present a step-by-step methodology for constructing the symplectic effective field theory referenced in the previous chapter. The main idea is to construct a self interacting real scalar effective field theory that represents a system of $\mathcal{A}$ interacting nucleons and to show how symplectic symmetry emerges from a simple field theoretical framework. Instead of solving the theory perturbatively we impose a condition on the scale parameter of the EFT such that the plane-wave solution satisfies the equations of motion, and all next-to-leading-order corrections and next-to-higher-order corrections to this solution are negligible. This in turn allows us to capture the relevant interaction by introducing an effective mass-like term that sets the strength of the driving force of the interaction; namely, quadrupole-quadrupole which in turn successfully captures the dynamics. The advantage of this approach is to utilize the fact that nucleons occupy harmonic oscillator like structures that allow a specific energy, therefore reducing the field theory into a quantum mechanical Hamiltonian that is suitable for nuclear structure calculations. Then we provide example applications for some nuclei like ^{12}C, ^{20}Ne and ^{166}Er.

5.1 HO Lagrangian and Its n-th Order Extension

As we discussed in the previous chapter, the simplest Lagrangian density for a real scalar field is

$$\mathcal{L} = \frac{1}{2}\partial_\mu\varphi\partial^\mu\varphi, \tag{5.1}$$

which is the Lagrangian of a harmonic oscillator for massless bosons which is simply putting $m = 0$ in Eq. (4.2). The construction of the EFT is accomplished by taking the Lagrangian density in Eq. (5.1) and naturally extending it to its n-th order

$$\mathcal{L}^{(n)} = \frac{\alpha^n}{2^{n+1}(n+1)!}\left(\partial_\mu\varphi\partial^\mu\varphi - nm^2\varphi^2\right)^{n+1}, \tag{5.2}$$

The total Lagrangian density is $\mathcal{L} = \sum_n \mathcal{L}^{(n)}$ and for $n = 0$ term we recover Eq. (5.1). We have added a new term $nm^2\varphi^2$ often called "the mass" term at every order. This term is

added in order to capture all possible combinations of interaction terms that could result from lowest powers of φ and $\partial_\mu\varphi\partial^\mu\varphi$. Including φ only shifts the equations of motion by a constant, therefore the lowest possible power is φ^2. α is the coupling coefficient of the theory. As we have shown the dimension of a Lagrangian density always has to be $[\mathcal{L}] = 4$ and since $[\partial_\mu\varphi] = 2$ which implies $[\alpha] = -4$ and therefore this is an EFT and is *non-renormalizable*.

The main advantage of this systematic construction of the Lagrangian density given by Eq. (5.2) is unique in the sense that the plane wave solution given by Eq.(4.6) satisfies the equations of motion at every n-th order if one imposes a specific condition on α. Furthermore excitations in nuclei have a narrow region of possible E_k energy values. Studies done with mean field models and also realistic interactions all support this claim. Moreover nuclear calculations using the NCSpM [16] and SA-NCSM [7] indicate that utilizing only one symplectic irrep is enough to recover nearly 70%-80% of the probability distribution. This is sufficient to reproduce nearly 90%-100% of the observables like energy spectra, B(E2) values and radii. This in turn then justifies the fact that symplectic basis states are labeled by N_ω that all have the same energy $\hbar\Omega = 41\mathcal{A}^{-1/3}$ MeV, where we recovered the SI units. This, alongside the imposed condition on α allows us to include all terms up to an arbitrary n-th order. At $n = 0$ the bosons are massless with energy $|E_k| = |\mathbf{k}|$ and for any arbitrary $n > 0$ a mass-like term is introduced through the self interaction that turns out to be the main driver of a $Q \cdot Q$ quadrupole-quadrupole type interaction.

The constructed EFT has to be suitable for describing nuclei, and therefore it is necessary to use discretized fields that we introduced in the previous chapter in Eq. (4.19) through localized plane waves within cubic elements of volume V with periodic boundary conditions. To reiterate, this condition transforms the plane waves into the following discrete form:

$$\varphi(\mathbf{r}, t) = \frac{1}{\sqrt{V}} \sum_{\mathbf{k}} \frac{b^+_{\mathbf{k}}}{\sqrt{|2E_k|}} e^{\iota k^\mu x_\mu} + \frac{b^-_{\mathbf{k}}}{\sqrt{|2E_k|}} e^{-\iota k^\mu x_\mu}, \tag{5.3}$$

where $b^+_{\mathbf{k}}$ creates a boson and $b_{\mathbf{k}}$ destroys a boson respectively with energy $|E_k| = |\mathbf{k}|$ by

acting on a $\left|n_k^b\right\rangle$ state, where n_k^b are the number of bosons with momentum $\mathbf{k}$.

Now that we identified the fields and operators we would like to use them to describe nucleons. Since each nucleon in the nucleus is represented by a pair of fields φ^2 in the EFT (to preserve the parity of each single-nucleon wave function), for a nucleus with $\mathcal{A}$ nucleons the Lagrangian given in Eq. (5.2) has to be generalized to

$$\mathcal{L}^{(n)} = \frac{\alpha^n}{2^{n+1}(n+1)!}\left(\partial_\mu\varphi_p\partial^\mu\varphi_p - nm^2\varphi_p^2\right)^{n+1}, \tag{5.4}$$

which is the Lagrangian of an $\mathcal{A}$-component real scalar field and is O($\mathcal{A}-1$) symmetric ($\mathcal{A}-1$ to remove the center-of-mass contribution). It has been established that the symplectic Sp(3,$\mathbf{R}$) group is a complimentary dual of the O($\mathcal{A}-1$) symmetry group [61] therefore it is symplectic meaning that the resulting Hamiltonian from it preserves symplectic symmetry and doesn't mix configurations belonging to different symplectic irreps. As for the p subscript is denotes the sum over all nucleons in the system described.

5.2 Parameters of SpEFT and the Plane Wave Solution

Let us find the condition on α for which the plane wave solution given by Eq. (4.6) satisfies the equations of motion for the Lagrangian in Eq. (5.2). At a specific n order we will have

$$\partial^\mu\frac{\partial\mathcal{L}^{(n)}}{\partial\varphi_{,\mu}} = \frac{\partial\mathcal{L}^{(n)}}{\partial\varphi}. \tag{5.5}$$

Calculating each derivative yields

$$\frac{\partial\mathcal{L}^{(n)}}{\partial\varphi} = \alpha^n\frac{n+1}{2^n(n+1)!}\left(\partial_\mu\varphi\partial^\mu\varphi - nm^2\varphi^2\right)^n(-nm^2\varphi), \tag{5.6}$$

$$\frac{\partial\mathcal{L}^{(n)}}{\partial\varphi_{,\mu}} = \alpha^n\frac{n+1}{2^n(n+1)!}\left(\partial_\nu\varphi\partial^\nu\varphi - nm^2\varphi^2\right)^n\partial_\mu\varphi, \tag{5.7}$$

$$\partial^\mu \frac{\partial \mathcal{L}^{(n)}}{\partial \varphi_{,\mu}} = \alpha^n \frac{n+1}{2^n(n+1)!}\big(\partial_\eta\varphi\partial^\eta\varphi - nm^2\varphi^2\big)^n \partial^\mu\partial_\mu\varphi$$
$$+\alpha^n \frac{n(n+1)}{2^n(n+1)!}\big(\partial_\eta\varphi\partial^\eta\varphi - nm^2\varphi^2\big)^{n-1}\big(2\partial_\nu\partial^\nu\varphi\partial^\mu\varphi\partial_\mu\varphi - 2nm^2\varphi\partial^\mu\varphi\partial_\mu\varphi\big). \tag{5.8}$$

Now summing over all possible n we get the equation of motion

$$\sum_{n=0}^{\infty} \alpha^n \frac{n+1}{2^n(n+1)!}\big(\partial_\eta\varphi\partial^\eta\varphi - nm^2\varphi^2\big)^n (\partial^\mu\partial_\mu\varphi + nm^2\varphi)$$
$$+\alpha^n \frac{n(n+1)}{2^n(n+1)!}\big(\partial_\eta\varphi\partial^\eta\varphi - nm^2\varphi^2\big)^{n-1}\big(2\partial_\nu\partial^\nu\varphi\partial^\mu\varphi\partial_\mu\varphi - 2nm^2\varphi\partial^\mu\varphi\partial_\mu\varphi\big) = 0. \tag{5.9}$$

Since the total Lagrangian density is $\mathcal{L} = \sum_n \mathcal{L}^{(n)}$ there is a sum over n. For $n = 0$ we will have $\partial^\mu\partial_\mu\varphi = 0$ which is the Klein-Gordon equation for massless bosons and the plane wave solution given in Eq. (4.6) satisfies it with $E^2 = k^2$ therefore the first $n = 0$ term disappears. As for $n > 0$, by plugging $\partial^\mu\partial_\mu\varphi = 0$ into Eq. (5.9) and since $\alpha^n \frac{n+1}{2^n(n+1)!}\big(\partial_\eta\varphi\partial^\eta\varphi - nm^2\varphi^2\big) \neq 0$ otherwise the Lagrangian would be zero so we can take it out of the equation we get

$$\sum_{n=0}^{\infty} \alpha^n \frac{n+1}{2^n(n+1)!}\Big((\partial_\eta\varphi\partial^\eta\varphi - nm^2\varphi^2)(nm^2\varphi) - n(2nm^2\varphi\partial^\mu\varphi\partial_\mu\varphi)\Big) = 0. \tag{5.10}$$

The above equation is not zero however if we pick the magnitude of α correctly for the leading order ($n = 1$) then the above equation can be made to be less than one. Since $\varphi \sim (b^+ + b^-)$ then the average maximum magnitude of $\langle f|\,\varphi\,|i\rangle \sim \sqrt{N_a}$ where $N_a = \sqrt{N_{\omega_f} N_{\omega_i}}$ is the geometric average number of bosons between the initial and final states. Since the above equation of motion is proportional to φ^3 then for $n = 1$ we roughly have

$$\alpha(N_a\sqrt{N_a}) \sim 0. \tag{5.11}$$

Therefore we have the following estimate for the magnitude of α

$$\alpha \sim \frac{1}{N_a\sqrt{N_a}}. \tag{5.12}$$

Establishing this magnitude also allows us to estimate the magnitude of m^2. To do this we need the field derivatives for which we have

$$\partial^\mu \varphi = \frac{1}{(2\pi)^{3/2}} \int_{-\infty}^{+\infty} \iota k_\mu \psi(\mathbf{k}, E) e^{\iota k^\nu x_\nu} dE d\mathbf{k},$$
$$\partial_\mu \varphi \partial^\mu \varphi = -\frac{1}{(2\pi)^3} \int_{-\infty}^{+\infty} \int_{-\infty}^{+\infty} k_{1\mu} k_2^\mu \psi(\mathbf{k}_1, E) \psi(\mathbf{k}_2, E) e^{\iota (k_1^\nu + k_2^\nu) x_\nu} dE_1 d\mathbf{k}_1 dE_2 d\mathbf{k}_2. \tag{5.13}$$

Using these and plugging them into Eq. (5.10) we get the following parametric equation (keeping in mind that for purposes of applying this to nuclei we would only keep one specific value of $E_\mathbf{k} = \hbar\Omega$ and hence the integrals drop out):

$$\sum_{n=1}^{\infty} \big(- |\mathbf{k}_1||\mathbf{k}_2| + \mathbf{k}_1 \cdot \mathbf{k}_2 - nm^2 \big) nm^2 + 2n^2 m^2 \big(|\mathbf{k}_1||\mathbf{k}_2| - \mathbf{k}_1 \cdot \mathbf{k}_2 \big) = 0. \tag{5.14}$$

Which gives the following formula for the mass parameter

$$m^2 = \frac{2n-1}{n} \big(|\mathbf{k}_1||\mathbf{k}_2| - \mathbf{k}_1 \cdot \mathbf{k}_2 \big). \tag{5.15}$$

Therefore this choice of the parameter guarantees that the plane wave satisfies the equation of motion for a specific energy value $|\mathbf{k}_1| = |\mathbf{k}_2| = \sqrt{\frac{g}{n}} \hbar\Omega$. This choice further reduces the formula to the following three cases

$$nm^2 = \begin{cases} g_n \hbar\Omega^2, & \text{if } \mathbf{k}_1 \perp \mathbf{k}_2 \\ 2\hbar\Omega^2, & \text{if } \mathbf{k}_1 \text{ is anti-parallel to } \mathbf{k}_2 \\ 0. & \text{if } \mathbf{k}_1 \text{ is parallel to } \mathbf{k}_2 \end{cases} \tag{5.16}$$

In the above equation where $g_n = \frac{2n-1}{n} g$ was introduced only for the $\mathbf{k}_1 \perp \mathbf{k}_2$ case since it is an effective description to the weight of the resulting interaction from such coupling between the fields, where g captures its strength. Given that α is determined by Eq. (5.12), g is the only parameter that will be fitted from one nuclear system to the other.

5.3 Sp(3,R) Algebra in the Interaction Picture

Since we are constructing a 4-dimensional EFT it is appropriate to represent the symplectic generators in the interaction picture (Heisenberg representation) where the operators explicitly depend on time. This is done through

$$b^{\pm}(t) = b^{\pm}e^{\pm\iota\Omega t}. \tag{5.17}$$

Using this definition and plugging it in Eq. (2.5)

$$\begin{aligned} A_{ij}(t) &= \frac{1}{2}b^{+}_{ip}b^{+}_{jp}e^{2\iota\Omega t}, \\ B_{ij}(t) &= \frac{1}{2}b^{-}_{ip}b^{-}_{jp}e^{-2\iota\Omega t}, \\ C_{ij}(t) &= \frac{1}{2}(b^{+}_{ip}b^{-}_{jp} + b^{-}_{jp}b^{+}_{ip}). \end{aligned} \tag{5.18}$$

The interaction picture clearly states that the symplectic operators A and B are the ones responsible for the dynamics in nuclei that could be described as vibrations in space and time. Whereas C is responsible only for static deformed configurations in nuclei that can rotate freely. This was perhaps implicitly evident from the fact that the Sp(3,$\mathbf{R}$) symmetry (A and B) is the dynamical extension of the SU(3) symmetry (C), but now it is explicitly evident through their representation in the interaction picture.

5.4 SpEFT Hamiltonian Derivation and Hermiticity

The Hamiltonian density at any n order is given by the Legendre transformation

$$\mathcal{H}^{(n)} = \dot{\varphi}\frac{\partial\mathcal{L}^{(n)}}{\partial\dot{\varphi}} - \mathcal{L}^{(n)}. \tag{5.19}$$

Using Eq. (5.7) and $\mu = 0$ (for the time component) we get the following

$$\frac{\partial\mathcal{L}^{(n)}}{\partial\dot{\varphi}} = \alpha^{n}\frac{n+1}{2^{n+1}(n+1)!}\left(\partial_{\nu}\varphi\partial^{\nu}\varphi - nm^{2}\varphi^{2}\right)^{n}2\dot{\varphi}. \tag{5.20}$$

Substituting it back in the Hamiltonian density formula we get

$$\mathcal{H}^{(n)} = \alpha^n \frac{2(n+1)}{2^{n+1}(n+1)!}\big(\partial_\nu\varphi\partial^\nu\varphi - nm^2\varphi^2\big)^n\dot{\varphi}^2 - \frac{\alpha^n}{2^{n+1}(n+1)!}\big(\partial_\mu\varphi\partial^\mu\varphi - nm^2\varphi^2\big)^{n+1}, \tag{5.21}$$

combining the terms we get

$$\mathcal{H}^{(n)} = \frac{\alpha^n}{2^{n+1}(n+1)!}\big(\partial_\nu\varphi\partial^\nu\varphi - nm^2\varphi^2\big)^n\big((2n+1)\dot{\varphi}^2 + \varphi'\cdot\varphi' + nm^2\varphi^2\big). \tag{5.22}$$

The Hamiltonian density in Eq. (5.22) is not Hermitian but the Hamiltonian density in Eq. (5.19) is by definition Hermitian. This is due to the fact when we calculated the term $\frac{\partial\mathcal{L}^{(n)}}{\partial\dot{\varphi}}$ we neglected all possible other combinations of $\dot{\varphi}$ with $\big(\partial_\nu\varphi\partial^\nu\varphi - nm^2\varphi^2\big)$. In reality this term should look like

$$\frac{\partial\mathcal{L}^{(n)}}{\partial\dot{\varphi}} = \alpha^n\frac{2(n+1)}{2^{n+1}(n+1)!}\Bigg(\dot{\varphi}\big(\partial_\nu\varphi\partial^\nu\varphi - nm^2\varphi^2\big)^n + \big(\partial_\nu\varphi\partial^\nu\varphi - nm^2\varphi^2\big)\dot{\varphi}\big(\partial_\nu\varphi\partial^\nu\varphi - nm^2\varphi^2\big)^{n-1}$$
$$+\big(\partial_\nu\varphi\partial^\nu\varphi - nm^2\varphi^2\big)^2\dot{\varphi}\big(\partial_\nu\varphi\partial^\nu\varphi - nm^2\varphi^2\big)^{n-2} + ... + \big(\partial_\nu\varphi\partial^\nu\varphi - nm^2\varphi^2\big)^n\dot{\varphi}\Bigg). \tag{5.23}$$

As evident from Eq. (5.23) there are $n+1$ terms which are different combinations of $\dot{\varphi}$ with $\big(\partial_\nu\varphi\partial^\nu\varphi - nm^2\varphi^2\big)$. This results into the following Hamiltonian density

$$\mathcal{H}^{(n)} = \frac{\alpha^n}{2^{n+1}(n+1)!}\Bigg(\big((2n+1)\dot{\varphi}^2 + \varphi'\cdot\varphi' + nm^2\varphi^2\big)\big(\partial_\nu\varphi\partial^\nu\varphi - nm^2\varphi^2\big)^n$$
$$+\big(\partial_\nu\varphi\partial^\nu\varphi - nm^2\varphi^2\big)\big((2n+1)\dot{\varphi}^2 + \varphi'\cdot\varphi' + nm^2\varphi^2\big)\big(\partial_\nu\varphi\partial^\nu\varphi - nm^2\varphi^2\big)^{n-1}$$
$$+\big(\partial_\nu\varphi\partial^\nu\varphi - nm^2\varphi^2\big)\big((2n+1)\dot{\varphi}^2 + \varphi'\cdot\varphi' + nm^2\varphi^2\big)\big(\partial_\nu\varphi\partial^\nu\varphi - nm^2\varphi^2\big)^{n-2}$$
$$+..... + \big(\partial_\nu\varphi\partial^\nu\varphi - nm^2\varphi^2\big)^n\big((2n+1)\dot{\varphi}^2 + \varphi'\cdot\varphi' + nm^2\varphi^2\big)\Bigg). \tag{5.24}$$

The above Hamiltonian density is Hermitian. Since the formula for the Hamiltonian density is very long we refrained from writing down all the terms and limited ourselves to only the

$n+1$-th term because it is easier for purposes of deriving a quantum mechanical Hamiltonian applicable for describing nuclear phenomena. However all terms are included in matrix element calculations up to an n-th order. Note that we also refrained from writing down all possible $n!$ combinations of $\left(\partial_\nu\varphi\partial^\nu\varphi - nm^2\varphi^2\right)$ with itself since they are all identical for matrix element calculations, hence the normalization factor of $(n+1)!$: $n!$ for identical combinations of $\left(\partial_\nu\varphi\partial^\nu\varphi - nm^2\varphi^2\right)$ combined with $n+1$ combinations with the $\left((2n+1)\dot{\varphi}^2 + \varphi'\cdot\varphi' + nm^2\varphi^2\right)$ term as we saw above.

Recovering the particle number for the fields, we have the following expression for the n-th order Hamiltonian

$$\mathcal{H}^{(n)} = \frac{\alpha^n}{2^{n+1}(n+1)!}\left(\dot{\varphi}^2_{p_1} - \varphi'_{p_1}\cdot\varphi'_{p_1} - nm^2\varphi^2_{p_1}\right)^n\left((2n+1)\dot{\varphi}^2_{p_2} + \varphi'_{p_2}\cdot\varphi'_{p_2} + nm^2\varphi^2_{p_2}\right). \tag{5.25}$$

The total Hamiltonian density at n-th order is a sum over all possible $n+1$ combinations of the $(n+1)$-th term in the second paranthesis in Eq. (5.25) with respect to the n terms in the first paranthesis.

The coupled fields in Eq. (5.25) are

$$\begin{aligned}
\varphi^2_p &= \frac{1}{V}\sum_{\mathbf{k},\mathbf{q}}\frac{1}{\sqrt{|2E_k||2E_q|}}\left(b^+_{p\mathbf{k}}e^{\iota k^\mu x_\mu} + b^-_{p\mathbf{k}}e^{-\iota k^\mu x_\mu}\right)\left(b^+_{p\mathbf{q}}e^{\iota q^\mu x_\mu} + b^-_{p\mathbf{q}}e^{-\iota q^\mu x_\mu}\right),\\
\dot{\varphi}^2_p &= \frac{1}{V}\sum_{\mathbf{k},\mathbf{q}}\frac{\iota E_k}{\sqrt{|2E_k|}}\frac{\iota E_q}{\sqrt{|2E_q|}}\left(b^+_{p\mathbf{k}}e^{\iota k^\mu x_\mu} - b^-_{p\mathbf{k}}e^{-\iota k^\mu x_\mu}\right)\left(b^+_{p\mathbf{q}}e^{\iota q^\mu x_\mu} - b^-_{p\mathbf{q}}e^{-\iota q^\mu x_\mu}\right),\\
\varphi'_p\cdot\varphi'_p &= \frac{1}{V}\sum_{\mathbf{k},\mathbf{q}}\frac{(-\iota\mathbf{k})}{\sqrt{|2E_k|}}\frac{(-\iota\mathbf{q})}{\sqrt{|2E_q|}}\left(b^+_{p\mathbf{k}}e^{\iota k^\mu x_\mu} - b^-_{p\mathbf{k}}e^{-\iota k^\mu x_\mu}\right)\left(b^+_{p\mathbf{q}}e^{\iota q^\mu x_\mu} - b^-_{p\mathbf{q}}e^{-\iota q^\mu x_\mu}\right).
\end{aligned} \tag{5.26}$$

From here on we will drop the index p denoting the sum over particle numbers from the fields above for convenience since they don't affect any of the derivations and will recover them at the end. As evident from the formulas above the creation and annihilation operators enter into the Hamiltonian in pairs of b^+b^+, b^-b^-, b^+b^- and b^-b^+. This allows us to describe them through the symplectic operators defined in Eqs. (5.18). This definition now will allow us

to transition from $\left|n_k^b\right\rangle$ to $|\sigma\rangle$ where N_ω will be equivalent to a state with number of bosons n_k^b created (destroyed) by $b_{\mathbf{k}}^+(b_{\mathbf{k}}^-)$ with momentum $\mathbf{k}$. Knowing this we can rewrite the fields in Eqs. (5.26) as

$$\begin{aligned}
\varphi^2 &= \frac{1}{V}\sum_{\mathbf{k},\mathbf{q}} \frac{1}{\sqrt{|2E_k||2E_q|}}\Big(Z_{\mathbf{k}}^+ Z_{\mathbf{q}}^+ + Z_{\mathbf{k}}^- Z_{\mathbf{q}}^- + Z_{\mathbf{k}}^+ Z_{\mathbf{q}}^- + Z_{\mathbf{k}}^- Z_{\mathbf{q}}^+\Big),\\
\dot{\varphi}^2 &= \frac{1}{V}\sum_{\mathbf{k},\mathbf{q}} \frac{\iota E_k}{\sqrt{|2E_k|}}\frac{\iota E_q}{\sqrt{|2E_q|}}\Big(Z_{\mathbf{k}}^+ Z_{\mathbf{q}}^+ + Z_{\mathbf{k}}^- Z_{\mathbf{q}}^- - Z_{\mathbf{k}}^+ Z_{\mathbf{q}}^- - Z_{\mathbf{k}}^- Z_{\mathbf{q}}^+\Big),\\
\varphi'\cdot\varphi' &= \frac{1}{V}\sum_{\mathbf{k},\mathbf{q}} \frac{(-\iota\mathbf{k})}{\sqrt{|2E_k|}}\frac{(-\iota\mathbf{q})}{\sqrt{|2E_q|}}\Big(Z_{\mathbf{k}}^+ Z_{\mathbf{q}}^+ + Z_{\mathbf{k}}^- Z_{\mathbf{q}}^- - Z_{\mathbf{k}}^+ Z_{\mathbf{q}}^- - Z_{\mathbf{k}}^- Z_{\mathbf{q}}^+\Big),
\end{aligned} \tag{5.27}$$

where we used the following notation

$$Z_{\mathbf{k}}^{\pm} = b_{\mathbf{k}}^{\pm} e^{\pm\iota k^\mu x_\mu}. \tag{5.28}$$

Substituting the formulas for the fields given in Eqs. (5.27) into the Hamiltonian density in Eq. (5.25) we get

$$\mathcal{H}^{(n)} = \frac{1}{2^{n+1}(n+1)!}\sum_{\mathbf{k}_1\mathbf{k}_2\ldots\mathbf{k}_{n+1}\mathbf{q}_1\mathbf{q}_2\cdots\mathbf{q}_{n+1}} \frac{\mathcal{Z}_1\mathcal{Z}_2.....\mathcal{Z}_n\Xi_{n+1}}{2^{n+1}\sqrt{E_{k_1}E_{k_2}.....E_{k_n+1}E_{q_1}E_{q_2}.....E_{q_n+1}}}\frac{\alpha^n}{V^{n+1}}, \tag{5.29}$$

where we used the following notations

$$\mathcal{Z}_n = \Big((-E_{k_n}E_{q_n}+\mathbf{k}_n\cdot\mathbf{q}_n-nm^2)(Z_{\mathbf{k}_n}^+Z_{\mathbf{q}_n}^+ + Z_{\mathbf{k}_n}^-Z_{\mathbf{q}_n}^-) - (-E_{k_n}E_{q_n}+\mathbf{k}_n\cdot\mathbf{q}_n+nm^2)(Z_{\mathbf{k}_n}^+Z_{\mathbf{q}_n}^- + Z_{\mathbf{k}_n}^-Z_{\mathbf{q}_n}^+)\Big).$$

$$\begin{aligned}
\Xi_{n+1} = \Big((&-(2n+1)E_{k_{n+1}}E_{q_{n+1}} - \mathbf{k}_{n+1}\cdot\mathbf{q}_{n+1} + nm^2)(Z_{\mathbf{k}_{n+1}}^+Z_{\mathbf{q}_{n+1}}^+ + Z_{\mathbf{k}_{n+1}}^-Z_{\mathbf{q}_{n+1}}^-)\\
&-(-(2n+1)E_{k_{n+1}}E_{q_{n+1}} - \mathbf{k}_{n+1}\cdot\mathbf{q}_{n+1} - nm^2)(Z_{\mathbf{k}_{n+1}}^+Z_{\mathbf{q}_{n+1}}^- + Z_{\mathbf{k}_{n+1}}^-Z_{\mathbf{q}_{n+1}}^+)\Big).
\end{aligned} \tag{5.30}$$

Now that we substituted in the fields we will finally calculate the Hamiltonian H.

5.5 Diagonal Coupling and Monopole Hamiltonian

The Hamiltonian is

$$H = \int_{-L}^{+L} \mathcal{H} dV. \tag{5.31}$$

Integrating $\mathcal{H}$, we notice that for every order n we have $n+1$ pairs of Z^+Z^+, Z^+Z^- and their conjugates multiplied with each other inside the integration. Let us consider a term like Z^+Z^+, for example, for the simplest case $n=0$, which gives a term like

$$\int_{-L}^{+L} b^+_{\mathbf{k}}(t) b^+_{\mathbf{q}}(t) e^{i(\mathbf{k}+\mathbf{q})\cdot\mathbf{r}} dV, \tag{5.32}$$

where we absorbed the time component of the exponent into the operators. This integral is zero because of the periodic boundary condition on $\mathbf{k}$ and $\mathbf{q}$ unless $\mathbf{k}+\mathbf{q}=0$. To generalize for $n+1$ pairs, each term Z^+Z^+ and Z^-Z^- has to have $\mathbf{k}+\mathbf{q}=0$, and each term Z^+Z^- and Z^-Z^+ has to have $\mathbf{k}-\mathbf{q}=0$. We call this "diagonal coupling" because for each pair in the integral we couple $\mathbf{k}$ to $\mathbf{q}$ for example $\mathbf{k}_1$ to $\mathbf{q}_1$, $\mathbf{k}_2$ to $\mathbf{q}_2$ and $\mathbf{k}_n$ to $\mathbf{q}_n$, etc. The result of this simple coupling is that each $\mathcal{Z}$ term in Eq. (5.29) doesn't interact with other similar terms, meaning the sums don't mix with each other inside the integral. This is the reason why $m^2 = \frac{2n-1}{n}(2E_k^2)$ (for anti-parallel case) doesn't include g_n which is a representative of that mixing. Similar to what we did for the HO Hamiltonian derivation we will pick $\mathbf{k}=-\mathbf{q}$ for Z^+Z^+ and Z^-Z^-, and pick $\mathbf{k}=\mathbf{q}$ for Z^+Z^- and Z^-Z^+ so they will survive the integration over the volume which results to

$$H^{(n)} = \frac{1}{2^{n+1}(n+1)!}\sum_{\mathbf{k}_1\mathbf{k}_2\ldots\mathbf{k}_{n+1}}\frac{1}{2^{n+1}E_{k_1}E_{k_2}.....E_{k_n+1}}\frac{\alpha^n}{V^n}\times$$
$$\Big((-E_{k_1}^2-\mathbf{k}_1^2-nm^2)(Z_{\mathbf{k}_1}^+Z_{-\mathbf{k}_1}^+ + Z_{\mathbf{k}_1}^-Z_{-\mathbf{k}_1}^-) - (-E_{k_1}^2+\mathbf{k}_1^2+nm^2)(Z_{\mathbf{k}_1}^+Z_{\mathbf{k}_1}^- + Z_{\mathbf{k}_1}^-Z_{\mathbf{k}_1}^+)\Big)\times$$
$$\Big((-E_{k_2}^2-\mathbf{k}_2^2-nm^2)(Z_{\mathbf{k}_2}^+Z_{-\mathbf{k}_2}^+ + Z_{\mathbf{k}_2}^-Z_{-\mathbf{k}_2}^-) - (-E_{k_2}^2+\mathbf{k}_2^2+nm^2)(Z_{\mathbf{k}_2}^+Z_{\mathbf{k}_2}^- + Z_{\mathbf{k}_2}^-Z_{\mathbf{k}_2}^+)\Big)\times$$
$$.....\times$$
$$\Big((-E_{k_n}^2-\mathbf{k}_n^2-nm^2)(Z_{\mathbf{k}_n}^+Z_{-\mathbf{k}_n}^+ + Z_{\mathbf{k}_n}^-Z_{-\mathbf{k}_n}^-) - (-E_{k_n}^2+\mathbf{k}_n^2+nm^2)(Z_{\mathbf{k}_n}^+Z_{\mathbf{k}_n}^- + Z_{\mathbf{k}_n}^-Z_{\mathbf{k}_n}^+)\Big)\times$$
$$\Big((-(2n+1)E_{k_{n+1}}^2+\mathbf{k}_{n+1}^2+nm^2)(Z_{\mathbf{k}_{n+1}}^+Z_{-\mathbf{k}_{n+1}}^+ + Z_{\mathbf{k}_{n+1}}^-Z_{-\mathbf{k}_{n+1}}^-)$$
$$-(-(2n+1)E_{k_{n+1}}^2-\mathbf{k}_{n+1}^2-nm^2)(Z_{\mathbf{k}_{n+1}}^+Z_{\mathbf{k}_{n+1}}^- + Z_{\mathbf{k}_{n+1}}^-Z_{\mathbf{k}_{n+1}}^+)\Big). \tag{5.33}$$

But $E_{k_1}^2 = \mathbf{k}_1^2$ and using the definiton of $\mathbf{k} = -\mathbf{q}$ and $m^2 = 0$ for $\mathbf{k} = \mathbf{q}$ by definition which further reduces Eq. (5.33) to

$$H^{(n)} = \frac{1}{2^{n+1}(n+1)!}\sum_{\mathbf{k}_1\mathbf{k}_2\ldots\mathbf{k}_{n+1}}\frac{1}{2^{n+1}E_{k_1}E_{k_2}.....E_{k_n+1}}\frac{\alpha^n}{V^n}\times$$
$$\Big((-2E_{k_1}^2-2(2n-1)E_{k_1}^2)(b_{\mathbf{k}_1}^+b_{-\mathbf{k}_1}^+e^{2\iota E_{k_1}t} + b_{\mathbf{k}_1}^-b_{-\mathbf{k}_1}^-e^{-2\iota E_{k_1}t})\Big)\times$$
$$.....\times\Big((-2E_{k_n}^2-2(2n-1)E_{k_n}^2)(b_{\mathbf{k}_n}^+b_{-\mathbf{k}_n}^+e^{2\iota E_{k_n}t} + b_{\mathbf{k}_n}^-b_{-\mathbf{k}_n}^-e^{-2\iota E_{k_n}t})\Big)\times$$
$$\Big(-2E_{k_{n+1}}^2(b_{\mathbf{k}_{n+1}}^+b_{-\mathbf{k}_{n+1}}^+e^{2\iota E_{k_{n+1}}t} + b_{\mathbf{k}_{n+1}}^-b_{-\mathbf{k}_{n+1}}^-e^{-2\iota E_{k_{n+1}}t})$$
$$+(2n+2)E_{k_{n+1}}^2(b_{\mathbf{k}_{n+1}}^+b_{\mathbf{k}_{n+1}}^- + b_{\mathbf{k}_{n+1}}^-b_{\mathbf{k}_{n+1}}^+)\Big). \tag{5.34}$$

Comparing the terms in the Hamiltonian to the symplectic operators defined in Eq. (5.18), it is easy to see that this Hamiltonian is symplectic in nature. What we mean is that symplectic symmetry emerges naturally from the EFT Lagrangian in Eq. (5.2) whose sole construction was done naturally by extending the harmonic oscillator Lagrangian into its n-th order. This implies that symplectic symmetry is an extension of the SU(3) symmetry of

the harmonic oscillator which algebraically was known and well understood through nuclear physics applications, but now it is evident that its origin is much more fundamental than previously thought.

In our effective field theory the nucleons are represented through their total energy quanta (bosons), which in turn can be created and destroyed with all possible energy values. This could be imagined as having infinite quantum mechanical harmonic oscillator systems, each with E_k where the nucleons are contained. Its application on a symplectic state further reduces this Hamiltonian. Only one term from each sum over $\mathbf{k}$ will survive namely the term where $E_k = \hbar\Omega$ which gives us

$$\begin{aligned} H^{(n)} = \frac{(-1)^n}{2^{n+1}(n+1)!}\frac{1}{2^{n+1}(\hbar\Omega)^{n+1}}\frac{\alpha^n}{V^n}\times \\ \Big(4n\hbar\Omega^2(b^+_{\mathbf{k}_1}b^+_{-\mathbf{k}_1}e^{2\iota\Omega t} + b^-_{\mathbf{k}_1}b^-_{-\mathbf{k}_1}e^{-2\iota\Omega t})\Big)\Big(4n\hbar\Omega^2(b^+_{\mathbf{k}_2}b^+_{-\mathbf{k}_2}e^{2\iota\Omega t} + b^-_{\mathbf{k}_2}b^-_{-\mathbf{k}_2}e^{-2\iota\Omega t})\Big)\times \\ ..... \times \Big(4n\hbar\Omega^2(b^+_{\mathbf{k}_n}b^+_{-\mathbf{k}_n}e^{2\iota\Omega t} + b^-_{\mathbf{k}_n}b^-_{-\mathbf{k}_n}e^{-2\iota\Omega t})\Big) \\ \times\Big(- 2\hbar\Omega^2(b^+_{\mathbf{k}_{n+1}}b^+_{-\mathbf{k}_{n+1}}e^{2\iota\Omega t} + b^-_{\mathbf{k}_{n+1}}b^-_{-\mathbf{k}_{n+1}}e^{-2\iota\Omega t}) + (2n+2)\hbar\Omega^2(b^+_{\mathbf{k}_{n+1}}b^-_{\mathbf{k}_{n+1}} + b^-_{\mathbf{k}_{n+1}}b^+_{\mathbf{k}_{n+1}})\Big). \end{aligned} \tag{5.35}$$

Now using the definitions in Eqs. (5.18), keeping in mind that we accounted for all possible combinations of the terms in respect to exchanging places with each other therefore the factorial term in front reduces to unity as discussed earlier and recovering the particle numbers we get

$$H^{(n)}_d(t) = \frac{(-n)^n}{2^{n+1}}\frac{4^{n+1}(\hbar\Omega)^{2(n+1)}}{2^{n+1}(\hbar\Omega)^{n+1}}\frac{\alpha^n}{V^n}(2A_{ii}+2B_{ii})^n\big(-2(A_{jj}+B_{jj})+(2n+2)C_{jj}\big). \tag{5.36}$$

Carrying out the necessary reductions we will finally get

$$H^{(n)}_d(t) = \begin{cases} (-n)^n(2\hbar\Omega)^{n+1}\frac{\alpha^n}{V^n}(A_{ii}+B_{ii})^n\big((n+1)C_{jj}-(A_{jj}+B_{jj})\big), & \text{if } n\geq 1 \\ \hbar\Omega C_{ii}. & \text{if } n=0 \end{cases} \tag{5.37}$$

The symplectic operators are time dependent and we represent this by $H \rightarrow H(t)$ in Eq. (5.37). This is a quantum mechanical Hamiltonian that is the natural extension to the harmonic oscillator Hamiltonian for $n \geq 1$ which represents a one-body interaction extended to arbitrary n order. It resulted from the diagonal coupling discussed above hence the d subscript and is solely responsible for generating monopole excitations in nuclei which do not contribute to the dynamics since they are just powers of $A_{ii} + B_{ii}$. They destroy the Leading order harmonic oscillator at every $n \geq 1$ which is unphysical and hence they have to be removed from the final Hamiltonian. What is responsible for dynamics are vibrations in space and time which result from the quadrupole excitations in nuclei that a result from off-diagonal couplings in the Hamiltonian in Eq. (5.29). The only term from the diagonal coupling that contributes to the Hamiltonian is the harmonic oscillator which is $H^{(0)} = \hbar\Omega C_{ii}$.

5.6 Off-Diagonal Coupling and Quadrupole Hamiltonian

In this section, we consider two pairs of Z^+Z^+, for example inside the integral resulting from multiplying two $\mathcal{Z}$ in Eq. (5.29), namely,

$$\int_{-L}^{+L} b^+_{\mathbf{k}_1}(t) b^+_{\mathbf{q}_1}(t) b^+_{\mathbf{k}_2}(t) b^+_{\mathbf{q}_2}(t) e^{i(\mathbf{k}_1+\mathbf{q}_1+\mathbf{k}_2+\mathbf{q}_2)\cdot\mathbf{r}} dV. \tag{5.38}$$

For $n = 1$, which as we discussed before, will be zero unless $\mathbf{k}_1 + \mathbf{q}_1 + \mathbf{k}_2 + \mathbf{q}_2 = 0$. We managed this before by picking $\mathbf{k}_1 + \mathbf{q}_1 = 0$ and $\mathbf{k}_2 + \mathbf{q}_2 = 0$, etc., which resulted to the diagonal coupling. However there are many possibilities to make $\mathbf{k}_1+\mathbf{q}_1+\mathbf{k}_2+\mathbf{q}_2 = 0$. What is particularly interesting is if we choose $\mathbf{k}_1+\mathbf{q}_2 = 0$ and $\mathbf{k}_2+\mathbf{q}_1 = 0$. This results into a pair of $A_{\mathbf{k}_1-\mathbf{k}_2}A_{\mathbf{k}_2-\mathbf{k}_1}$ which creates a boson pair with momentum $\mathbf{k}_1$ and $-\mathbf{k}_2$ respectively and create another pair with momentum $\mathbf{k}_2$ and $-\mathbf{k}_1$ respectively such as the total momentum of both pairs is conserved. If we pick $\mathbf{k}_1 = -\mathbf{k}_2$ this will result to the diagonal coupling Hamiltonian in Eq. (5.37) derived in the previous section. However we can pick $|\mathbf{k}_1| = |\mathbf{k}_2|$ such that $\mathbf{k}_1 \perp \mathbf{k}_2$. This reduces $A_{\mathbf{k}_1-\mathbf{k}_2}A_{\mathbf{k}_2-\mathbf{k}_1}$ to $A_{ij}A_{ji}$ which creates two boson pairs in

the i-th and j-th direction such that $i \neq j$. The same argument applies to other terms like $Z^+Z^+Z^-Z^-$, $Z^+Z^+Z^+Z^-$, $Z^+Z^+Z^+Z^-$, $Z^-Z^-Z^+Z^-$ etc. The expression for the off-diagonal Hamiltonian depends on n. If n is odd then we have $n+1$ even pairs of $Z^{\pm}$ that all could be coupled to each other resulting into $(n-1)/2$ identical pairs and one unique pair. If n is even then we have $n+1$ odd pairs, from which we can form either $n/2$ identical pairs, and a unique pair or $(n-2)/2$ identical pairs and two unique pairs. This results into three off-diagonal Hamiltonians, one for odd n and two for even n for $n > 0$, since for $n = 0$ only diagonal coupling is possible. The resulting expressions will contain terms like $A_{ij}A_{ji}$, $C_{ij}C_{ji}$, $B_{ij}C_{ji}$ etc., which can be represented in terms of Q_{ij} and K_{ij} resulting into three expansions that together with the HO Hamiltonian will form the final desired quantum mechanical Hamiltonian. The off-diagonal coupling will result to the following possible couplings $\forall n$ of all possible terms in pairs that survive the integration over the volume of the Hamiltonian in Eq. (5.29). After coupling terms in Eq. (5.29) off-diagonally we are interested in applying

Table 5.1. All possible couplings in pairs of two Z operators. There are 16 possible terms. Only 8 are shown since the other 8 are conjugates and have identical couplings.

$Z^+_{\mathbf{k}_n} Z^+_{\mathbf{q}_n} Z^+_{\mathbf{k}_{n+1}} Z^+_{\mathbf{q}_{n+1}}$	$\mathbf{k}_n = -\mathbf{q}_{n+1}, \mathbf{k}_{n+1} = -\mathbf{q}_n$
$Z^+_{\mathbf{k}_n} Z^+_{\mathbf{q}_n} Z^-_{\mathbf{k}_{n+1}} Z^-_{\mathbf{q}_{n+1}}$	$\mathbf{k}_n = \mathbf{q}_{n+1}, \mathbf{k}_{n+1} = \mathbf{q}_n$
$Z^+_{\mathbf{k}_n} Z^+_{\mathbf{q}_n} Z^+_{\mathbf{k}_{n+1}} Z^-_{\mathbf{q}_{n+1}}$	$\mathbf{k}_n = \mathbf{q}_{n+1}, \mathbf{k}_{n+1} = -\mathbf{q}_n$
$Z^+_{\mathbf{k}_n} Z^+_{\mathbf{q}_n} Z^-_{\mathbf{k}_{n+1}} Z^+_{\mathbf{q}_{n+1}}$	$\mathbf{k}_n = -\mathbf{q}_{n+1}, \mathbf{k}_{n+1} = \mathbf{q}_n$
$Z^+_{\mathbf{k}_n} Z^-_{\mathbf{q}_n} Z^+_{\mathbf{k}_{n+1}} Z^-_{\mathbf{q}_{n+1}}$	$\mathbf{k}_n = \mathbf{q}_{n+1}, \mathbf{k}_{n+1} = \mathbf{q}_n$
$Z^+_{\mathbf{k}_n} Z^-_{\mathbf{q}_n} Z^-_{\mathbf{k}_{n+1}} Z^+_{\mathbf{q}_{n+1}}$	$\mathbf{k}_n = -\mathbf{q}_{n+1}, \mathbf{k}_{n+1} = -\mathbf{q}_n$
$Z^-_{\mathbf{k}_n} Z^+_{\mathbf{q}_n} Z^-_{\mathbf{k}_{n+1}} Z^+_{\mathbf{q}_{n+1}}$	$\mathbf{k}_n = \mathbf{q}_{n+1}, \mathbf{k}_{n+1} = \mathbf{q}_n$

it to a symplectic state, which results to a quantum mechanical Hamiltonian. To avoid diagonal terms like A_{ii} B_{ii} and C_{ii} resulted from $\mathbf{k}_n = \mathbf{k}_{n+1}$ $\forall n$ we pick $|\mathbf{k}_n| = |\mathbf{k}_{n+1}|$ such that $\mathbf{k}_n \perp \mathbf{k}_{n+1}$ $\forall n$. This results into terms like $A_{ij}A_{ji}$ for example. As discussed for any

two $\mathcal{Z}$ in Eq. (5.29) we have

$$\begin{aligned}
&4(E^2+nm^2)^2(A_{ij}A_{ji}+B_{ij}B_{ji}+A_{ij}B_{ji}+B_{ij}A_{ji})\\
&-4(E^4-n^2m^4)(A_{ij}\mathcal{Q}_{ji}+B_{ij}\mathcal{Q}_{ji}+\mathcal{Q}_{ij}B_{ji}+\mathcal{Q}_{ij}A_{ji})\\
&+4(E^2-nm^2)^2\mathcal{Q}_{ij}\mathcal{Q}_{ji}. \qquad (5.39)
\end{aligned}$$

Expressing the symplectic operators in Eq. (5.39) in terms of the quadrupole and kinetic tensors we get

$$\begin{aligned}
&(E^2+nm^2)^2(Q_{ij}Q_{ji}+K_{ij}K_{ji}-Q_{ij}K_{ji}-K_{ij}Q_{ji})\\
&-(E^4-n^2m^4)(2Q_{ij}Q_{ji}-2K_{ij}K_{ji})\\
&+(E^2-nm^2)^2(Q_{ij}Q_{ji}+K_{ij}K_{ji}+Q_{ij}K_{ji}+K_{ij}Q_{ji})=\\
&4n^2m^4Q_{ij}Q_{ji}+4E^4K_{ij}K_{ji}-4nm^2E^2(Q_{ij}K_{ji}+K_{ij}Q_{ji}). \qquad (5.40)
\end{aligned}$$

As for the unique term resulting from coupling the $\mathcal{Z}_n$-th term to Ξ_{n+1}-th term in Eq. (5.29) we have

$$\begin{aligned}
&4((2n+1)E^4-n^2m^4+2n^2m^2E^2)(A_{ij}A_{ji}+B_{ij}B_{ji}+A_{ij}B_{ji}+B_{ij}A_{ji})\\
&+4(-(2n+1)E^4-n^2m^4-2(n+1)nm^2E^2)(A_{ij}\mathcal{Q}_{ji}+B_{ij}\mathcal{Q}_{ji})\\
&+4(-(2n+1)E^4-n^2m^4+2(n+1)nm^2E^2)(\mathcal{Q}_{ij}B_{ji}+\mathcal{Q}_{ij}A_{ji})\\
&+4((2n+1)E^4-n^2m^4-2n^2m^2E^2)\mathcal{Q}_{ij}\mathcal{Q}_{ji}. \qquad (5.41)
\end{aligned}$$

Expressing the symplectic operators in Eq. (5.41) in terms of the quadrupole and kinetic tensors we get

$$\begin{aligned}
&((2n+1)E^4 - n^2m^4 + 2n^2m^2E^2)(Q_{ij}Q_{ji} + K_{ij}K_{ji} - Q_{ij}K_{ji} - K_{ij}Q_{ji}) \\
&+(-(2n+1)E^4 - n^2m^4 - 2(n+1)nm^2E^2)(Q_{ij}Q_{ji} - K_{ij}K_{ji} + Q_{ij}K_{ji} - K_{ij}Q_{ji}) \\
&+(-(2n+1)E^4 - n^2m^4 + 2(n+1)nm^2E^2)(Q_{ij}Q_{ji} - K_{ij}K_{ji} - Q_{ij}K_{ji} + K_{ij}Q_{ji}) \\
&+((2n+1)E^4 - n^2m^4 - 2n^2m^2E^2)(Q_{ij}Q_{ji} + K_{ij}K_{ji} + Q_{ij}K_{ji} + K_{ij}Q_{ji}). \qquad (5.42)
\end{aligned}$$

Finally combining them gives

$$\begin{aligned}
&-4n^2m^4Q_{ij}Q_{ji} + 4(2n+1)E^4K_{ij}K_{ji} \\
&-4n^2m^2E^2(Q_{ij}K_{ji} + K_{ij}Q_{ji}) \\
&-4(n+1)nm^2E^2(Q_{ij}K_{ji} - K_{ij}Q_{ji}). \qquad (5.43)
\end{aligned}$$

Note that the last term in Eq. (5.43) is not Hermitian. However as we explained in section 5.4, there will be a Hermitian conjugate term resulting from other possible perturbations. For every possible term where we have $(Q_{ij}K_{ji} - K_{ij}Q_{ji})$ we will get its conjugate from other perturbations resulting to $-(Q_{ij}K_{ji} - K_{ij}Q_{ji})$ which cancel each other. Keeping this in mind, we get the following for the Hamiltonian for an arbitrary odd n where $E = \hbar\Omega$

$$\begin{aligned}
H_{od}^{(n=odd)}(t) = &\frac{(n+1)!}{2^{n+1}(n+1)!}\frac{\hbar\Omega^{2(n+1)}}{(2\hbar\Omega)^{n+1}}\frac{\alpha^n}{V^n}\times \\
&\big(4g_n^2Q_{ij}Q_{ji} + 4K_{ij}K_{ji} - 4g_n\{Q_{ij}, K_{ji}\}\big)^{(n-1)/2}\times \\
&\big(-4g_n^2Q_{ij}Q_{ji} + 4(2n+1)K_{ij}K_{ji} - 4ng_n\{Q_{ij}, K_{ji}\}\big), \qquad (5.44)
\end{aligned}$$

where the *od* denotes the off-diagonal coupling and $\{Q_{ij}, K_{ji}\}$ is the anti-commutator. Canceling the coefficients we get

$$H_{od}^{(n=odd)}(t) = \frac{(\hbar\Omega)^{n+1}}{2^{n+1}}\frac{\alpha^n}{V^n}\big(g_n^2 Q_{ij}Q_{ji} + K_{ij}K_{ji} - g_n\{Q_{ij}, K_{ji}\}\big)^{(n-1)/2}\times \\ \big(-g_n^2 Q_{ij}Q_{ji} + (2n+1)K_{ij}K_{ji} - ng_n\{Q_{ij}, K_{ji}\}\big). \tag{5.45}$$

For $n > 0$ and $n = even$ we have two options, as discussed. The first option is to couple all identical terms off-diagonally and couple the $n+1$-th term diagonally which results to

$$H_{od}^{(n=even)}(t) = \frac{(\hbar\Omega)^{n+1}}{2^{n+1}}\frac{\alpha^n}{V^n}\big(g_n^2 Q_{ij}Q_{ji} + K_{ij}K_{ji} - g_n\{Q_{ij}, K_{ji}\}\big)^{n/2}\times \\ \big((n+1)C_{ll} - (A_{ll} + B_{ll})\big). \tag{5.46}$$

The other possibility is having one of the identical terms coupled diagonally and the rest off-diagonally which gives terms proportional to powers of $(A_{ll} + B_{ll})$ and therefore we won't consider them either since they also destroy the harmonic oscillator structure.

Combining the Hamiltonian expansion terms we get the final Hamiltonian that is

$$H(t) = \hbar\Omega C_{ii} + \sum_{n=odd}\frac{(\hbar\Omega)^{n+1}}{2^{n+1}}\frac{\alpha^n}{V^n}\big(g_n^2 Q_{ij}Q_{ji} + K_{ij}K_{ji} - g_n\{Q_{ij}, K_{ji}\}\big)^{(n-1)/2}\times \\ \big(-g_n^2 Q_{ij}Q_{ji} + (2n+1)K_{ij}K_{ji} - ng_n\{Q_{ij}, K_{ji}\}\big) \\ + \sum_{n=even}\frac{(\hbar\Omega)^{n+1}}{2^{n+1}}\frac{\alpha^n}{V^n}\big(g_n^2 Q_{ij}Q_{ji} + K_{ij}K_{ji} - g_n\{Q_{ij}, K_{ji}\}\big)^{n/2}\big((n+1)C_{ll} - (A_{jj} + B_{jj})\big). \tag{5.47}$$

Each n-th term in this Hamiltonian is a $n+1$-body interaction. Therefore our Hamiltonian includes all possible interaction terms up to infinity except the ones resulting from triple, four or higher off-diagonal coupling terms that can also produce a new power series of three-body and four-body interaction terms, for example like $Q_{ij}Q_{jf}Q_{fi}$ and $Q_{ij}Q_{jf}Q_{fl}Q_{li}$ respectively. We will not cover these within the scope of this thesis and will limit ourselves only up to

two off-diagonal coupling terms, and the resulting interactions and their respective powers.

The resulting Hamiltonian from the EFT in Eq. (5.47) is effectively a two parameter theory, namely $\frac{\alpha}{V}\hbar\Omega$ and g_n. The first parameter α which has the dimension of inverse energy density and therefore $\frac{\alpha}{V}$ will have dimensions of inverse energy $[\frac{\alpha}{V}] = -1$. Multiplying it with $\hbar\Omega$ will give us the desired dimensionless parameter of the theory $\frac{\alpha}{V}\hbar\Omega$. In Eq. (5.12) we showed that $\alpha \sim 1/N_a^{3/2}$ in order for the plane wave solution to be justified. To recover its full dimensions it is appropriate to pick $\alpha = \frac{V_{\mathcal{A}}}{N_a^{3/2}\hbar\Omega}$ where $V_{\mathcal{A}} = \frac{4}{5}\pi R^3$ and $R = 1.2\mathcal{A}^{1/3}$ are the average volume of the nucleus and radius respectively. α is chosen such as it is self consistently determined for the nucleus for which the theory is applied to. So we have $\frac{\alpha}{V}\hbar\Omega = \frac{V_{\mathcal{A}}}{N_a^{3/2}}/V$, and as $V \to \infty$ we should recover the continuous Hilbert space and $H^{(n\neq 1)} \to 0$. The maximum magnitude of a matrix element for a term in the Hamiltonian, for example like $Q_{ij}Q_{ji}$, scales as $Q_{ij}Q_{ji} \sim N_a^2$. This implies that in theory we could have a symplectic state that includes infinite number of bosons (excitation quanta). Therefore V has to be picked in such a way that when $N_a \to \infty$ then $H^{(n\neq 1)} \to 0$. Since the volume of the harmonic oscillator is proportional to $N_a^{3/2}$ therefore the volume of the box in which the Hamiltonian will be quantized and diagonalized should be picked such as $V \sim N_a^{3/2}$. This simply states that the volume has to be able to contain the dynamics especially the underlying dominant deformation and vibrations of nuclei, and has to scale appropriately. This choice reduces $\frac{\alpha}{V}\hbar\Omega = \frac{V_{\mathcal{A}}}{N_a^3} \sim \frac{\mathcal{A}}{N_a^3}$. The physical meaning of this parameter is that configurations with higher number of bosons (excitations) will have smaller contributions to the Hamiltonian and therefore the observables. This is evident from the fact that a matrix element in the Hamiltonian will effectively scale as $H^{(n\neq 0)} \sim \frac{\mathcal{A}}{N_a}$ which tells us that for a system with $\mathcal{A}$ nucleons we need N_a bosons to describe them with. $\frac{\alpha}{V}\hbar\Omega$ sets the scale of our theory. If $\frac{\alpha}{V}\hbar\Omega << 1$ then the plane wave solution is justified and the harmonic oscillator structure is preserved. But if $\frac{\alpha}{V}\hbar\Omega \sim 1$ then higher order corrections to the plane wave solution become relevant and $Q \cdot Q$ destroys the HO structure. As we add more nucleons to the system their corresponding boson excitations have to also increase appropriately such as

we can treat them as plane waves. This further emphasizes the fact that this scale is valid as long as a shell structure description is appropriate for the system we are studying.

The second parameter of our theory is g_n which is the strength of the quadrupole operator because only the quadrupole terms in Eq. (5.47) carry this parameter. This coefficient tells us the strength of the quadrupole tensor relative to the kinetic tensor. It is evident from the fact that if $g_n = 0$ then we would get a power series of $K_{ij}K_{ji}$. It is therefore the careful choice of $g_n > 1$ for $\forall n$ that balances the weight of the interaction between $Q_{ij}Q_{ji}$, $K_{ij}K_{ji}$ and $Q_{ij}K_{ji}$.

The parameter g_n is expressed in terms of the mass-like parameter introduced in Eq. (5.16) to represent the strength of the interaction. It results from off-diagonal coupling that depends on n which has a simple physical interpretation

$$g_n = \frac{2n-1}{n} g. \tag{5.48}$$

Its consequence is the following: the energy of the bosons contributing to the formation of a given final symplectic configuration starting from an initial one decreases as we consider more pairs of them. This simple explanation makes $g_1 = g$ and $g_\infty = 2g$ and as $n \to \infty$ the weight of $Q_{ij}Q_{ji}$ will scale as

$$\lim_{n\to\infty} \frac{(\hbar\Omega)^{n+1}}{2^{n+1}} \frac{\alpha^n}{V^n} g_n^{n+1} = 0. \tag{5.49}$$

Although we have a new parameter g_n at every order of the Hamiltonian, we only need to determine g through which g_n will be determined, therefore our theory is effectively a two parameter theory; namely, $\frac{V_A}{N_a^3}$ and g. As for the magnitude of g it follows a simple pattern. Initial studies suggest that there is a possibility for a way to determine a universal functional for g, which can be then used for any nucleus. This could be done by applying the Hamiltonian to different nuclei that have different leading symplectic irreps and then trying to reproduce the best energy spectra, B(E2) values and radii. In this thesis, we fit only the

value of g to a given nucleus and only to a given symplectic irrep that describes most of the physics of the rotational band of the ground state.

5.7 Time Average of the SpEFT Hamiltonian

The Hamiltonian in Eq. (5.47) depends on time implicitly. This dependence comes through the symplectic operators defined in Eqs. (5.18) and since they enter in pairs into the two-body interaction terms they will have the following time factors $e^{\pm 4\iota\Omega t}$ for $A_{ij}A_{ji}$ and $B_{ij}B_{ji}$, $e^{\pm 2\iota\Omega t}$ for $A_{ij}C_{ji}$ and $B_{ij}C_{ji}$, unity for $A_{ij}B_{ji}$ and $C_{ij}C_{ji}$ (+ for A-s and - for B-s). It is evident that the time independent terms, like $A_{ij}B_{ji}$ and $C_{ij}C_{ji}$ are responsible for rotations. As for the dynamical terms, time dependent parts, they are responsible for vibrations in nuclei.

The time dependence has to be integrated out. This is done by averaging the Hamiltonian over the time period that the nucleons interact with each other.

$$H = \frac{1}{T}\int_0^T H(t)dt, \tag{5.50}$$

where T is the upper time limit in which the strong interaction propagates and it is of order $T = \frac{2R}{c} = \frac{2\times 10^{-15}}{3\times 10^{8}} \sim 10^{-23}s$. This allows us to evaluate the integral in the limit of $T \to 0$ which implies that the self interacting fields in our EFT interact almost simultaneously

$$H = \lim_{T\to 0}\frac{1}{T}\int_0^T H(t)dt. \tag{5.51}$$

Time independent terms come out of this integral unchanged. As for the time dependent ones let us show an explicit example like $e^{4\iota\Omega t}$ which will be to the power of $\frac{n+1}{2}$ for $n = odd$ and to power of $\frac{n}{2}$ for $n = even$. For the odd ones we have

$$H = \lim_{T\to 0}\frac{1}{T}\int_0^T e^{2(n+1)\iota\Omega t}dt = \lim_{T\to 0}\frac{e^{2(n+1)\iota\Omega T}-1}{2(n+1)\iota\Omega T} = 1. \tag{5.52}$$

This proves that the time dependent terms also come out unchanged except they drop their

exponential time factors. Same proof applies to the even expansion terms as well. Finally the Hamiltonian in Eq. (5.47) could be applied to any nucleus as though it is independent of time.

5.8 Carbon-12

Carbon is the fourth most abundant chemical element in the observable universe by mass after hydrogen, helium, and oxygen. It is one of the main elements that forms organic life as we know it. The formation of carbon occurs within the so called CNO cycle (after Carbon-Nitrogen-Oxygen) that takes place within giant and supergiant stars through the triple-alpha process that is the main driver of nuclear fusion. The resulting carbon nuclei from this process are in their first excited 0^+ state, the Hoyle state. Therefore understanding the nuclear structure of carbon has significant importance for astrophysical applications mainly determining reaction rates and abundances of elements that could help improve our understanding of the formation of stars and visible matter.

^{12}C has 6 protons and 6 neutrons. Filling particles along the shells of a harmonic oscillator potential that can contain $2(N_h+1)(N_h+2)$ oscillator quanta at each shell, where N_h is the major oscillator shell number, we will have 4 nucleons in $N_h = 0$ and 8 nucleons in $N_h = 1$. This gives us the number of bosons at the bandhead level

$$N_\sigma = 4 \times 0 + 8 \times 1 + \frac{3}{2}(12-1) = 24.5, \tag{5.53}$$

where $\frac{3}{2}12$ is the vacuum energy for 12 nucleons and we subtracted 1.5 to remove the center of mass contribution. As for $(\lambda_\sigma, \mu_\sigma)$ we count starting from the highest shell closure, so 8 nucleons in $N_h = 1$ of which 4 at $(n_z, n_x, n_y) = (1, 0, 0)$ and 4 at $(n_z, n_x, n_y) = (0, 1, 0)$ so we have $4 \times [(1, 0, 0) + (0, 1, 0)] = (4, 4, 0)$ which gives $(\lambda_\sigma, \mu_\sigma) = (0, 4)$. So the leading symplectic irrep at the 0p-0h configuration that is used to describe the ground state is $24.5(0, 4)$, and Hoyle state is believed to belong to the $28.5(12, 0)$ symplectic irrep at the 4p-4h level.

The Hamiltonian is diagonalized for $24.5(0, 4)$ and $28.5(12, 0)$ symplectic irreps using

$g = 6.1$ which was sufficient to reproduce energies, B(E2) and radii. The results are presented in Fig. (5.1) for the ground state and in Fig. (5.3) for the Hoyle state. Comparing these results to Fig. (2.5) we clearly see the advantages of our SpEFT Hamiltonian; namely, we capture similar results for the rotational band of the ground state and the Hoyle state without using a spin-orbit term or the need to subtract a centroid term. The convergence of the results for the ground state was achieved in a model space of $N_{max} = 14$. This is easily demonstrated by the convergence of the B(E2) values in Fig. (5.8). The probability distribution is presented in Fig. (5.2) for the ground state and Fig. (5.4) for the Hoyle state. As for the radius mean squared (rms) we get 2.4 fm compared to an experimental value of 2.43(2) fm for the ground state and 2.77 fm for the Hoyle state compared to an experimental value of 2.89(4) fm. All the results shown are with the Hamiltonian in (5.47), where we include terms up to $n \leq 4$ which are sufficient for observables to converge.

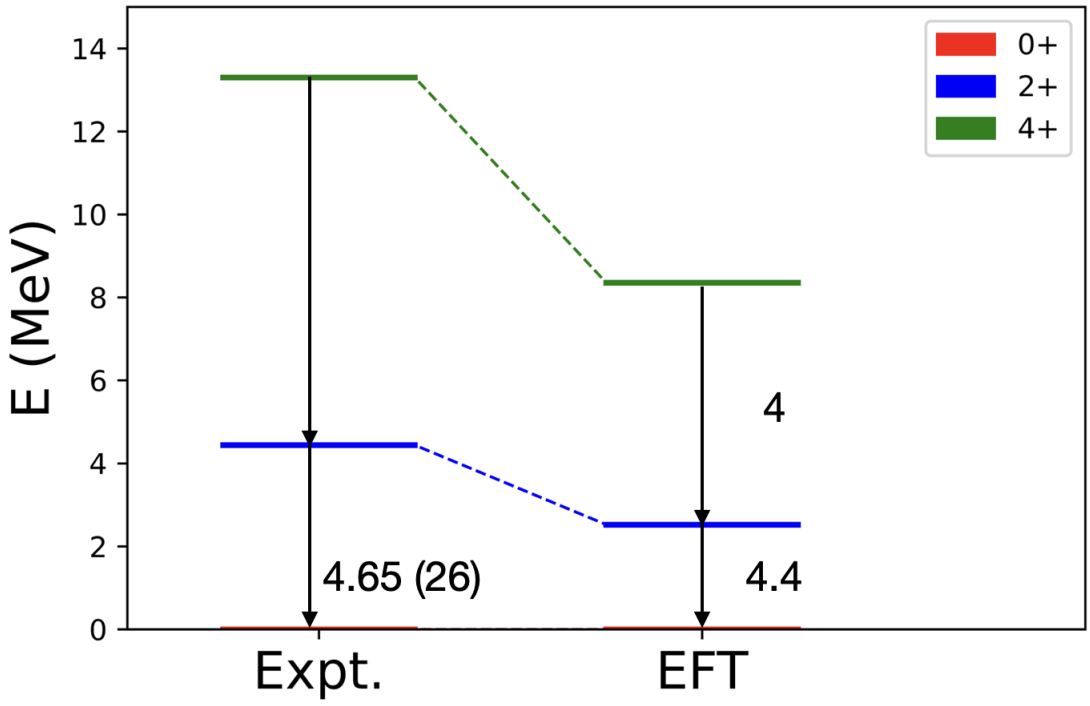

Figure 5.1. The energy spectrum and BE(2) values of the $24.5(0,4)$ symplectic irrep for ^{12}C within SpEFT in $N_{max} = 14$ model space (EFT) compared to experimental data (Expt.) [62]. BE(2) values are in W.u.

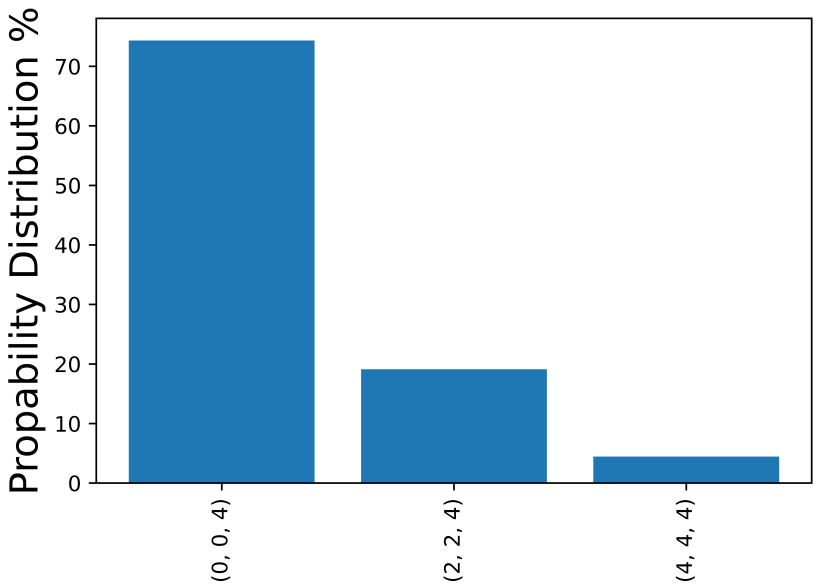

Figure 5.2. The probability distribution of the ground state 0^+ for ^{12}C in $N_{max} = 14$ model space for each $(N_n, \lambda_\omega, \mu_\omega)$ configuration.

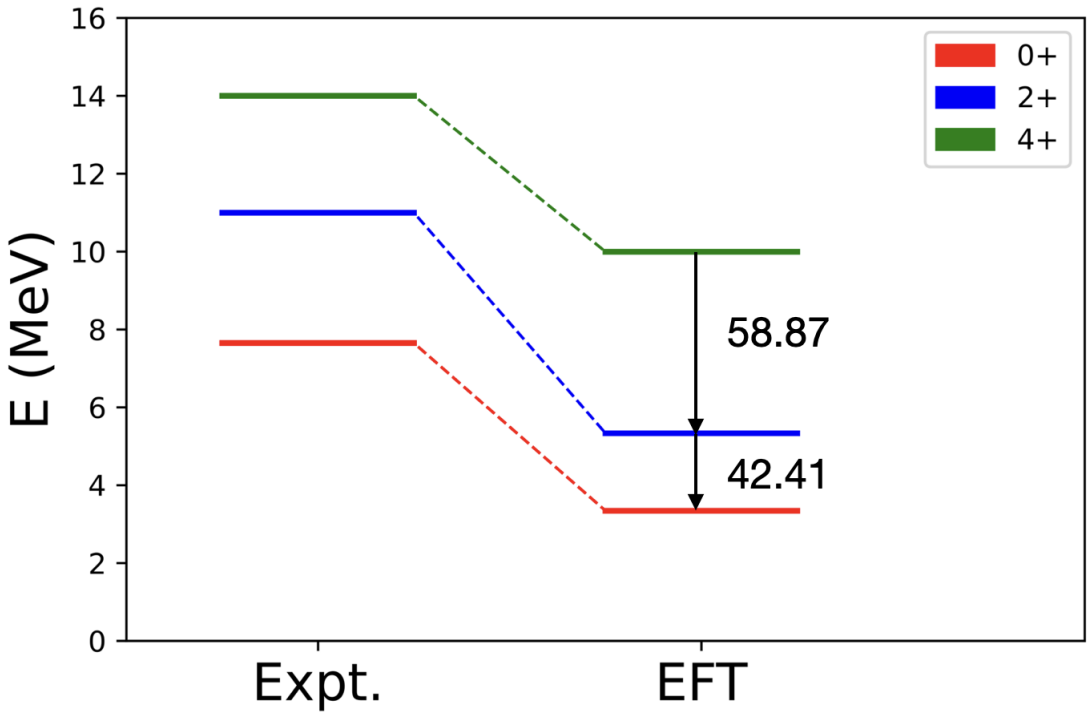

Figure 5.3. The energy spectrum and BE(2) values of the $28.5(12, 0)$ symplectic irrep for ^{12}C within SpEFT in $N_{max} = 14$ model space relative to the ground state (EFT) compared to experimental data (Expt.) [62]. Experimental BE(2) values are not available. BE(2) values are in W.u.

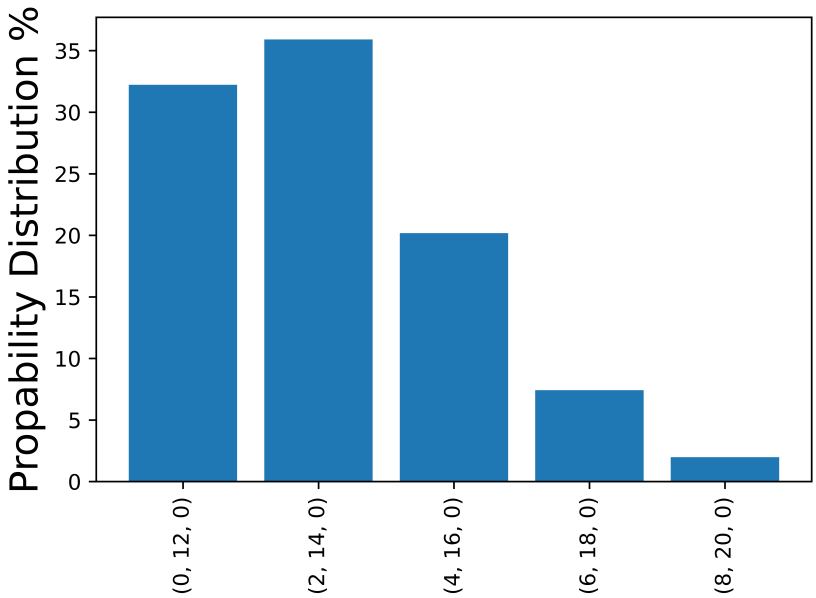

Figure 5.4. The probability distribution of the Hoyle state (first excited 0^+) for ^{12}C in $N_{max} = 14$ model space for each $(N_n, \lambda_\omega, \mu_\omega)$ configuration.

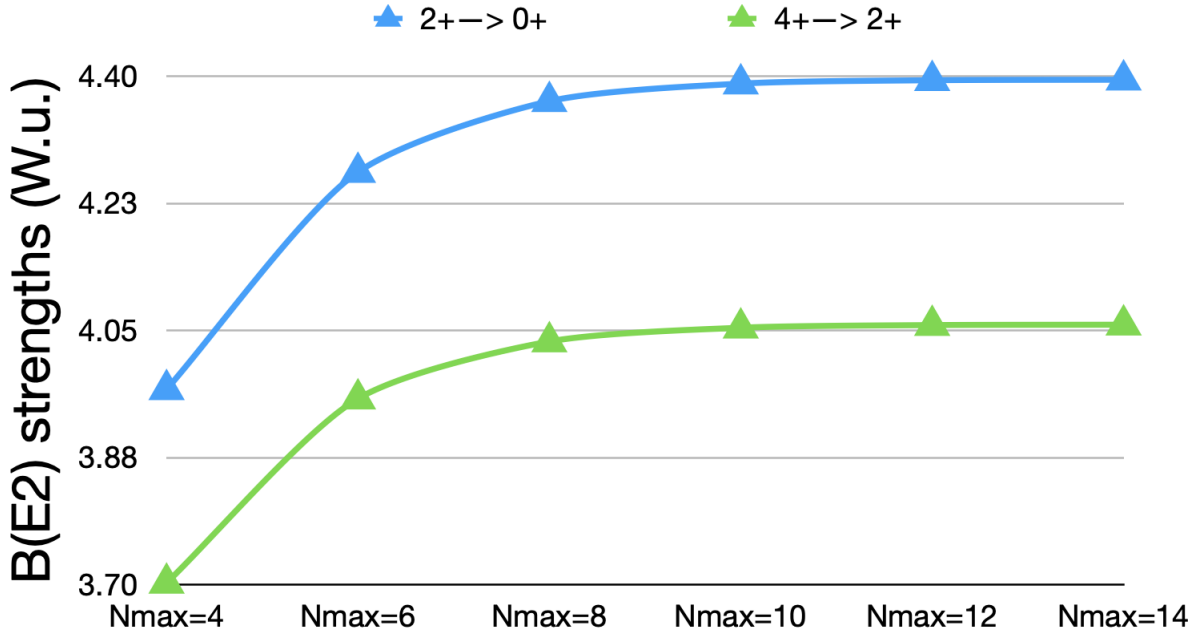

Figure 5.5. B(E2) strengths for the two transitions plotted at different N_{max} values show convergence as we near $N_{max} = 10$

5.9 Neon-20

^{20}Ne is a nucleus with 10 protons and 10 neutrons. Its ground state behaves like nearly a perfect rigid rotor. This makes it interesting to see if our EFT can capture this rotational

band. Moreover the terms $K_{ij}K_{ji}$ and $Q_{ij}K_{ji}$ in Eq. (5.47) should capture the irrotational behavior in nuclei and this makes ^{20}Ne the perfect candidate to study within our theory. It fills 4 nucleons in $N_h = 0$, 12 nucleons in $N_h = 1$ and 4 in $N_h = 2$. This gives the number of bosons at the bandhead level

$$N_\sigma = 4 \times 0 + 12 \times 1 + 4 \times 2 + \frac{3}{2}(20 - 1) = 48.5. \tag{5.54}$$

So we have $N_\sigma = 48.5$ bosons that form the symplectic bandhead for ^{20}Ne. As for $(\lambda_\sigma, \mu_\sigma)$ we count starting from the highest shell closure so 4 nucleons in $N_h = 2$ and they all fill the state $(n_z, n_x, n_y) = (2, 0, 0)$ so we have $4 \times (2, 0, 0) = (8, 0, 0)$ which gives $(\lambda_\sigma, \mu_\sigma) = (8, 0)$.

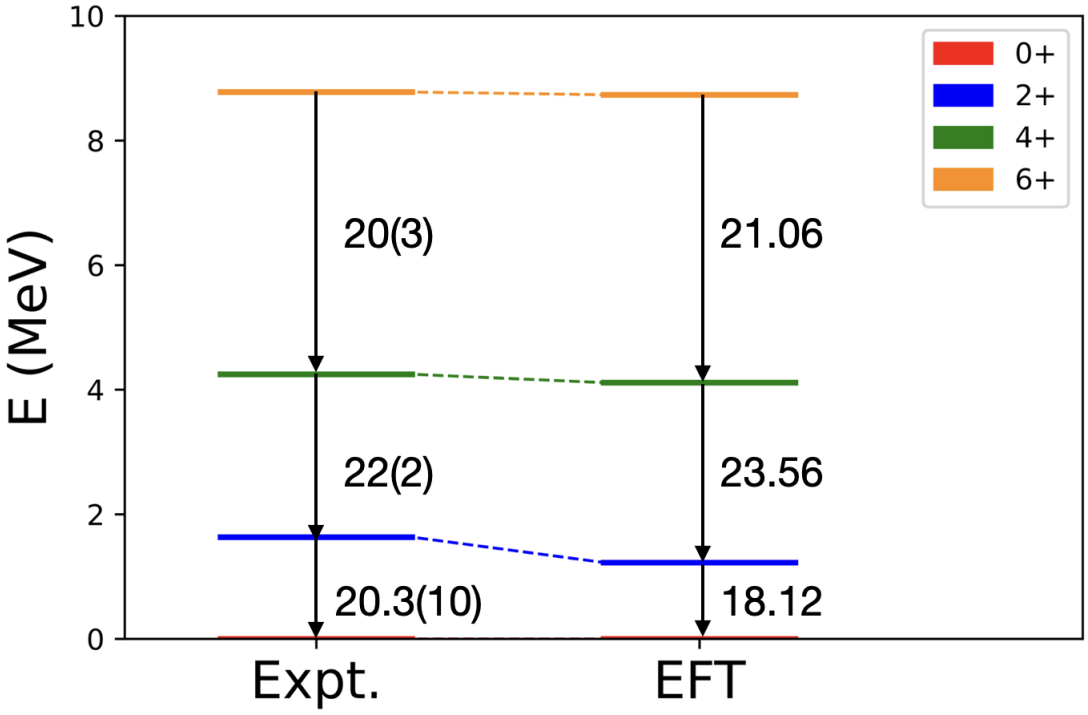

Figure 5.6. The energy spectrum and BE(2) values of the 48.5(8, 0) symplectic irrep for ^{20}Ne within SpEFT in $N_{max} = 16$ model space (EFT) compared to experimental data (Expt.) [63]. BE(2) values are in W.u.

It was found that $g = 8.6$ was sufficient to reproduce energies, B(E2) and radii. The results presented in Fig. (5.6) are remarkable. The developed SpEFT Hamiltonian reproduces nearly perfect energy spectra and B(E2) transitions with only one fitted parameter.

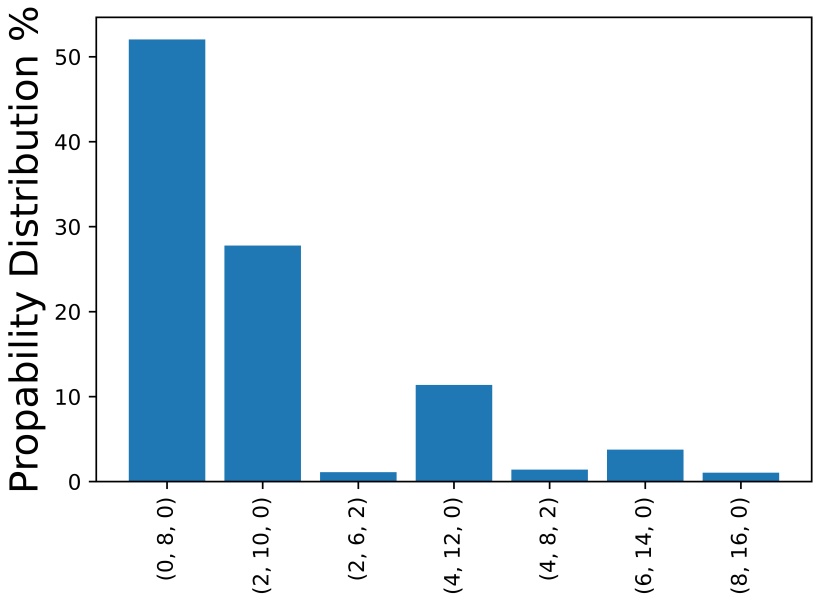

Figure 5.7. The probability distribution of the ground state 0^+ for ^{20}Ne in $N_{max} = 16$ model space for each $(N_n, \lambda_\omega, \mu_\omega)$ configuration.

The probability distribution is presented in Fig. (5.7). The convergence of the results was achieved in a model space of $N_{max} = 16$ demonstrated by the convergence of the B(E2) values in Fig. (5.8). As for the radius mean squared (rms) we get 2.8 fm compared to an experimental value of 2.87(3) fm. All the results shown are with the Hamiltonian in (5.47), where we include terms up to $n \leq 4$ which are sufficient for observables to converge.

5.10 Erbium-166

Finally, to prove that the SpEFT Hamiltonian is applicable to heavy nuclei, we apply it to a heavy nucleus like ^{166}Er. This nucleus is interesting since its lowest leading symplectic configuration at the lowest HO energy level comes at $N_\sigma = 799.5$, but the authors in [64] showed that the ground state rotational band of ^{166}Er could be described by $826.5(78, 0)$. This is a common occurrence in heavy nuclei. The higher lying symplectic bandheads that are maximally deformed are favored energetically and their energy drops below the symplectic bandhead $N_\sigma = 799.5$. To test this, we apply the SpEFT Hamiltonian with $g = 70$ to the $826.5(78, 0)$ symplectic irrep in a model space of $N_{max} = 14$ and the results shown in Fig. (5.9) are in remarkable agreement with experiment. The probability distribution for ^{166}Er

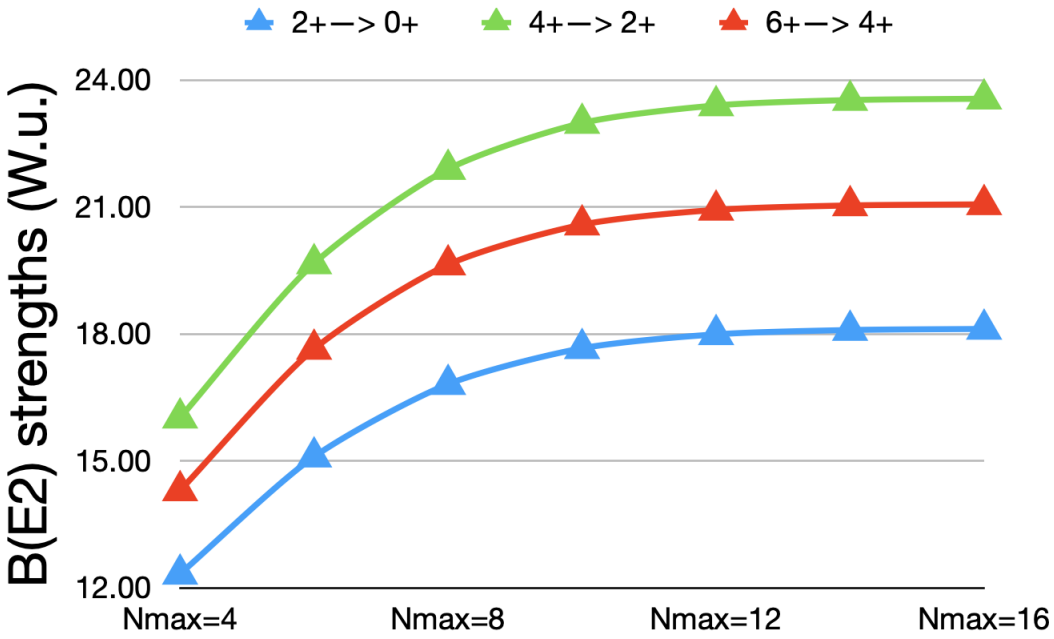

Figure 5.8. BE(2) strengths for the three transitions plotted at different N_{max} values show convergence as we near $N_{max} = 16$

presented in Fig. (5.10) shows a different pattern compared to ^{12}C and ^{20}Ne. The dominant configurations that contribute to the wave function of the ground state for Erbium move towards higher N_n, contrary to the cases for Carbon and Neon, for which the leading order contributions to the ground state came from the bandheads. We get 5.39 fm for the radius of ^{166}Er.

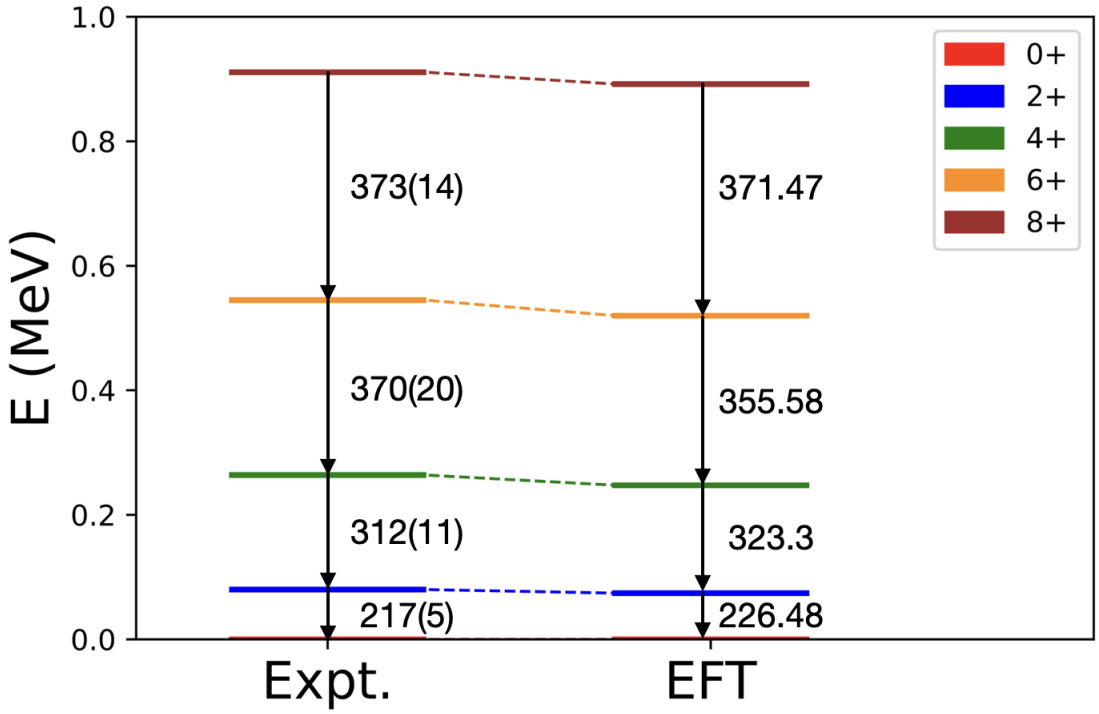

Figure 5.9. The energy spectrum and BE(2) values of the $826.5(78, 0)$ symplectic irrep for ^{166}Er within SpEFT in $N_{max} = 14$ model space (EFT) compared to experimental data (Expt.) [65]. BE(2) values are in W.u.

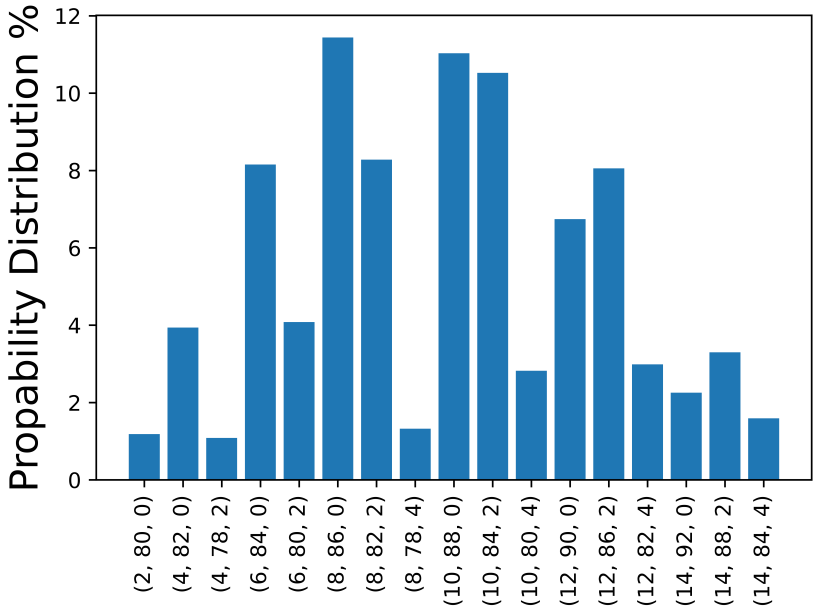

Figure 5.10. The probability distribution of the ground state 0^+ for ^{166}Er in $N_{max} = 14$ model space for each $(N_n, \lambda_\omega, \mu_\omega)$ configuration.

6 Conclusions

In this thesis we explored the historical evolution of nuclear physics as an established field of science. We then followed on by emphasizing the importance of special symmetries in nuclear physics and then focused in on the symplectic symmetry as an extension of the Elliott Model as a model of choice for gaining reasonable results within relatively small model spaces. Additionally, we outlined a step-by-step process of how to calculate the matrix elements of symplectic operators that formed the interaction in NCSpM.

We then examined two approaches that established the theoretical underpinning of a deformed symplectic model that is the logical extension of a many-particle generalization of the Nilsson Model. First of which was constructing the quantum equivalent of a canonical transformation for mapping the non-deformed symplectic algebra onto its deformed counterpart, and within that framework advanced a unitary canonical transformation that preserves the symplectic symmetry and provided a simple example by applying it to the harmonic oscillator Hamiltonian. The second approach was through providing analytic results for transformation coefficients between spherical, cylindrical and Cartesian basis states of the 3D-HO between deformed and non-deformed sates, and observed how their probability distributions change as a function of deformation.

The crown jewel of this thesis was to explore the emergence of symplectic symmetry within a field theory framework for which we developed a symplectic effective field theory. A many-body microscopic theory applicable from light to heavy nuclei because it takes full advantage of the dynamical symmetry group which is an extension of the complete, multi-shell isotropic harmonic oscillator; namely, it is underpinned by the Sp(3,$\mathbf{R}$) symmetry group, which when restricted to a single shell reduces to Elliott's SU(3) theory. To reemphasize, it allows one to create an alternative complete shell-model theory from the ground up starting from a simple real scalar field theory Lagrangian that implicitly and explicitly exposes the ubiquitous nature of the dominance of deformation in atomic nuclei. It shows the emergence of Sp(3,R), which is the dynamical symmetry group of the three dimensional harmonic oscillator, and

that has now been shown to reproduce — typically to a 70-80 percent level in its probability distribution — with the remaining 20-30 percent due to mixing of the symmetry that is driven by terms of lesser importance that lead for its mixing. The primary structure of atomic nuclei can be characterized in terms of a single irreducible representation of the symplectic group which in many cases is sufficient to reproduce the experimentally observed energy spectra. And furthermore, since the quadrupole moment is part of the symplectic algebra by construction, it automatically yields observed B(E2) values without the need for introducing an ad hoc effective charge into the theory. Each such symplectic structure is but a small fraction of the full NCSM shell-model space, which means it can be used to integrate coherent-state-like structures into the theory that is capable of reproducing observed B(E2) strengths and radii in smaller model spaces without the need of large supercomputers. We successfully demonstrated its capabilities by applying it on ^{12}C, ^{20}Ne and ^{166}Er. The results were in remarkable agreement with experiment.

Appendix: Copyright Information

Symmetries and canonical transformations in nuclei

Cite as: AIP Conference Proceedings **2150**, 040002 (2019); https://doi.org/10.1063/1.5124603
Published Online: 03 September 2019

David Kekejian, Jerry P. Draayer and Kristina D. Launey

Physics Letters A 384 (2020) 126162

Contents lists available at ScienceDirect

Physics Letters A

www.elsevier.com/locate/pla

Overlaps of deformed and non-deformed harmonic oscillator basis states

David Kekejian [a,*], Jerry P. Draayer [a], Tomáš Dytrych [a,b], Kristina D. Launey [a]

[a] Department of Physics and Astronomy, Louisiana State University, Baton Rouge, LA 70803-4001, USA
[b] Nuclear Physics Institute, Czech Academy of Sciences, 25068 Řež, Czech Republic

ARTICLE INFO

Article history:
Received 11 May 2019
Received in revised form 16 November 2019
Accepted 18 November 2019
Available online 25 November 2019
Communicated by M.G.A. Paris

Keywords:
Harmonic oscillator
Deformed overlaps
Interbasis expansion

ABSTRACT

A systematic approach for expanding non-deformed harmonic oscillator basis states in terms of deformed ones, and vice versa, is presented. The objective is to provide analytical results for calculating these overlaps (transformation brackets) between deformed and non-deformed basis states in spherical, cylindrical, and Cartesian coordinates. These overlaps can be used for reducing the complexity of different research problems that employ three-dimensional harmonic oscillator basis states, for example as used in coherent state theory and the nuclear shell-model, especially within the context of *ab initio* symmetry-adapted no-core shell model.

1. Introduction

The harmonic oscillator (HO) is perhaps the most frequently used concept in all of physics. Applications that employ HO concepts span from classical to quantum mechanics [1–6]. The fact that the Hamiltonian of the HO is very simple, incredibly intuitive, and analytically solvable makes it a desirable starting point for gaining initial insight into a broad range of physical phenomena.

The use of the three-dimensional (3D) HO for studying nuclear phenomena reaches back to the Nilsson single-particle model [7], and more generally to Elliott's many-particle SU(3) theory [8]. SU(3) enters because it is the symmetry of the 3D-HO, coupled with the fact that low-lying nuclear configurations can be considered in lowest order to be simple harmonic excitations around locally defined minima.

More recently, the use of an extended SU(3)-based theory has been shown to be advantageous in advanced *ab initio* nuclear structure studies because the SU(3) framework enables one to reduce the size of model spaces that are required to capture the dominant dynamics of complex nuclear systems. Applications using the so-called symmetry-adapted no-core shell-model (SA-NCSM) illustrate this well through successful studies up to and including medium-mass nuclei using SU(3) coupled basis states [9–13].

While all harmonic oscillator basis states can be considered to be equivalent, depending on the specific nature of the problem, some choices may be preferable to others; for example, spherical basis states ($|nlm\rangle$) have l as a good quantum number whereas cylindrical basis states ($|nn_zm\rangle$) do not; nevertheless, these are equivalent in the sense that both form complete sets. In particular, as first shown by the work of Nilsson cited above [7], it is advantageous to use a deformed basis to fold the dominant effects of deformation into smaller model spaces, an early result that anticipates and underpins the importance of providing easy-to-use transformations between these schemes – developed below – in anticipation of their use in more complex many-particle environments that these results can enable.

In this paper, we give analytic expressions for transformations between single-particle deformed and single-particle non-deformed spherical, cylindrical and Cartesian basis states; namely, for the overlaps $\langle\widetilde{nl}m|nlm\rangle$, $\langle\widetilde{nn}_zm|nn_zm\rangle$ and $\langle\widetilde{n}_x\widetilde{n}_y\widetilde{n}_z|n_xn_yn_z\rangle$ respectively, where a tilde is used to denote deformation.

First we will calculate the transformation coefficients between non-deformed cylindrical and spherical basis states, namely $\langle nn_zm|nlm\rangle$ [14–16] which in turn will be used to calculate the $\langle\widetilde{nl}m|nlm\rangle$.

2. Non-deformed spherical versus cylindrical basis states

To calculate the $\langle nn_zm|nlm\rangle$, we begin by expanding a given $|nlm\rangle$ state in terms of all possible cylindrical states $|nn_zm\rangle$,

* Corresponding author.
E-mail address: dkekejian@lsu.edu (D. Kekejian).

https://doi.org/10.1016/j.physleta.2019.126162
0375-9601/

References

[1] A. Bohr and B. R. Mottelson. *Nuclear Structure, Vol. II: Nuclear Deformation.* W. A. Benjamin, Reading, Mas- sachusetts,USA, 1975.

[2] P. O. Hess, M. Seiwert, J. Maruhn, and W. Greiner. General collective model and its application to $^{238}_{92}$**U**. *Zeitschrift fuer Physik A, Atoms and Nuclei*, 296:147–163, 1980.

[3] J. P. Elliott. Collective motion in the nuclear shell model. ii. the introduction of intrinsic wave-functions. *Proceedings of the Royal Society. A. Mathematical, Physical and Engineering Sciences*, 245(1243), 1958.

[4] P. Navrátil, J. P. Vary, and B. R. Barrett. Large-basis ab initio no-core shell model and its application to ^{12}C. *Phys. Rev. C*, 62:054311, 2000.

[5] B. R. Barrett, P. Navrátil, and J. P. Vary. Ab initio no core shell model. *Progress in Particle and Nuclear Physics*, 69(Supplement C):131 – 181, 2013.

[6] P. Navrátil, J. P. Vary, and B. R. Barrett. Properties of ^{12}C in the ab initio nuclear shell model. *Phys. Rev. Lett.*, 84:5728–5731, Jun 2000.

[7] T. Dytrych, K. D. Launey, J. P. Draayer, D. J. Rowe, J. L. Wood, G. Rosensteel, C. Bahri, D. Langr, and R. B. Baker. Physics of nuclei: Key role of an emergent symmetry. *Phys. Rev. Lett.*, 124:042501, Jan 2020.

[8] K. D. Launey, T. Dytrych, and J. P. Draayer. Symmetry-guided large-scale shell-model theory. *Progress in Particle and Nuclear Physics*, 89:101 – 136, 2016.

[9] T. Dytrych, K. D. Sviratcheva, J. P. Draayer, C. Bahri, and J. P. Vary. Ab initio symplectic no-core shell model. *Journal of Physics G: Nuclear and Particle Physics*, 35(12):123101, 2008.

[10] T. Dytrych, K. D. Sviratcheva, C. Bahri, J. P. Draayer, and J. P. Vary. Evidence for symplectic symmetry in ab initio no-core shell model results for light nuclei. *Phys. Rev. Lett.*, 98:162503, Apr 2007.

[11] T. Dytrych, K. D. Launey, J. P. Draayer, P. Maris, J. P. Vary, E. Saule, U. Catalyurek, M. Sosonkina, D. Langr, and M. A. Caprio. Collective modes in light nuclei from first principles. *Phys. Rev. Lett.*, 111:252501, Dec 2013.

[12] T. Dytrych, A. C. Hayes, K. D. Launey, J. P. Draayer, P. Maris, J. P. Vary, D. Langr, and T. Oberhuber. Electron-scattering form factors for ^{6}Li in the ab initio symmetry-guided framework. *Phys. Rev. C*, 91:024326, 2015.

[13] K. D. Launey, A. C. Dreyfuss, J. P. Draayer, T. Dytrych, and R. Baker. Emergence of cluster structures and collectivity within a no-core shell-model framework. *Journal of Physics: Conference Series*, 569(1):012061, 2014.

[14] G. Rosensteel and D. J. Rowe. Nuclear Sp$(3, r)$ model. *Phys. Rev. Lett.*, 38:10–14, Jan 1977.

[15] A. C. Dreyfuss, K. D. Launey, T. Dytrych, J. P. Draayer, and C. Bahri. Hoyle state and rotational features in carbon-12 within a no-core shell-model framework. *Physics Letters B*, 727(4):511–515, 2013.

[16] G. K. Tobin, M. C. Ferriss, K. D. Launey, T. Dytrych, J. P. Draayer, A. C. Dreyfuss, and C. Bahri. Symplectic no-core shell-model approach to intermediate-mass nuclei. *Phys. Rev. C*, 89:034312, Mar 2014.

[17] H. Geiger. The scattering of the α-particles by matter. *Proceedings of the Royal Society of London. Series A, Containing Papers of a Mathematical and Physical Character*, 83:492, 1910.

[18] H. Geiger and E. Marsden. On a diffuse reflection of the α-particles. *Proceedings of the Royal Society of London. Series A, Containing Papers of a Mathematical and Physical Character*, 82(557):495–500, 1909.

[19] B. R. Webber and E. A. Davis. Commentary on 'the scattering of α and β particles by matter and the structure of the atom' by e. rutherford (philosophical magazine 21 (1911) 669–688). *Philosophical Magazine*, 92(4):399–405, 2012.

[20] J. Chadwick. Possible existence of a neutron. *Nature*, 192:312, 1932.

[21] D. Rowe and J. Wood. Fundamentals of nuclear models. 1:19–20, 2010.

[22] V. Zelevinsky and A. Volya. Physics of atomic nuclei. 1:20, 2017.

[23] M. G. Mayer. On closed shells in nuclei. ii. *Phys. Rev.*, 75:1969–1970, Jun 1949.

[24] O. Haxel, J. H. D. Jensen, and H. E. Suess. On the "magic numbers" in nuclear structure. *Phys. Rev.*, 75:1766–1766, Jun 1949.

[25] S. G. Nilsson. Binding states of individual nucleons in strongly deformed nuclei. *Kong. Dan. Vid. Sel. Mat. Fys. Med.*, 29N16:1–69, 1955.

[26] I. Stetcu and J. Rotureau. Effective interactions and operators in the no-core shell model. *Progress in Particle and Nuclear Physics*, 69(Supplement C):182 – 224, 2013.

[27] P. Brussard and P. Glaudemans. Shell-model applications in nuclear spectroscopy. *Progress in Particle and Nuclear Physics*, 1977.

[28] I. Shavitt. The history and evolution of configuration interaction. *Molecular Physics*, 94(1):3–17, 1998.

[29] R. Roth and P. Navrátil. *ab initio* study of ^{40}Ca with an importance-truncated no-core shell model. *Phys. Rev. Lett.*, 99:092501, Aug 2007.

[30] P. Rochford and D.J. Rowe. The survival of rotor and SU(3) bands under strong spin-orbit symmetry mixing. *Physics Letters B*, 210(1):5 – 9, 1988.

[31] V. G. Gueorguiev, J. P. Draayer, and C. W. Johnson. SU(3) symmetry breaking in lower fp-shell nuclei. *Phys. Rev. C*, 63:014318, Dec 2000.

[32] C. Bahri and D. J. Rowe. SU(3) quasi-dynamical symmetry as an organizational mechanism for generating nuclear rotational motions. *Nuclear Physics A*, 662(1):125 – 147, 2000.

[33] G. Rosensteel and D.J. Rowe. Phase transitions and quasi-dynamical symmetry in nuclear collective models, iii: The U(5) to SU(3) phase transition in the IBM. *Nuclear Physics A*, 759(1), 2005.

[34] G. Rosensteel and D. J. Rowe. On the algebraic formulation of collective models iii. the symplectic shell model of collective motion. *Annals of Physics*, 126(2):343, 1980.

[35] G. Rosensteel. Irreducible u(3) tensor interactions in the symplectic collective model. *Nuclear Physics A*, 341(3):397, 1980.

[36] J. Escher and J. P. Draayer. Fermion realization of the nuclear Sp(6,R) model. *Journal of Mathematical Physics*, 39(10):5123, 1998.

[37] D. J. Rowe. Microscopic theory of the nuclear collective model. *Reports on Progress in Physics*, 48(10):1419–1480, oct 1985.

[38] J. P. Draayer and Yoshimi Akiyama. Wigner and racah coefficients for su3. *Journal of Mathematical Physics*, 14(12):1904–1912, 1973.

[39] Yoshimi Akiyama and J. P. Draayer. A user's guide to fortran programs for wigner and racah coefficients of su(3). *Computer Phys. Commun.*, 5:405–415, 1973.

[40] D J Rowe. Analytical expressions for the matrix elements of the non-compact symplectic algebra. *Journal of Physics A: Mathematical and General*, 17(8):L399–L403, jun 1984.

[41] G. Rosensteel. Analytic formula for quadrupole-quadrupole matrix elements. *Phys. Rev. C*, 42:2463–2468, Dec 1990.

[42] J. P. Draayer and G. Rosensteel. Major shell centroids in the symplectic collective model. *Physics Letters B*, 125(4):237–239, 1983.

[43] A. C. Dreyfuss. Alpha capture reaction rates for nucleosynthesis within an ab initio framework. *LSU Doctoral Dissertations. 5105*, 2019.

[44] D. Kekejian, J. P. Draayer, and K. D. Launey. Symmetries and canonical transformations in nuclei. *AIP Conference Proceedings*, 2150(1):040002, 2019.

[45] D. Kekejian, J. P. Draayer, T. Dytrych, and K. D. Launey. Overlaps of deformed and non-deformed harmonic oscillator basis states. *Physics Letters A*, 384(7):126162, 2020.

[46] Kh.P. Gnatenko. System of interacting harmonic oscillators in rotationally invariant noncommutative phase space. *Physics Letters A*, 382(46):3317 – 3324, 2018.

[47] M.C. Baldiotti, R. Fresneda, and D.M. Gitman. Quantization of the damped harmonic oscillator revisited. *Physics Letters A*, 375(15):1630 – 1636, 2011.

[48] S. Binder, A. Ekstrom, G. Hagen, T. Papenbrock, and K. A. Wendt. Effective field theory in the harmonic oscillator basis. *Phys. Rev. C*, 93:044332, 2016.

[49] Giuseppe Dito and Francisco J. Turrubiates. The damped harmonic oscillator in deformation quantization. *Physics Letters A*, 352(4):309 – 316, 2006.

[50] A. Anderson. Canonical transformations in quantum mechanics. *Annals of Physics*, 232(2):292, 1994.

[51] P. A. Mello and M. Moshinsky. Nonlinear canonical transformations and their representations in quantum mechanics. *Journal of Mathematical Physics*, 16(10):2017, 1975.

[52] J. Deenen, M. Moshinsky, and T.H Seligman. Canonical transformations to action and angle variables and their representations in quantum mechanics: Iii. the general problem. *Annals of Physics*, 127(2):458, 1980.

[53] D.N. Poenaru, R.A. Gherghescu, A.V. Solov'yov, and W. Greiner. Hemispheroidal quantum harmonic oscillator. *Physics Letters A*, 372(33):5448 – 5451, 2008.

[54] J. P. Draayer. A deformed potential many-particle theory. *Retrospective Theses and Dissertations*, 3731, 1968.

[55] Shi-Hai Dong. Interbasis expansions for isotropic harmonic oscillator. *Physics Letters A*, 376(15):1262, 2012.

[56] C. Truesdell. On the Addition and Multiplication Theorems for the Special Functions. *Proceedings of the National Academy of Sciences, Mathematics*, page 752, 1950.

[57] M. D. Schwartz. *Quantum Field Theory and the Standard Model*. 2013.

[58] M. Srednicki. *Quantum Field Theory*. Cambridge University Press, 2007.

[59] L. D. Landau and E. M. Lifshitz. *The Classical Theory of Fields*. Butterworth-Heinemann, 1980.

[60] R. Machleidt and D.R. Entem. Chiral effective field theory and nuclear forces. *Physics Reports*, 503(1):1–75, 2011.

[61] M. Moshinsky and C. Quesne. Linear canonical transformations and their unitary representations. *Journal of Mathematical Physics*, 12(8):1772, 1971.

[62] J. H. Kelley, J. E. Purcell, and C. G. Sheu. Energy levels of light nuclei A = 12. *Nuclear Physics A*, 968:71–253, 2017.

[63] D. R. Tilley, C. M. Cheves, J. H. Kelley, S. Raman, and H. R. Weller. Energy levels of light nuclei, A = 20. *Nuclear Physics A*, 636(3):249–364, 1998.

[64] D. J. Rowe. The fundamental role of symmetry in nuclear models. 2013.

[65] C. M. Baglin. Nuclear data sheets for A = 168. *Nuclear Data Sheets*, 111(7):1807–2080, 2010.

Vita

David Kekejian is of Armenian ethnicity and is from Aleppo, Syria. Always intrigued by the elementary processes that dictate nature, he decided to pursue sciences. After graduating from Karen Jeppe Armenian high school in 2009 he traveled to Armenia for his undergraduate studies. He graduated from Yerevan State University with honors in 2014 with a BS in physics. Finally, he decided to attend LSU to get his doctorate in theoretical nuclear physics.